



the
abdus salam
international centre for theoretical physics

ICTP 40th Anniversary

SMR 1564 - 36

SPRING COLLEGE ON SCIENCE AT THE NANOSCALE
(24 May - 11 June 2004)

NANOCRYSTALS

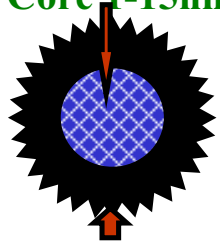
C. B. MURRAY
I.B.M. Thomas J. Watson Research Centre
Yorktown Heights, NY, U.S.A.

These are preliminary lecture notes, intended only for distribution to participants.

Semiconductor Nanocrystals (Dots, Cubes, Wires and Superlattices)

K. S. Cho, F. X. Redl, D. Talapin, C. B. Murray and C. R. Kagan

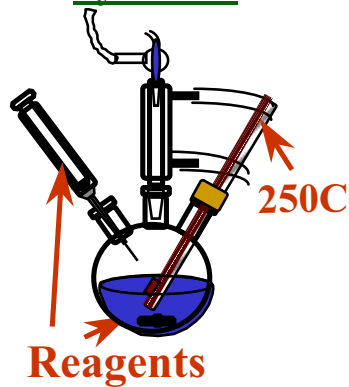
Inorganic
Core 1-15nm



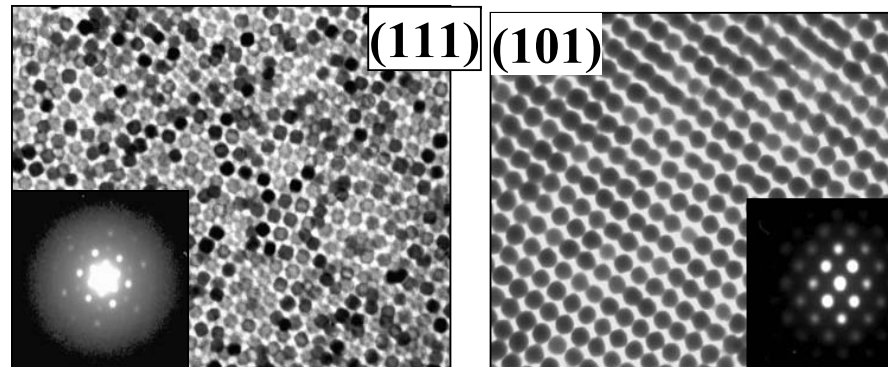
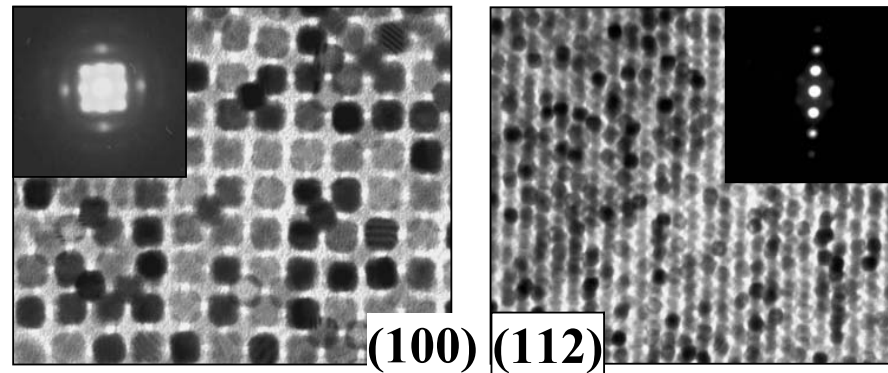
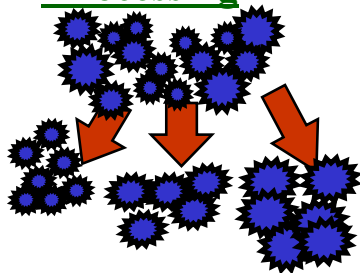
Surfactants
1-4 nm thick

- (1) Synthesize, characterize and integrate nanostructured materials.
- (2) Probe the limits conventional materials/device scaling.
- (3) Harness mesoscopic properties for future technology.
- (4) Explore the potential of self-assembly for nanofabrication.

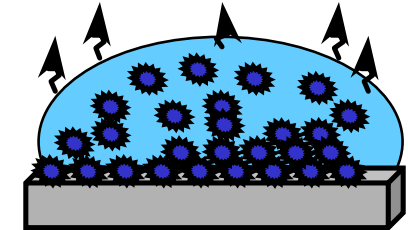
Synthesis



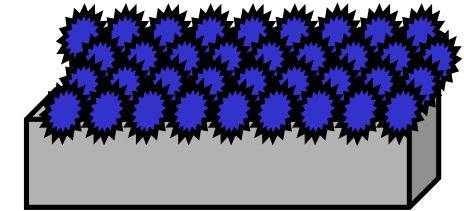
Size Selective
Processing



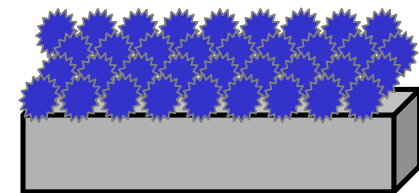
Film Growth:
Self-Assembly



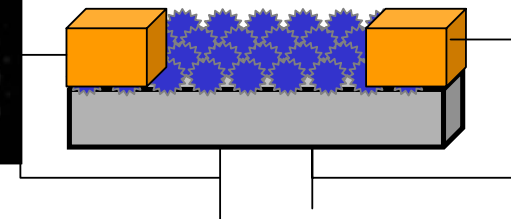
Nanocrystal Superlattice



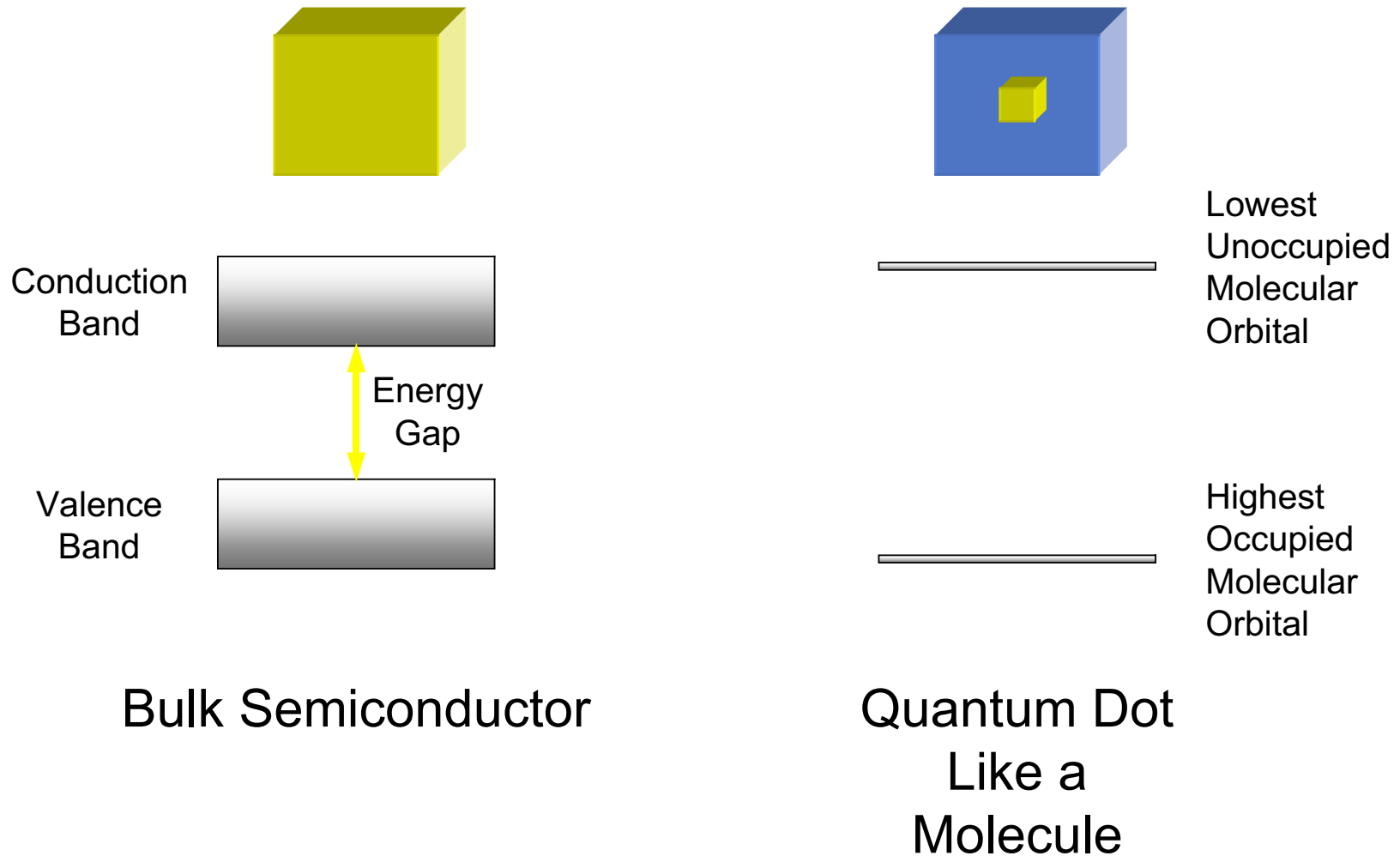
Annealed Superlattice



Nanowires



Basic Physics of Semiconductor Quantum Dots



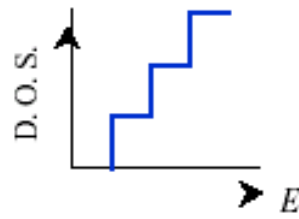
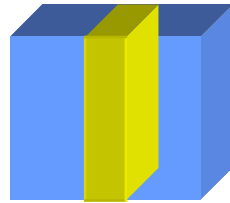
Quantum Confinement

Low Dimensional Structures



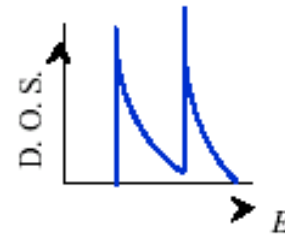
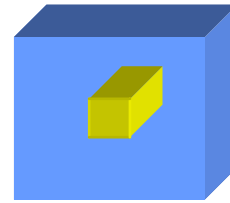
3D
Bulk Semiconductor

$$\rho_c(E) \propto \sqrt{(E - E_c)}$$



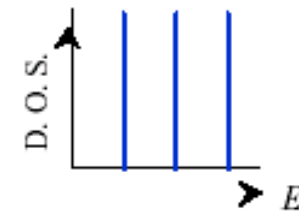
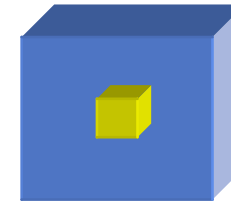
2D
Quantum Well

$$\rho_c(E) = \text{constant}$$



1D
Quantum Wire

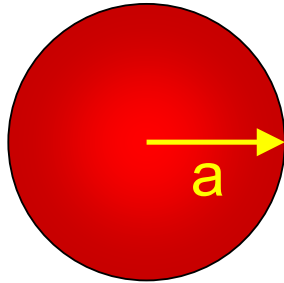
$$\rho_c(E) \propto \frac{1}{\sqrt{(E - E_n)}}$$



0D
Quantum Dot

$$\rho_c(E) \propto \delta(E - E_n)$$

Particle-in-a-Sphere

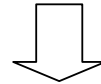


$$\Phi(r, \theta, \phi) = C \frac{j_l(k_{n,l} r) Y_l^m(\theta, \phi)}{r}$$

$Y_l^m(\theta, \phi)$ is a spherical harmonic

$j_l(k_{n,l} r)$ is the l^{th} order spherical Bessel function

$$k_{n,l} = \frac{\alpha_{n,l}}{a}$$

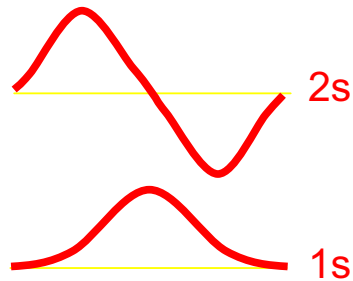


$$E_{n,l} = \frac{\hbar^2 k_{n,l}^2}{2m_0} = \frac{\hbar^2 \alpha_{n,l}^2}{2m_0 a^2}$$

Discrete energy levels

size-dependence

Potential V



r

solutions give
hydrogen-like orbitals with
quantum numbers

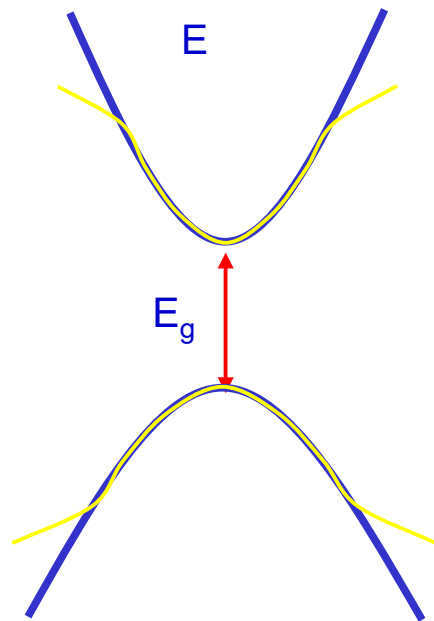
n (1, 2, 3 ...)

l (s, p, d ...)

m_j

The Quantum Dot is a Semiconductor

The Effective Mass Approximation parabolic conduction and valence bands



Direct Bandgap Semiconductor

n=conduction band

$$E_k^c = \frac{\hbar^2 k^2}{2m_{eff}^c} + E_g$$

k

n=valence band

$$E_k^v = -\frac{\hbar^2 k^2}{2m_{eff}^v}$$

Bloch's Theorem

$$\Psi_{nk}(\vec{r}) = u_{nk}(\vec{r}) \exp(i\vec{k} \cdot \vec{r})$$

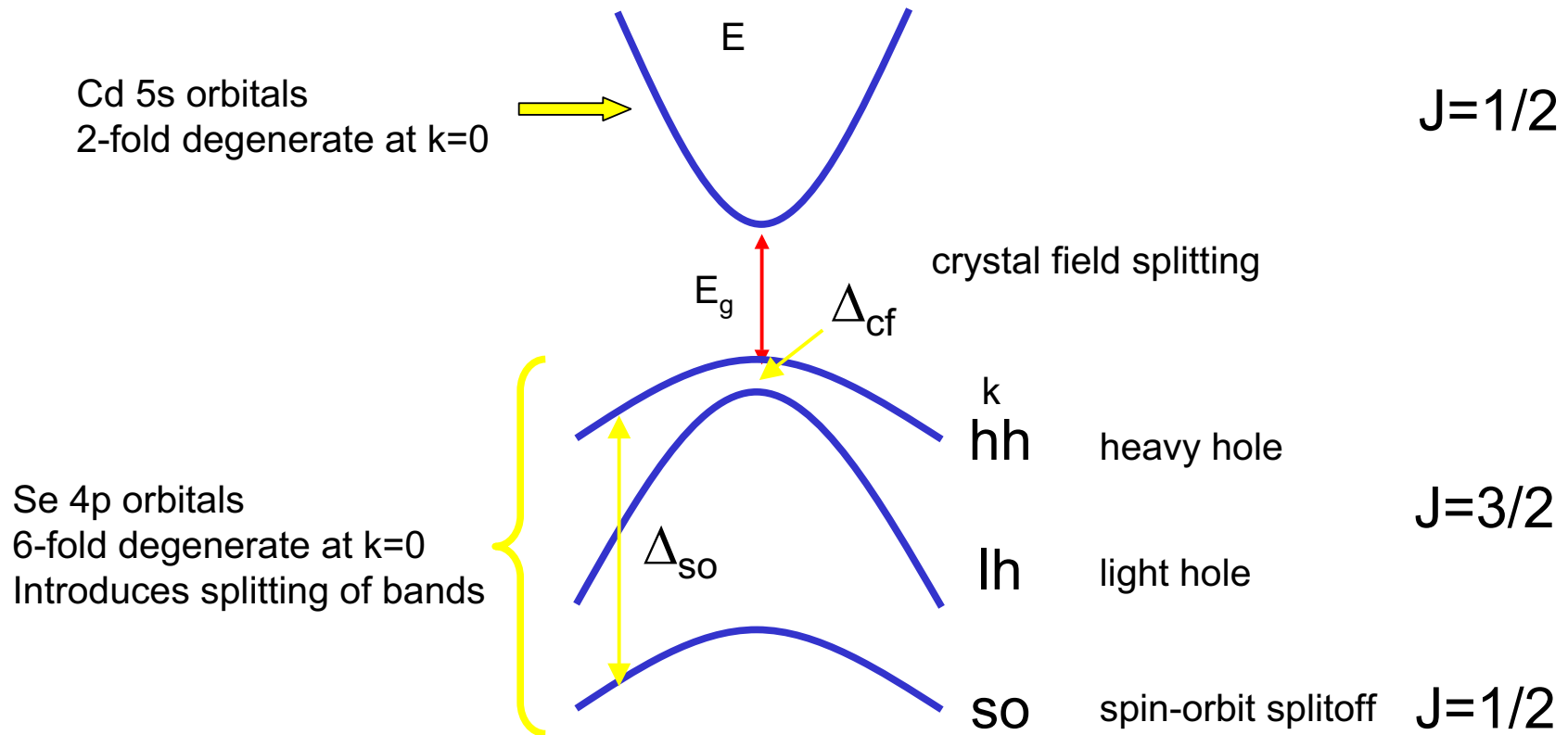
with periodicity of crystal lattice

Free particles treated
by effective mass:

- describing graphically the curvature of the bands
- representing the potential presented by the lattice

Real Band Structure

Example: CdSe



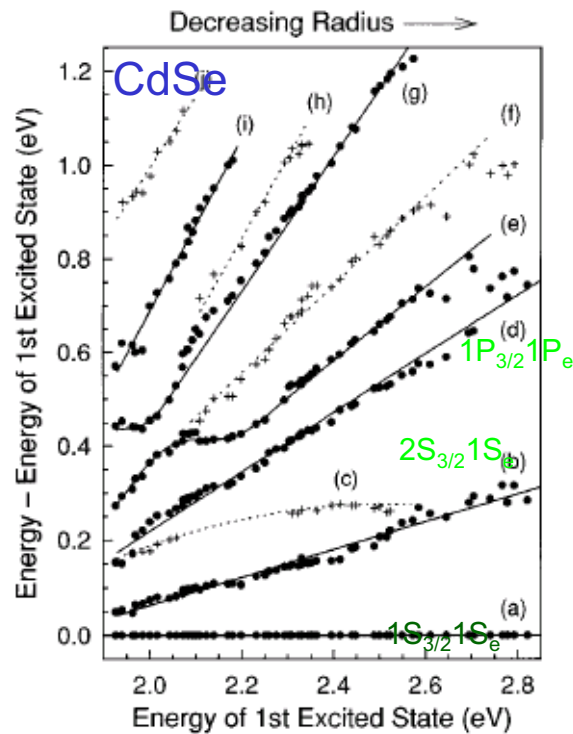
$$J = L + S$$

where L =orbital angular momentum

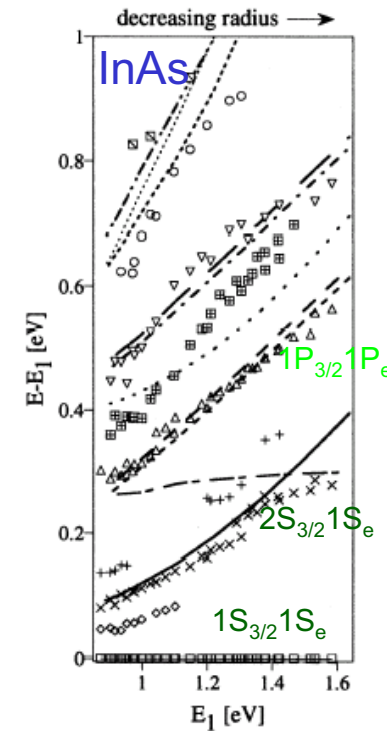
S =spin angular momentum

J good quantum number due to strong spin-orbit coupling

Size Evolution of Electronic States



Low Band gap InAs modeling must also account for valence-conduction band coupling



D. J. Norris, M. G. Bawendi, Phys. Rev. B **53**, 16338 (1996).

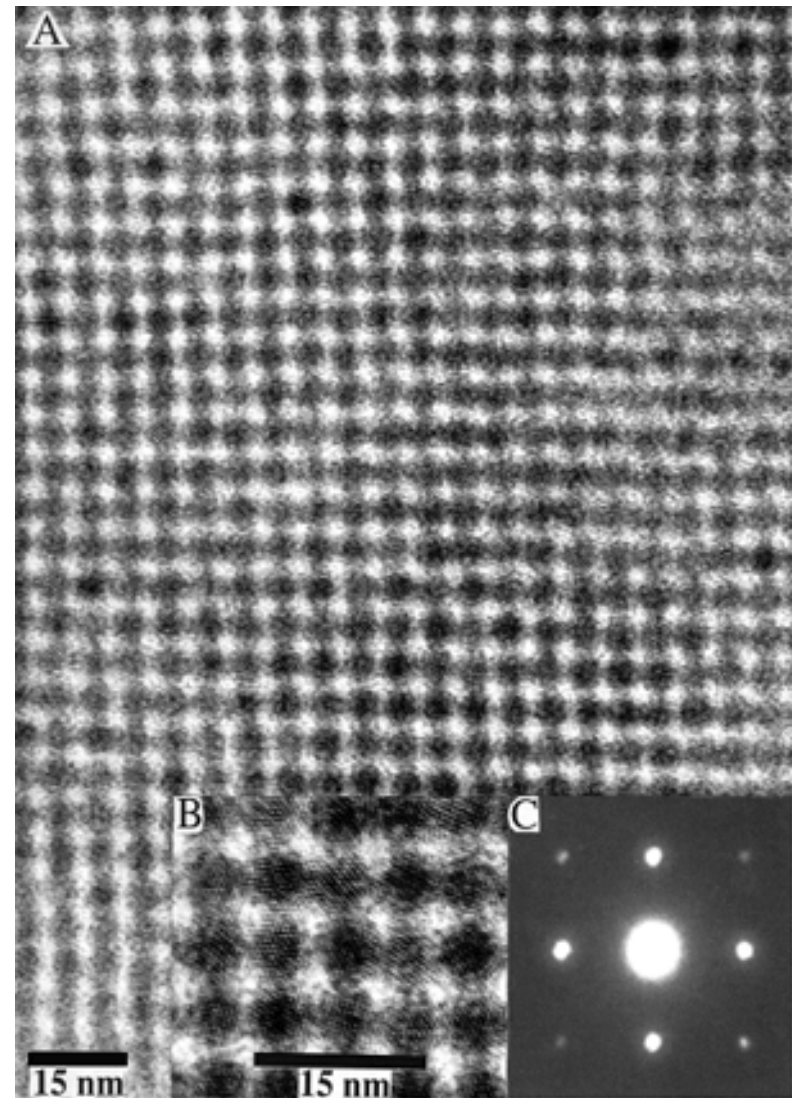
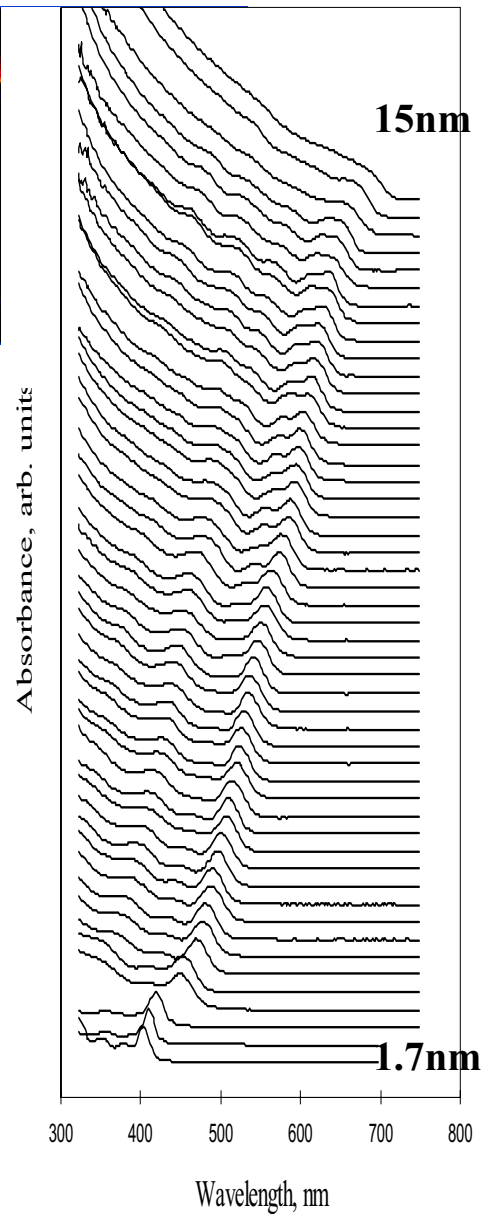
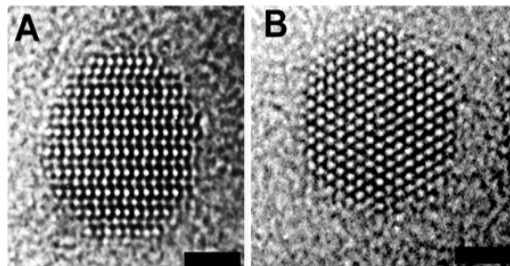
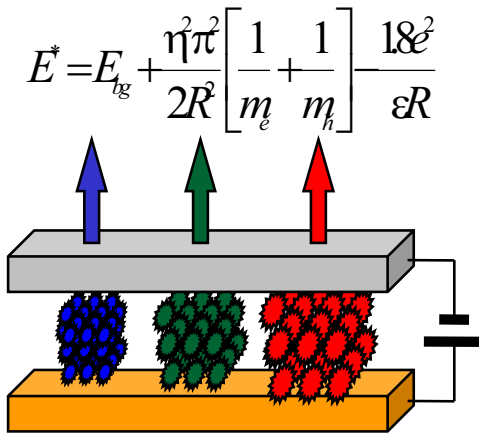
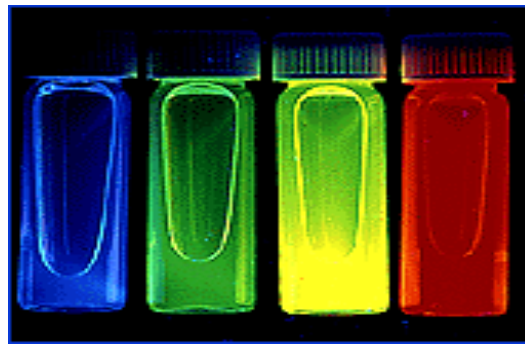
U. Banin et al., J. Chem. Phys. **109**, 2306 (1998).

$F=J+L$ where L =envelope angular momentum
 J =Bloch-band edge angular momentum

Hole states labeled by $n_h L_F$ [$L_F=L + (L+2)$]

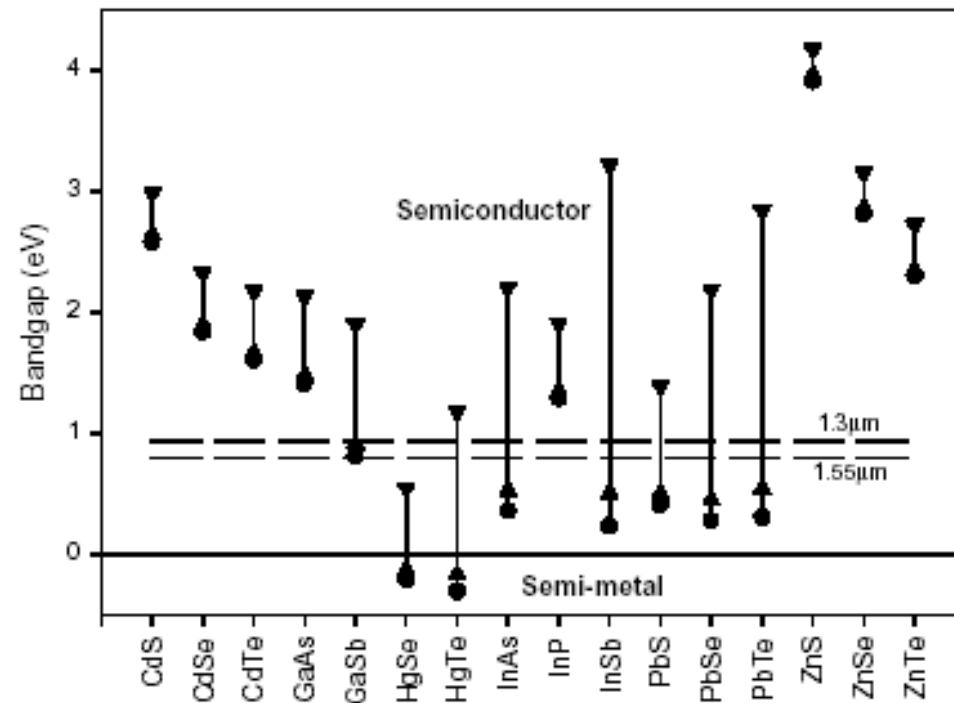
Electron states labeled $n_e L_e$

Colloidal CdSe Nanocrystals (Quantum dots).



5 nm σ <5% CdSe Nanocrystals

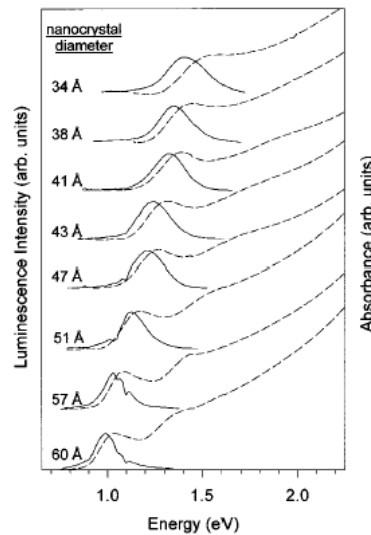
Semiconductor Materials



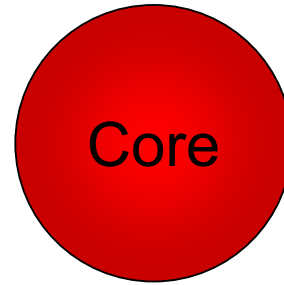
Range from 30 nm QDs to bulk crystal

Graph from H. Weller, Pure Appl. Chem. **72**, 295 (2000).

Absorption Spectra of Semiconductor Nanocrystals

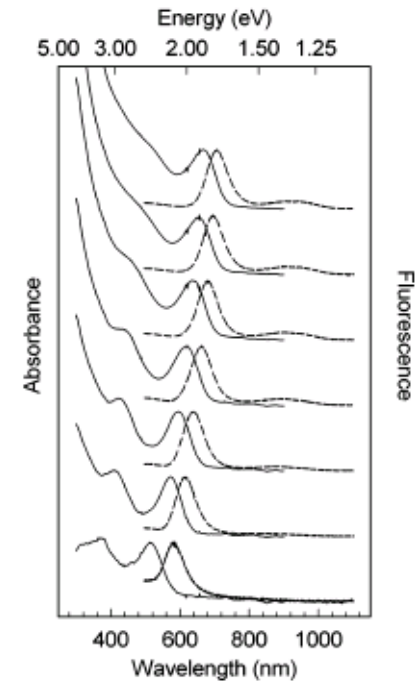


Changing the Core

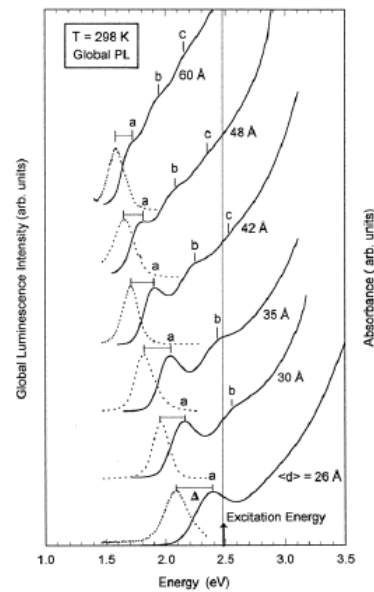


← InAs

HgS →



A. P. Alivisatos, UC Berkeley

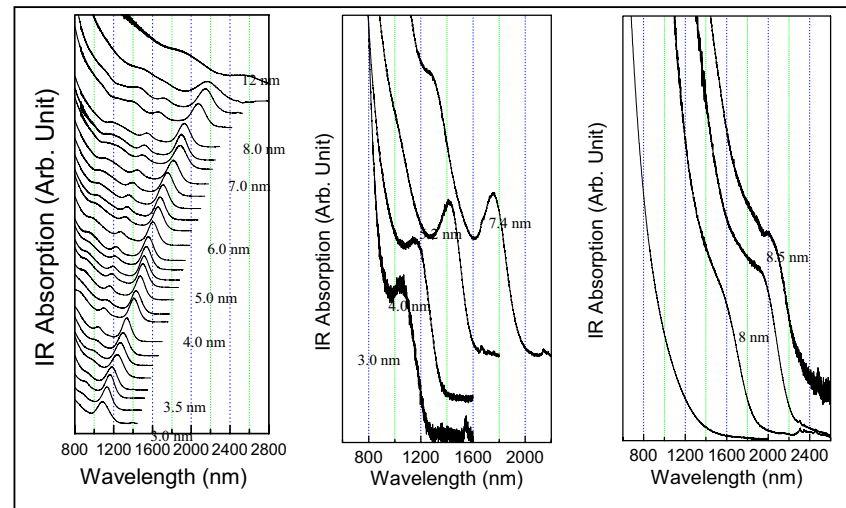


← InP

PbSe

PbS

PbTe

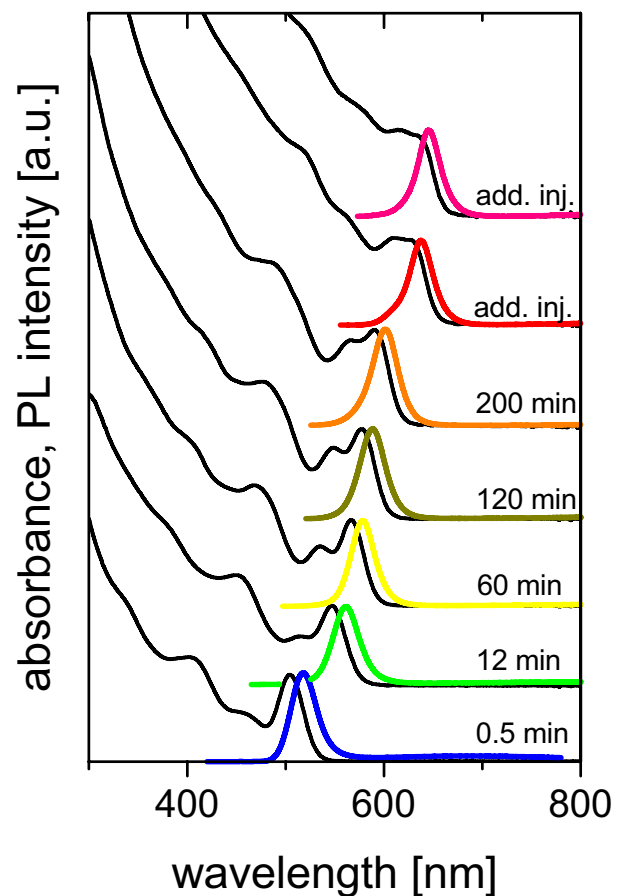
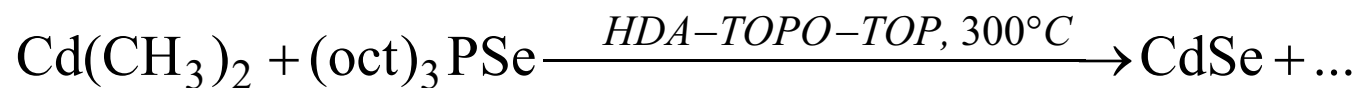


O. Micic, A. Nozik, NREL

C. B. Murray, IBM

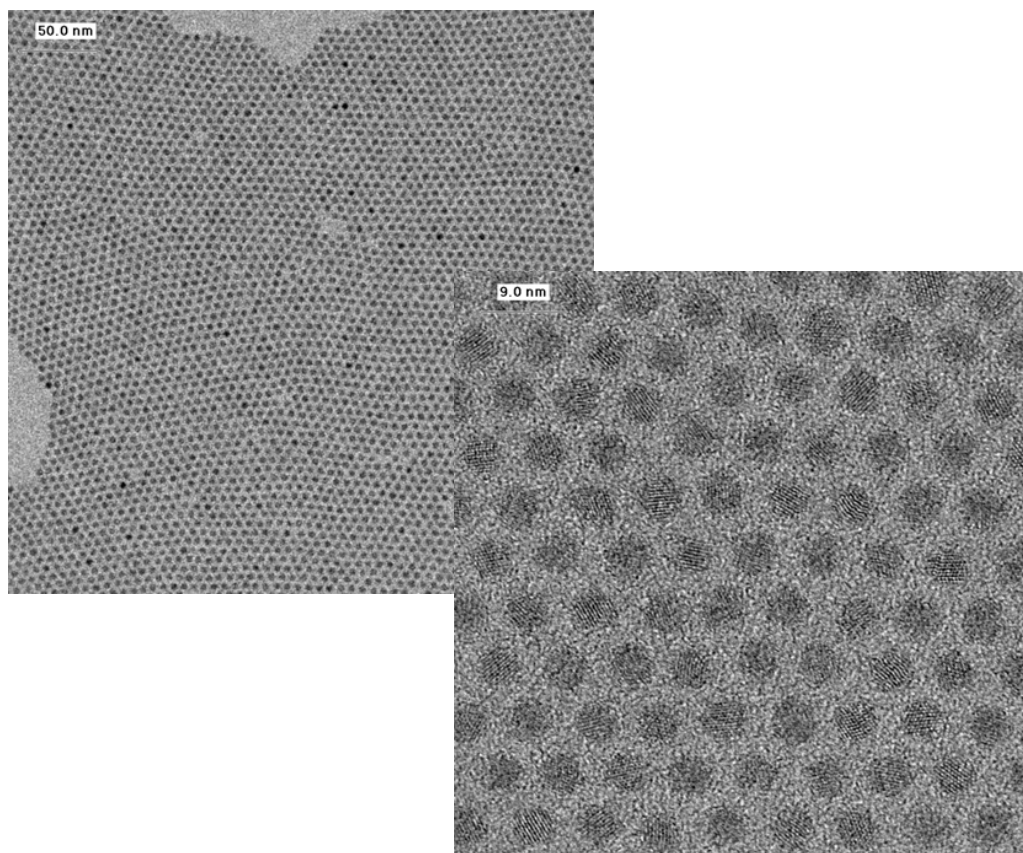
NRL group

Synthesis of monodisperse CdSe nanocrystals

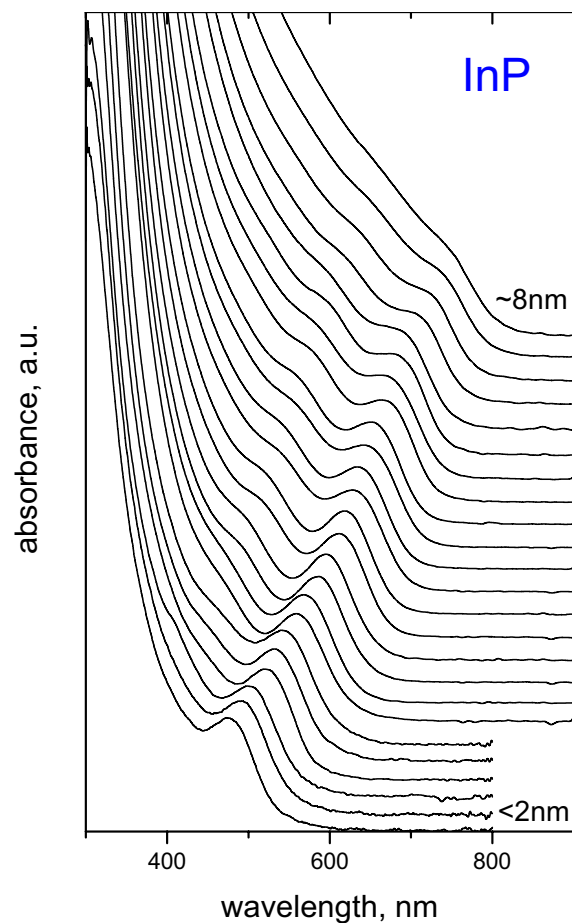
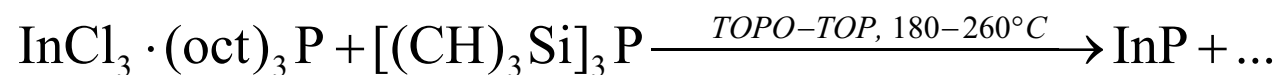


UV-Vis and PL spectra of CdSe nanocrystals in growth at 300°C

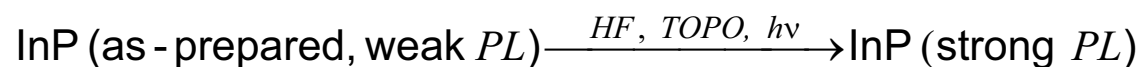
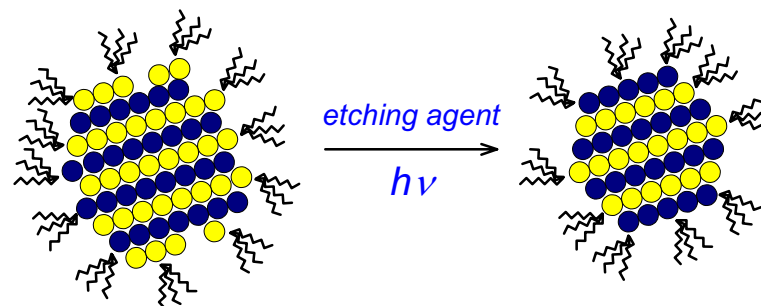
TEM and HRTEM images of as-prepared CdSe nanocrystals.



III-V semiconductor nanocrystals : InP



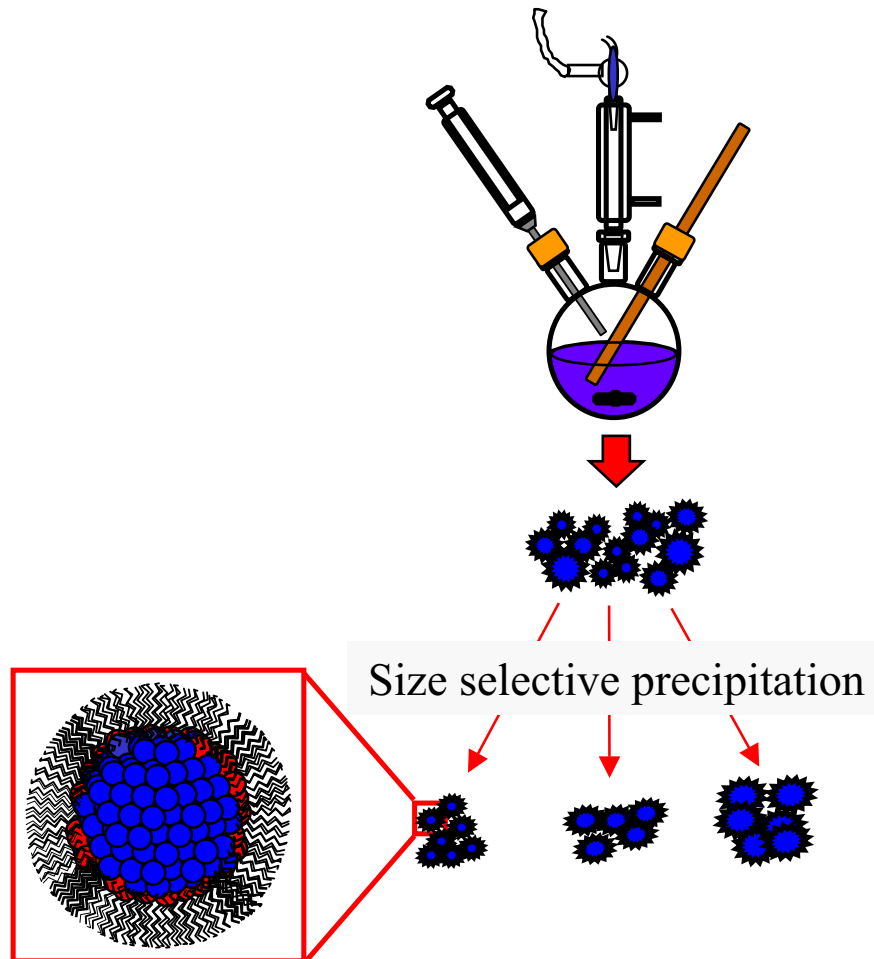
Size-dependent evolution of absorption spectra of InP colloidal quantum dots



PL quantum efficiency ~25-40%

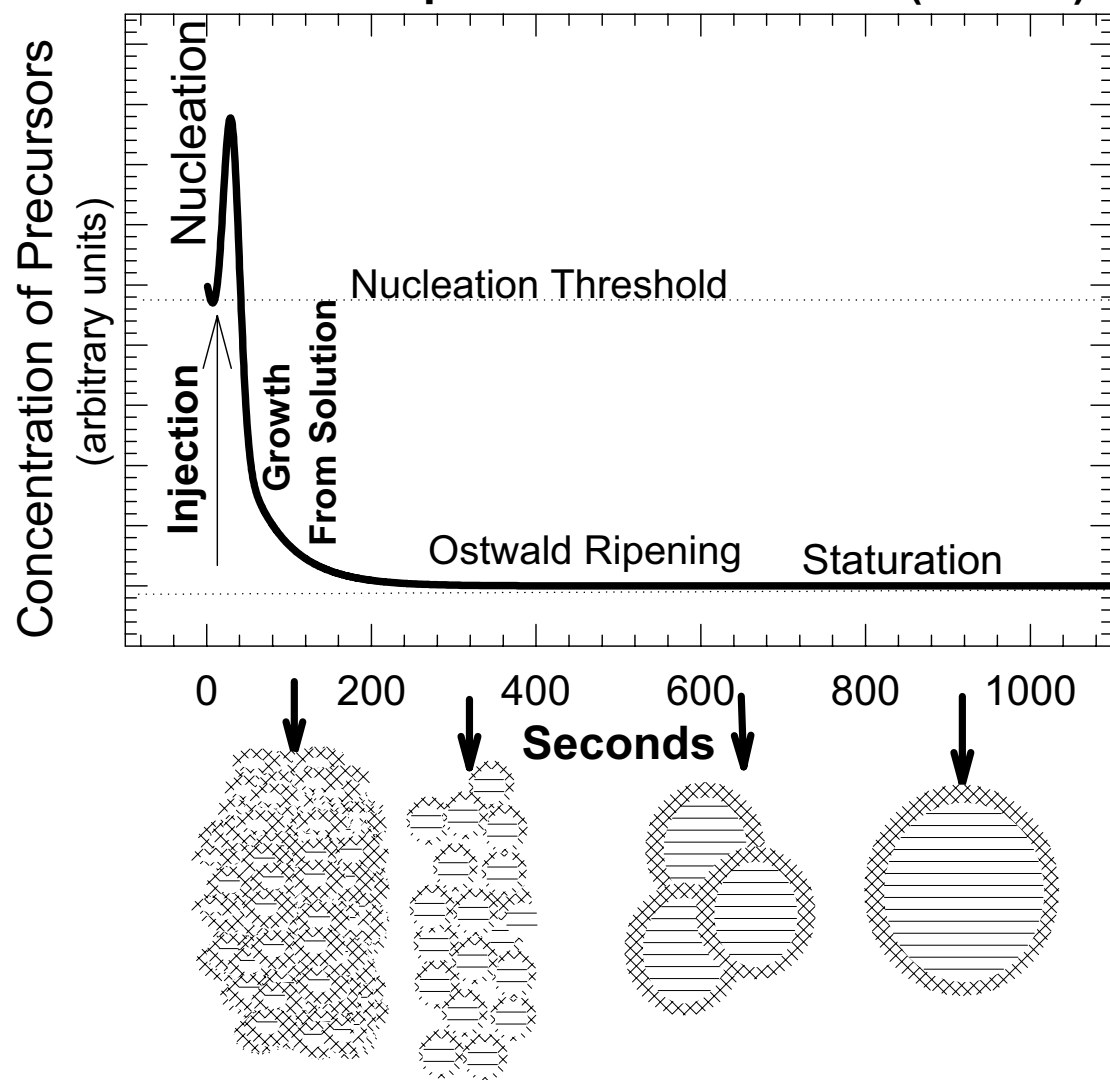
Synthesis and Characterization of Monodisperse Nanoparticles

C. B. Murray IBM

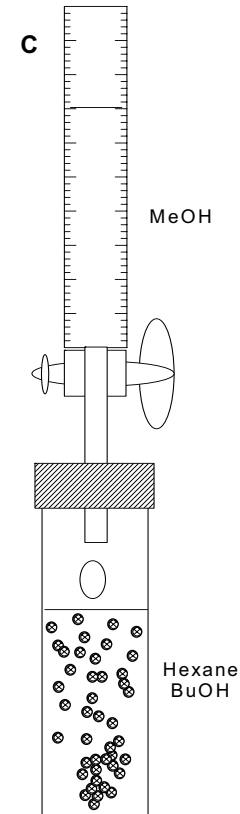
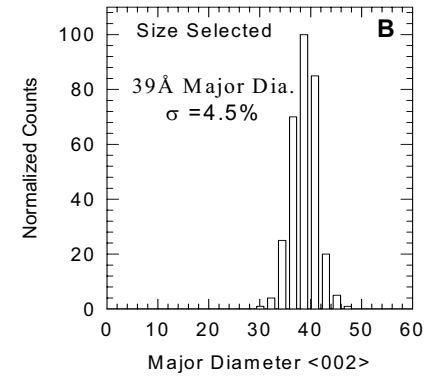
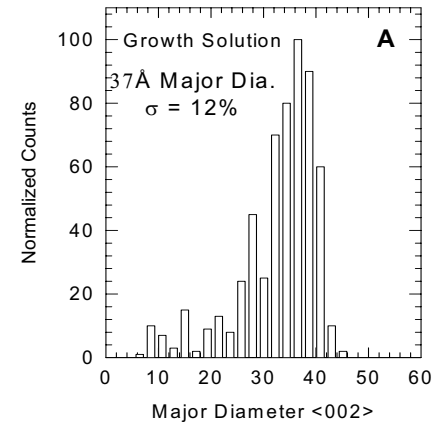
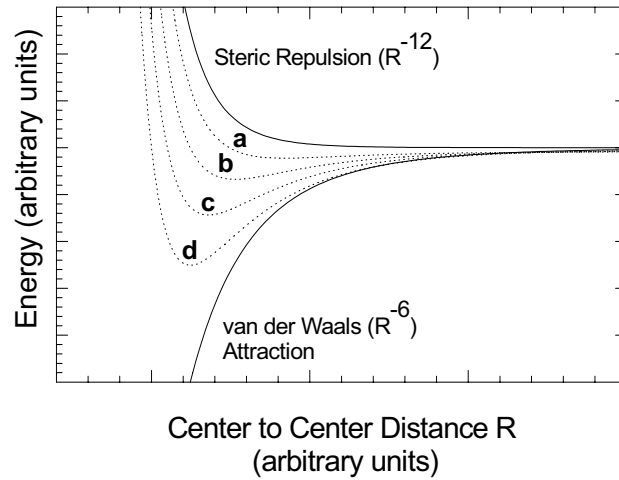
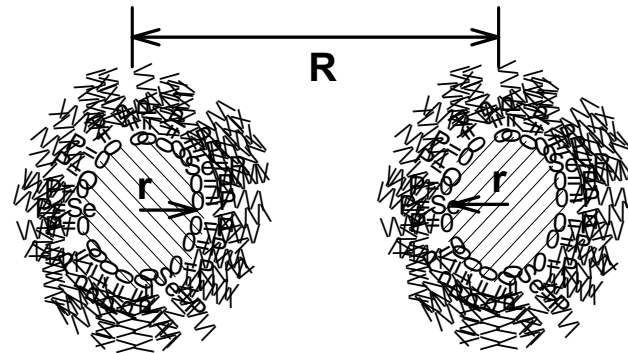


A

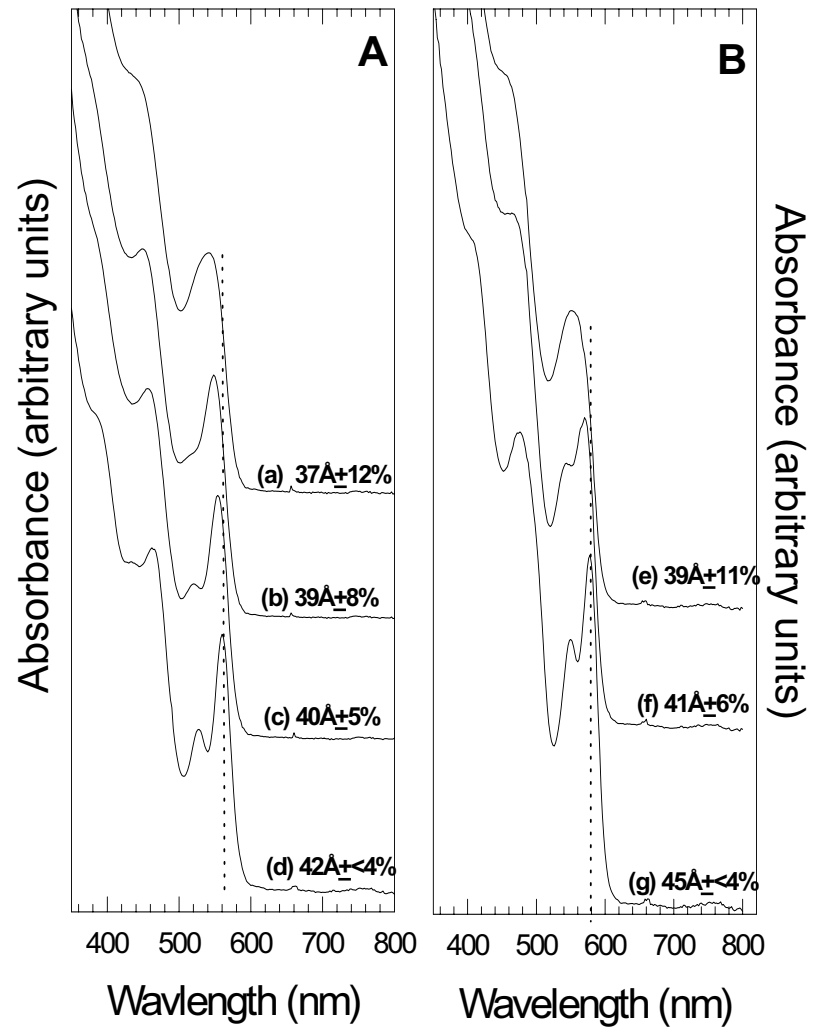
Monodisperse Colloid Growth (La Mer)



Size selective processing:



Results of size selected Percipitation



Organometallic synthesis of the II-VI Semiconductor Nanocrystals

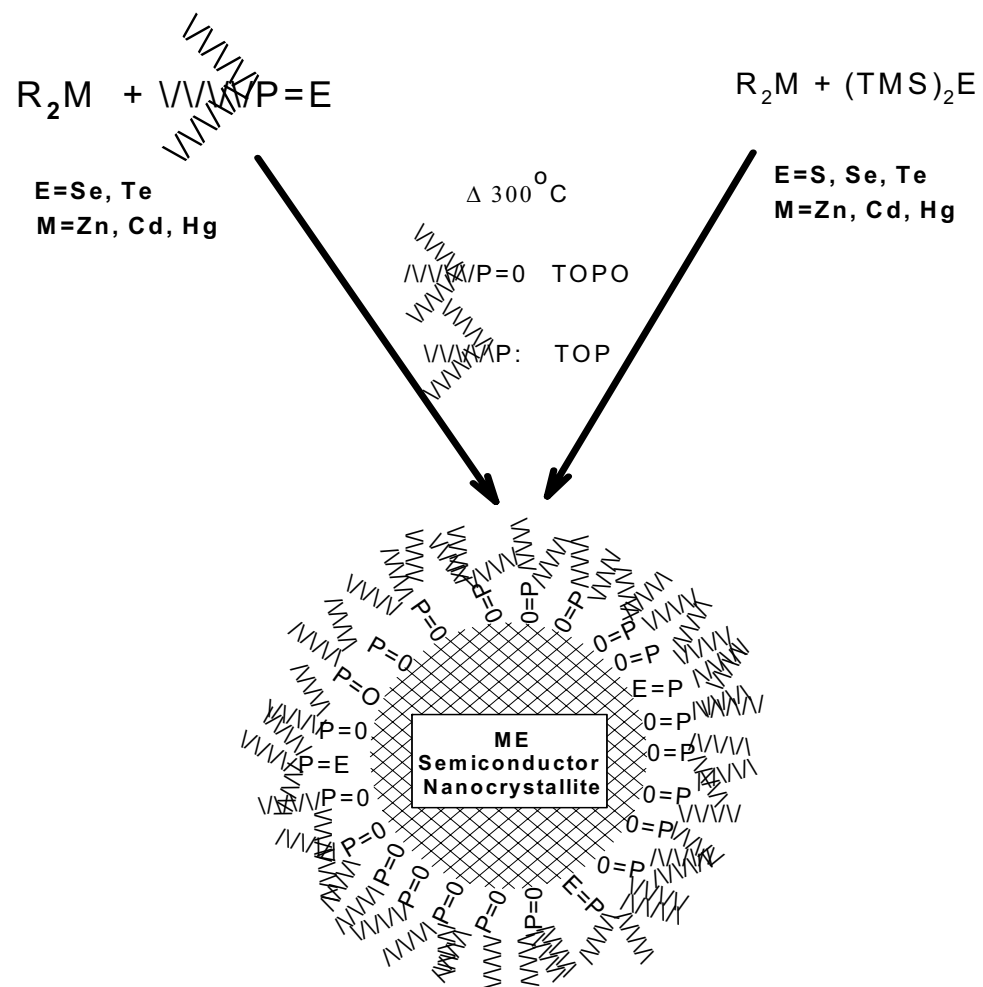
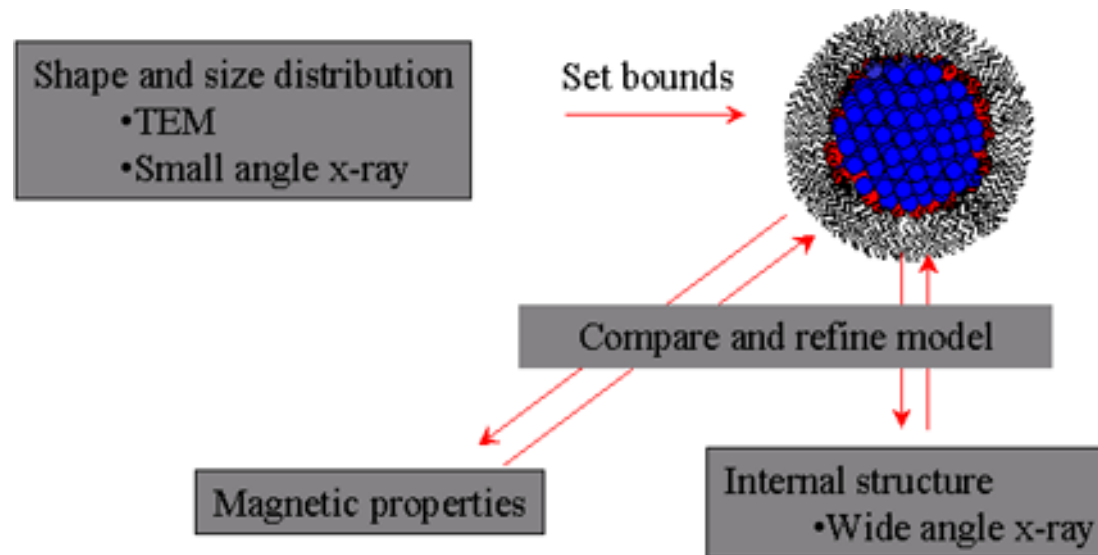


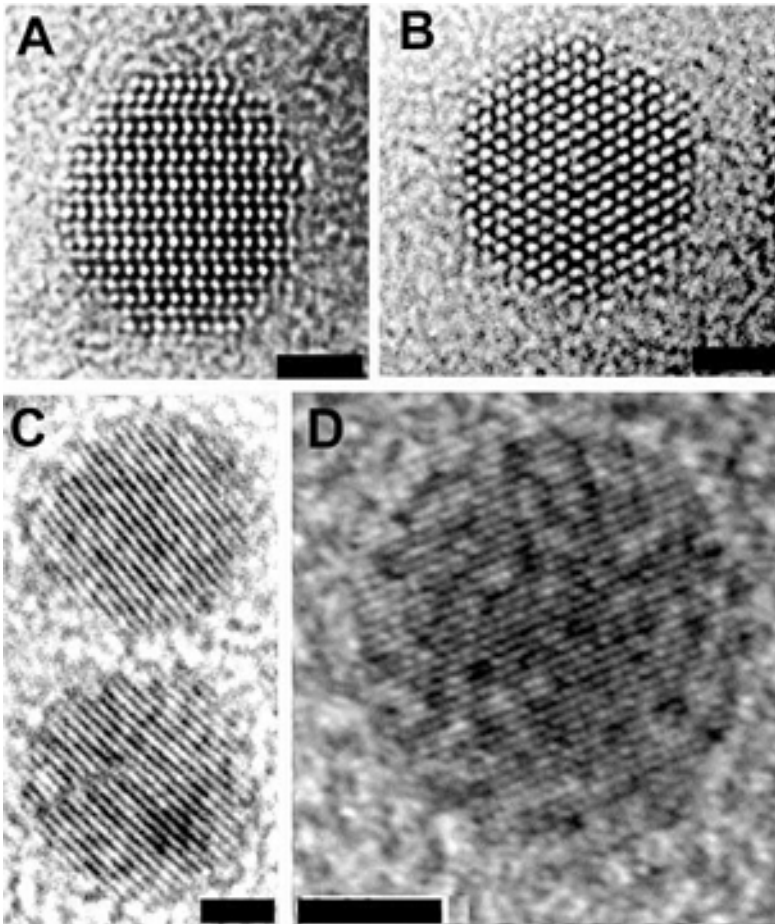
FIG. 2.1 Cartoon of the reaction scheme for the production of monodisperse II-VI nanocrystallites by rapid pyrolysis in coordinating solvents.

Atomistic approach to structural characterization

- Nanoparticles are measured using a wide variety of techniques
- Standard approach
 - Specific modeling for each measurement.
 - Difficult to produce single unified model.
- Atomistic approach
 - Model of nanoparticle built up atom-by-atom.
 - Single model used for each technique.
 - Self-consistent, systematic and extensible methodology.



High Resolution TEM Images reveal internal lattice.

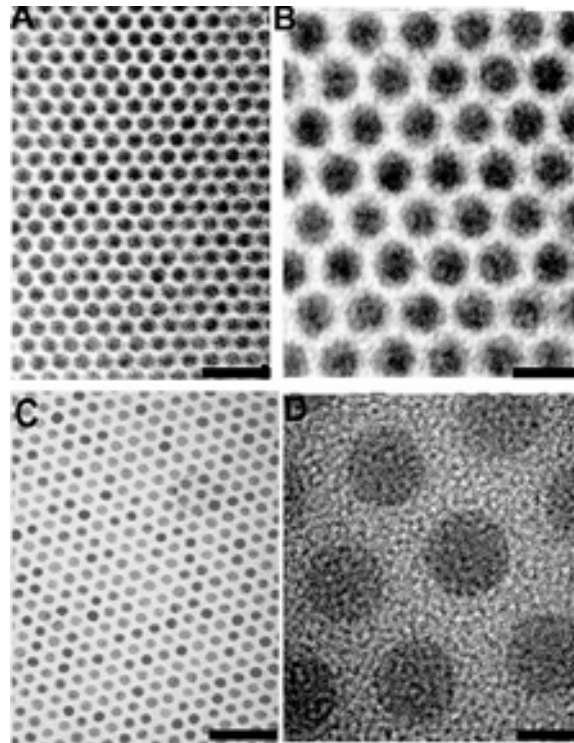


A & B CdSe

C CdTe

D Cobalt

Low Mag TEM allows determination
of average size and shape:



CdSe

Cobalt

Modeling of x-ray diffraction:

The Debye equation which is valid in the kinematical approximation is shown in equation 4.6 ⁽⁸⁾.

$$I(q) = I_0 \sum_m \sum_n F_m F_n \frac{\sin(qr_{m,n})}{qr_{m,n}}$$

(4.6)

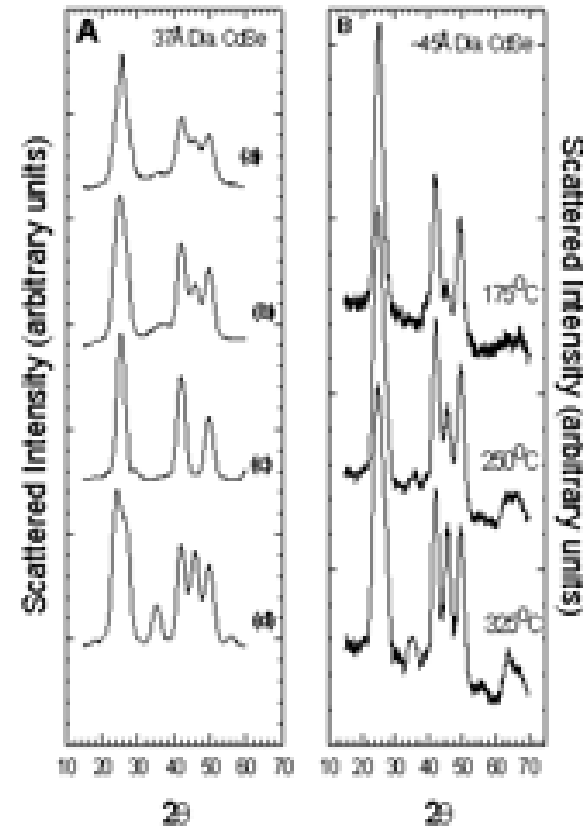
Where $I(q)$ is the scattered intensity, I_0 is the incident intensity, q is the scattering parameter [$q = 4\pi\sin(\theta)/\lambda$] for X-rays of wavelength λ diffracted through angle θ .

The distance between atoms m and n is r_{mn} . A discrete form of the Debye is shown in equation (4.7) ⁽⁹⁾.

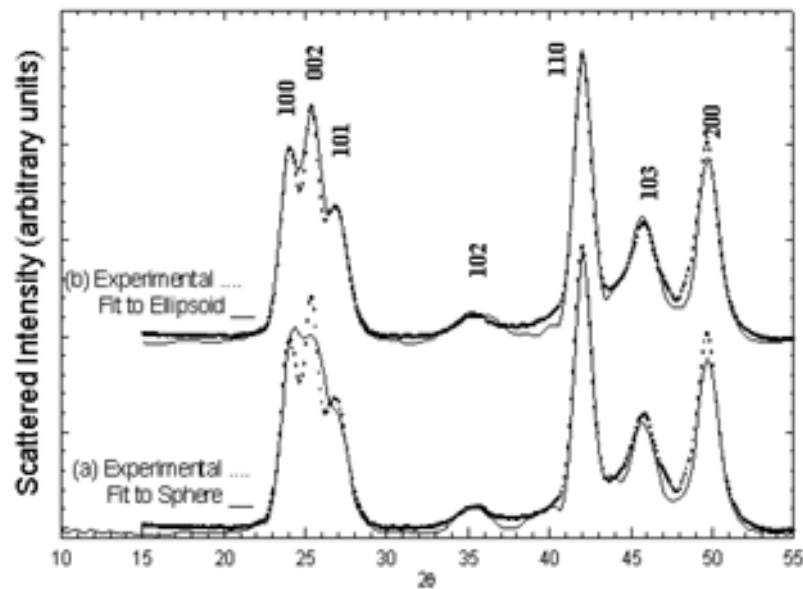
(4.7)

$$I(q) = I_0 \frac{f^2(q)}{q} \sum_k \frac{\rho(r_k)}{r_k} \sin(qr)$$

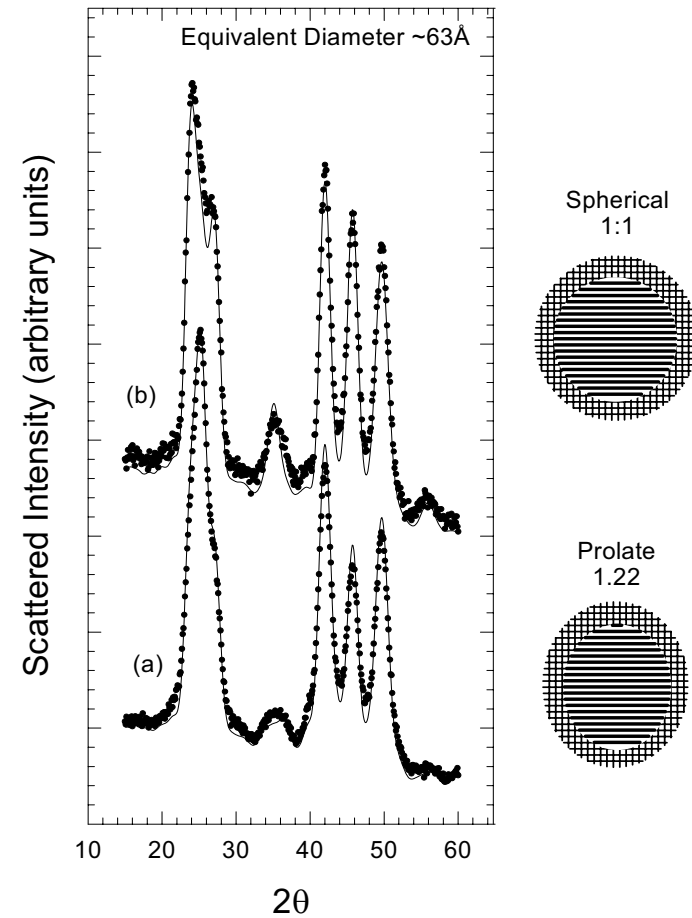
where I_0 is the incident intensity, $f(q)$ is the angle dependent scattering factor, q is the scattering parameter [$4\pi\sin(\theta)/\lambda$] for X-rays of wavelength λ diffracted through angle θ . The sum is over all inter atomic distances, and $\rho(r_k)$ is the number of times a given interatomic distance r_k occurs. Since the number of discrete interatomic distances in an ordered structure grows much more slowly than the total number of distances, using the discrete form of the equation is significantly more efficient in the simulation of large crystallites ⁽⁹⁾.



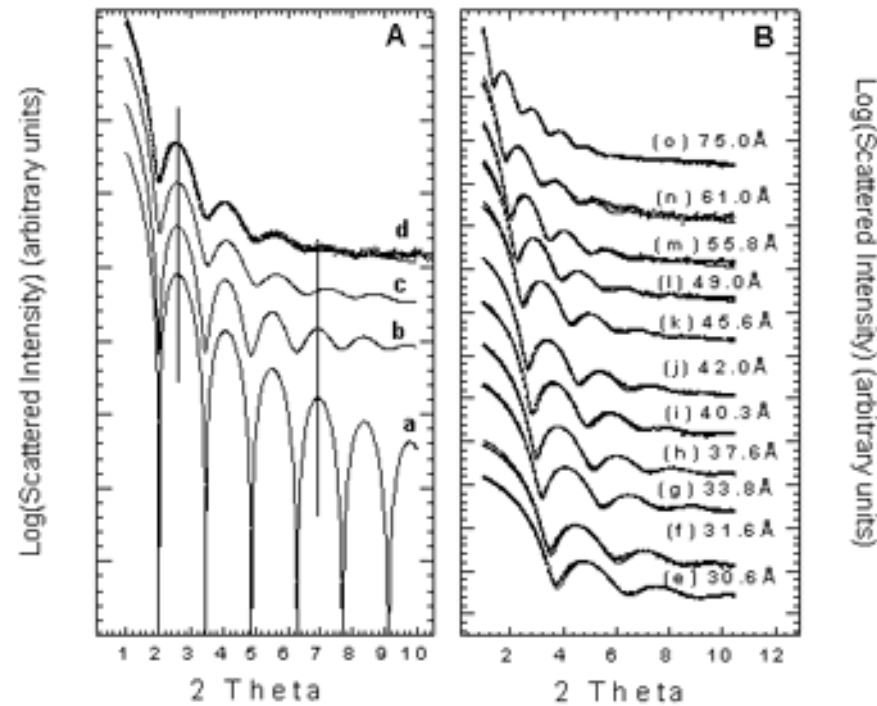
Modeling Stacking faults



Modeling NP Shape



Small angle X-ray Scattering SAXS



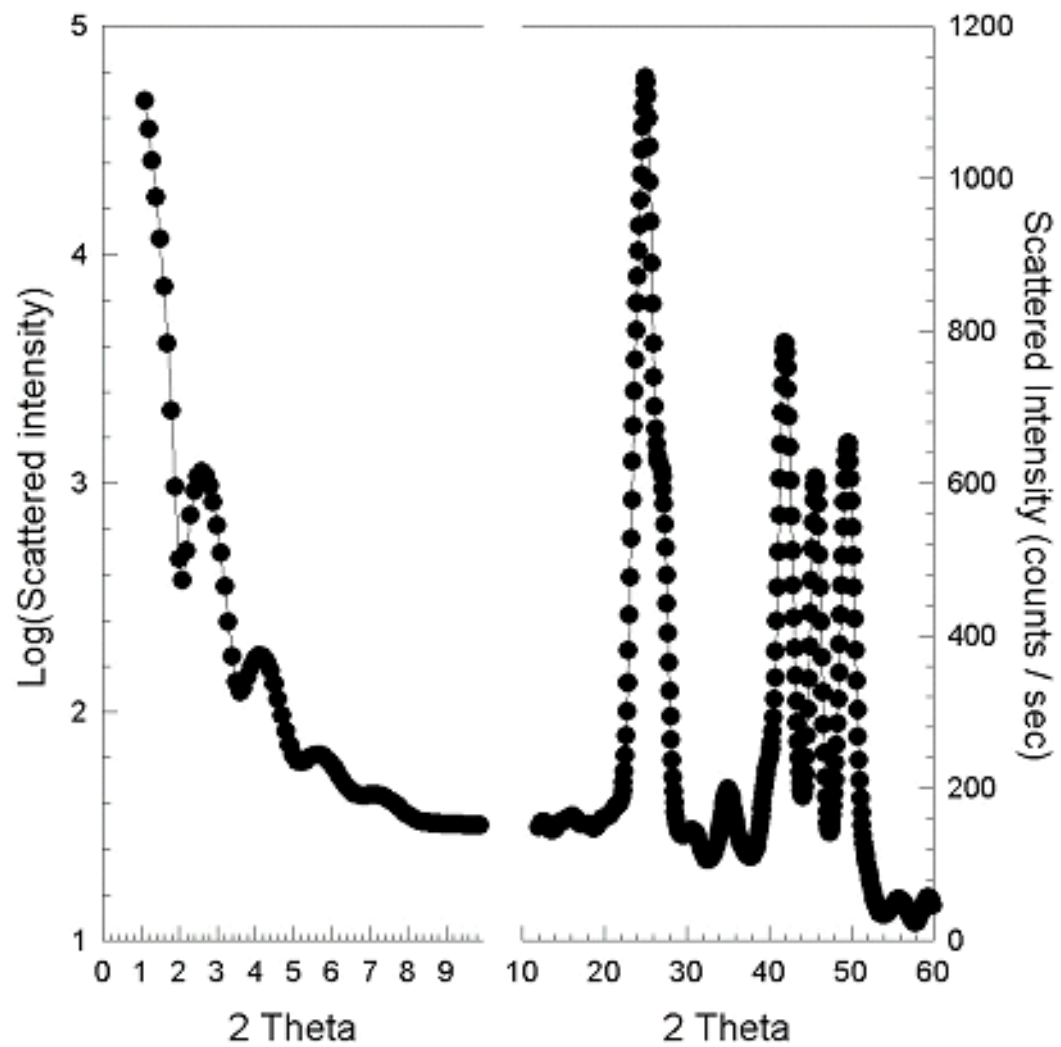
$$(4.8) \quad I(q) = I_0 N [(\rho - \rho_o)^2 \frac{4}{3} \pi R^3 [3 \frac{\sin(qR) - qR \cos(qR)}{(qR)^3}]]^2$$

Where ρ and ρ_o are the electron density of the particle and the dispersing medium respectively. I_0 is the incident intensity and N is the number of particles. $F(q)$ is the material form factor (the fourier transform of the shape of the scattering object) and is the origin of the oscillations observed. Thus for a spherical particle of radius R

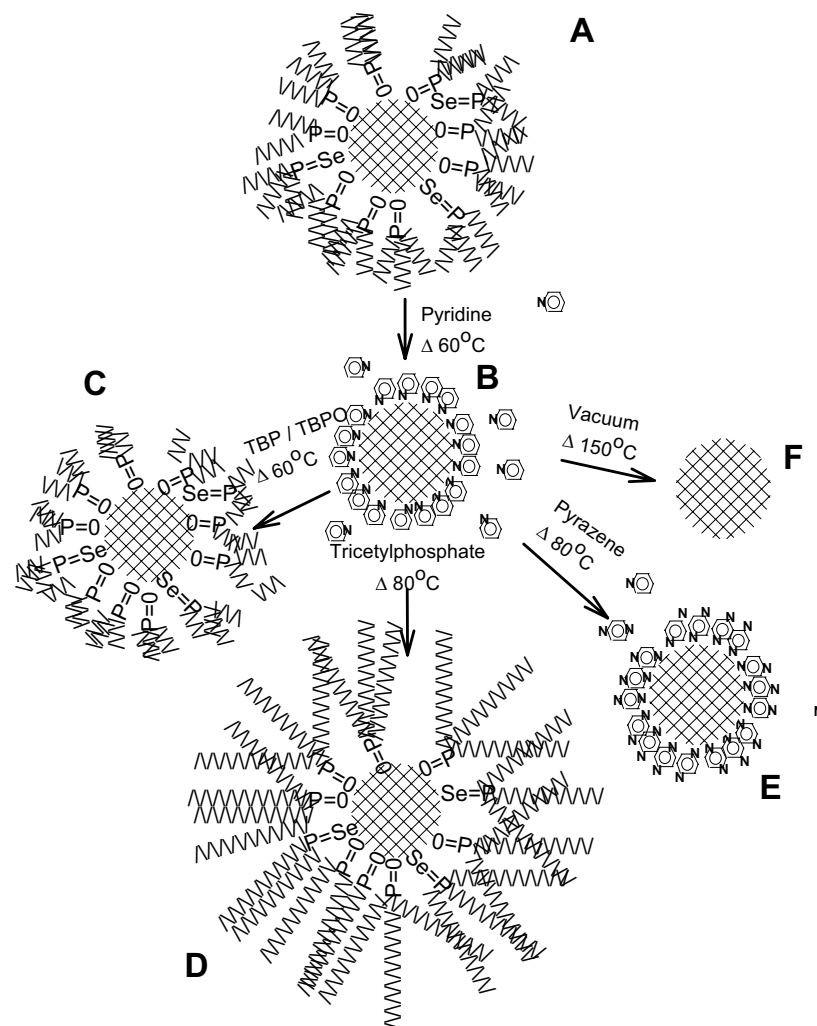
$$(4.9) \quad I(q) = I_0 N (\rho - \rho_o)^2 F^2(q)$$

$$(4.10) \quad F(q) = \frac{4}{3} \pi R^3 [3 \frac{\sin(qR) - qR \cos(qR)}{(qR)^3}]$$

Combined SAXS and WAXS Modeling.

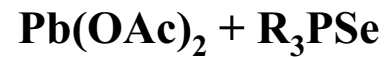
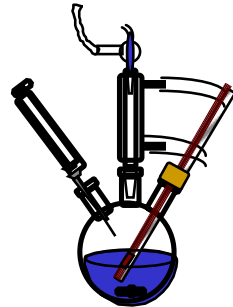


Cap exchange to modify surface:



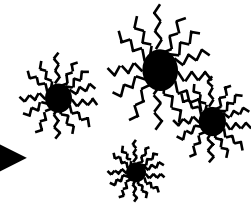
Wet Chemical Synthesis of PbSe Nanocrystals and Superlattices

Synthesis



oleic acid,

R_3P , $T=150\text{ C}$

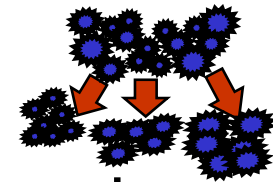


PbSe

R= octyl

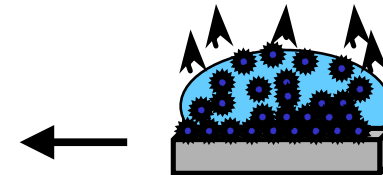
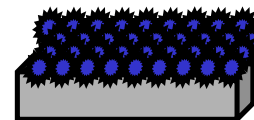
Size Selective Processing

Size selective precipitation in solvent/ non solvent pairs like hexane-methanol

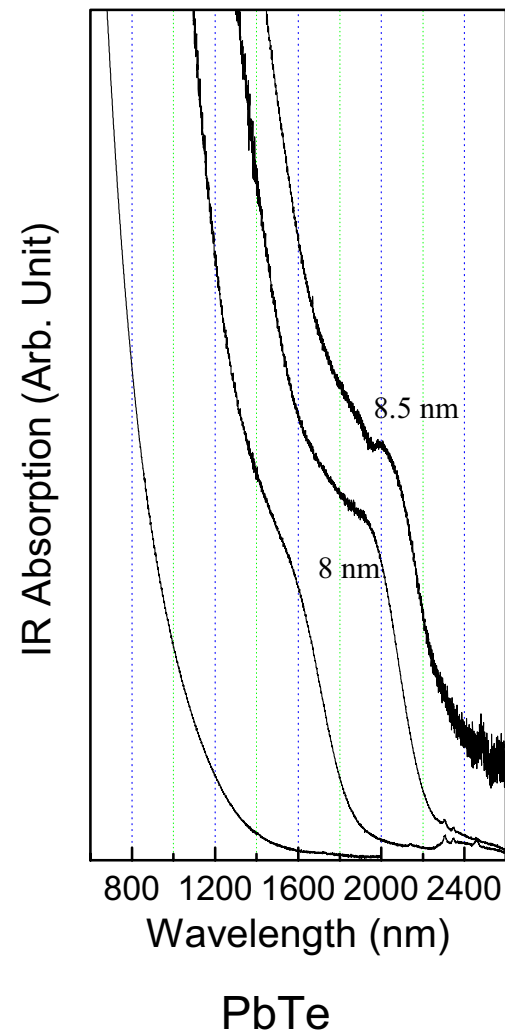
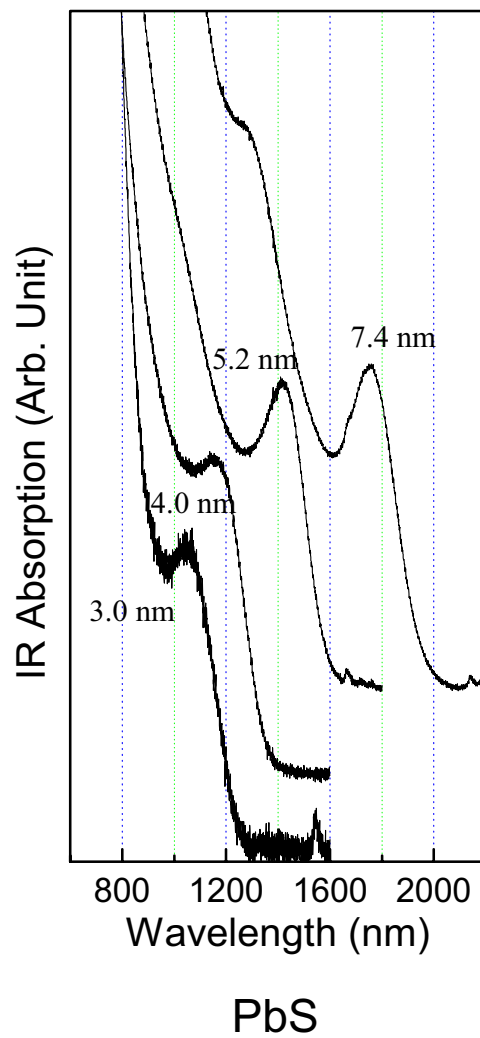
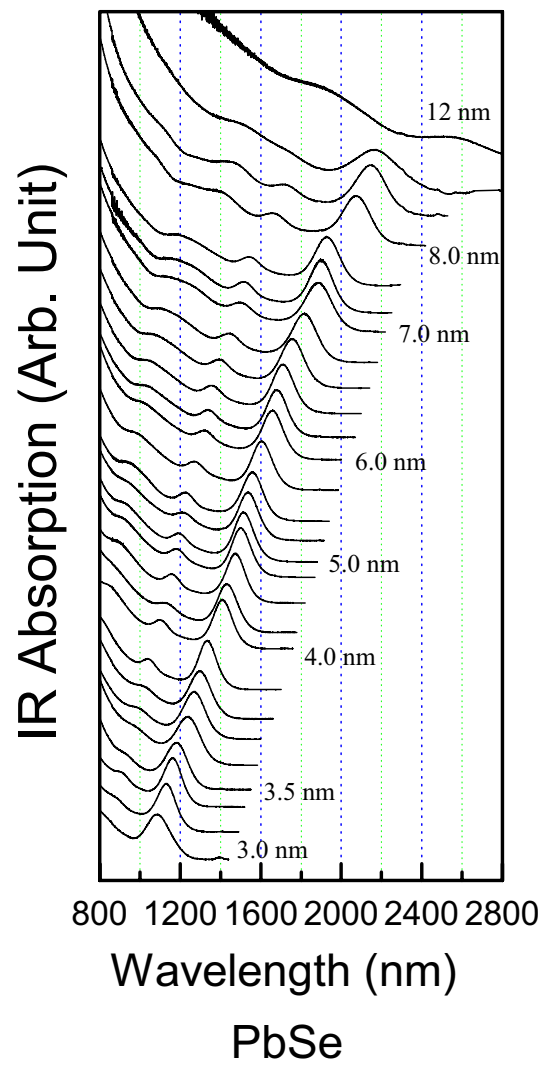


Self Assembly

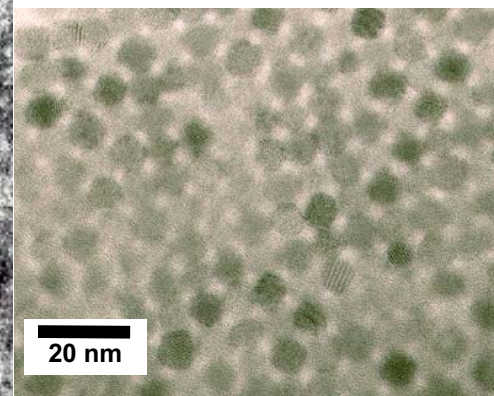
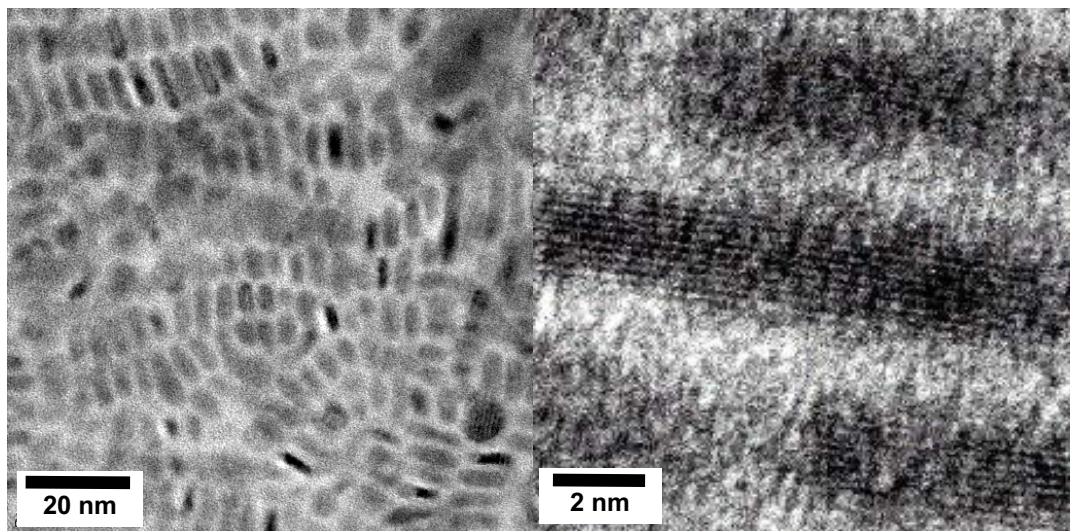
Evaporation of the solvent



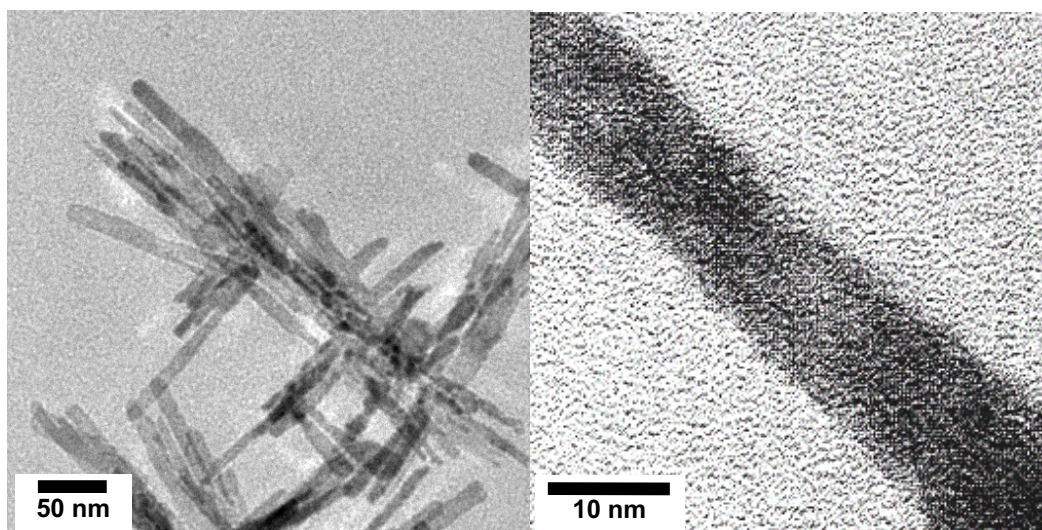
IR Absorption of Lead Chalcogenides NCs



PbTe, PbS Nanocrystal and Nanorod

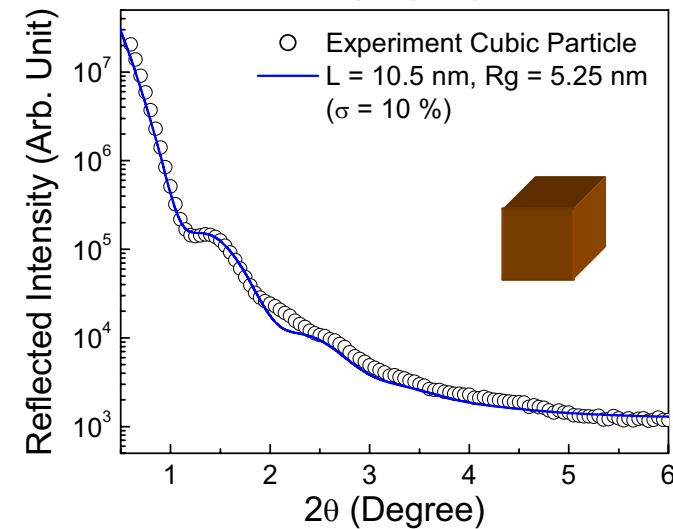
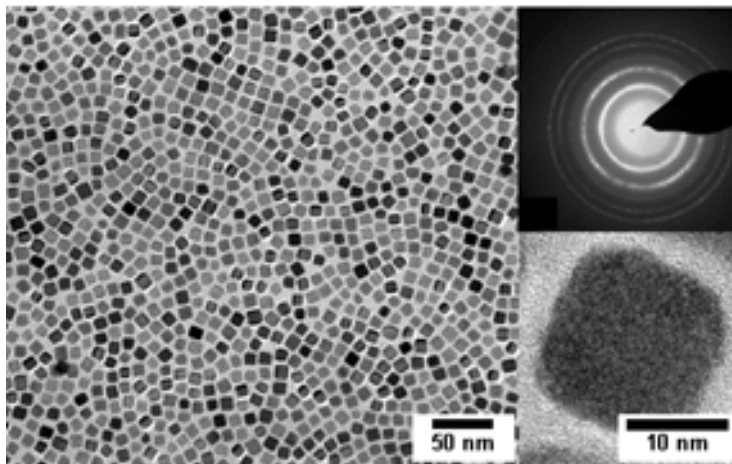
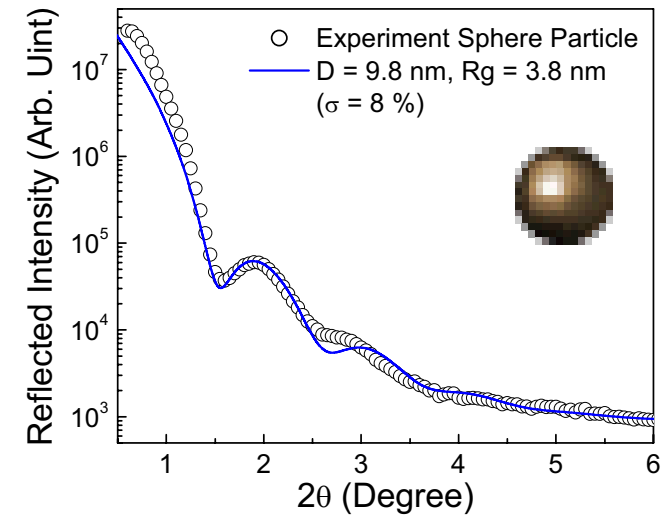
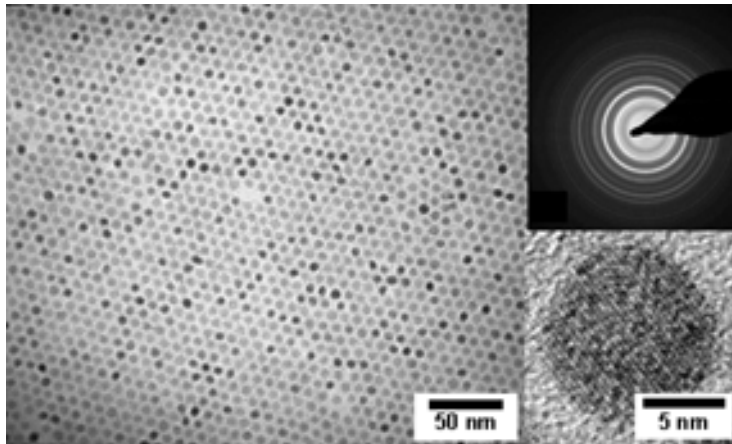


PbTe forms rod-shape nanoparticles in the early – stage of synthesis

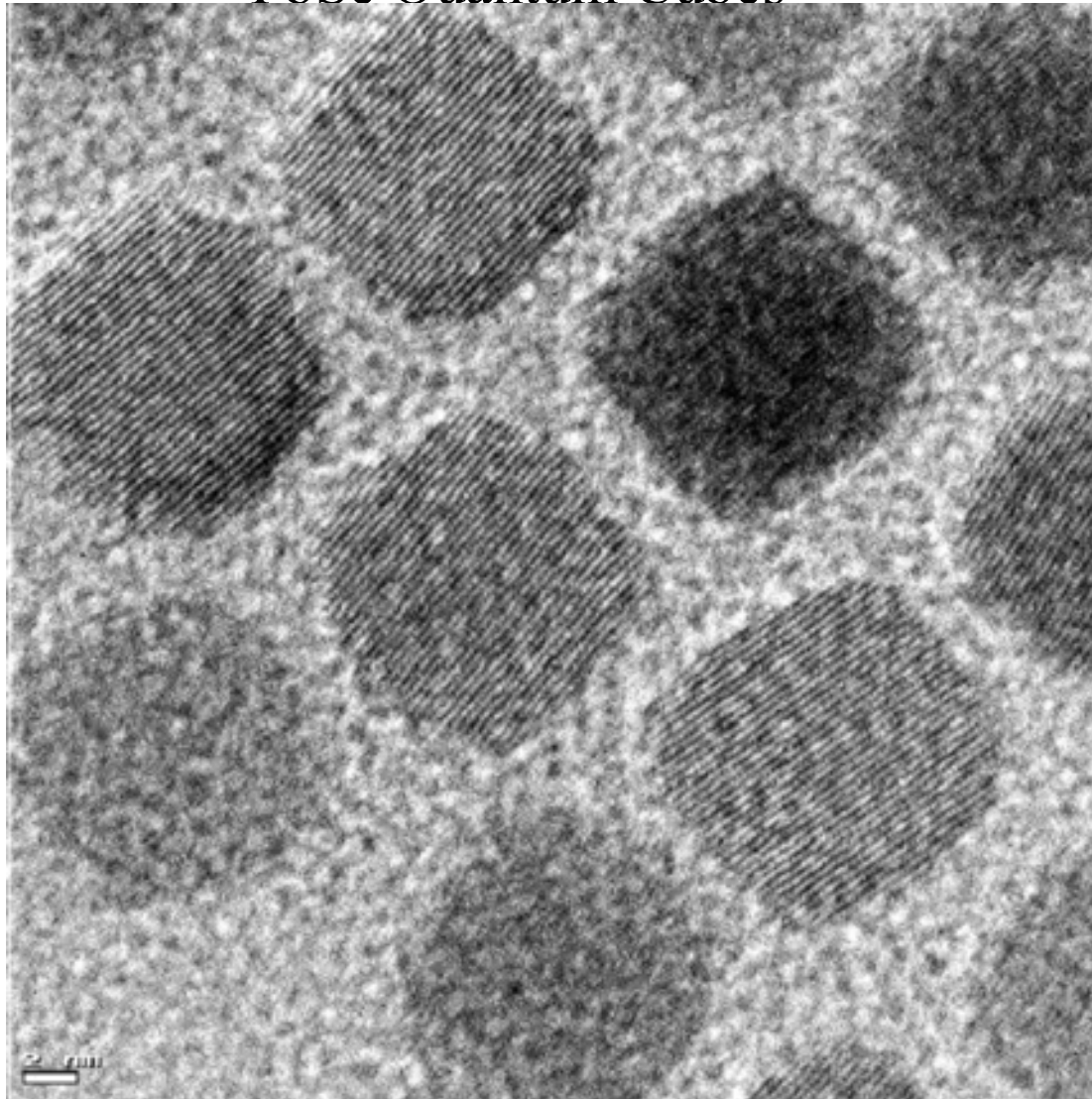


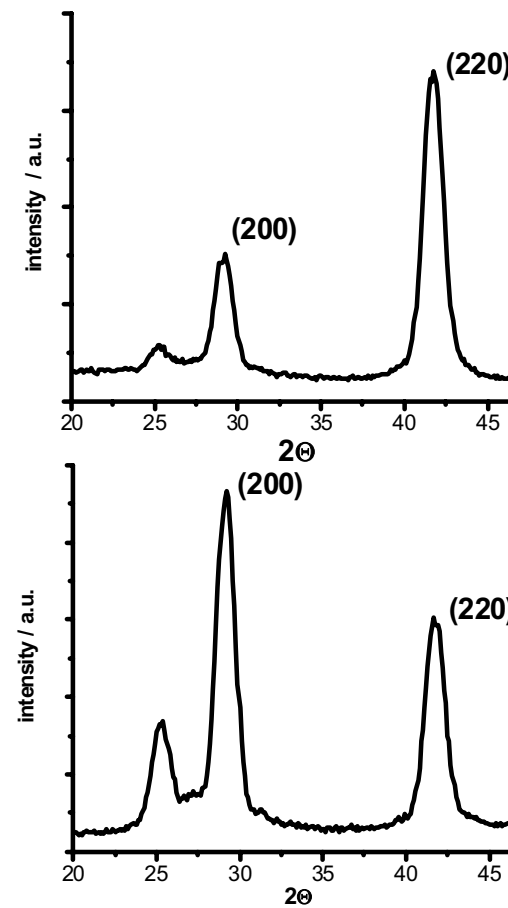
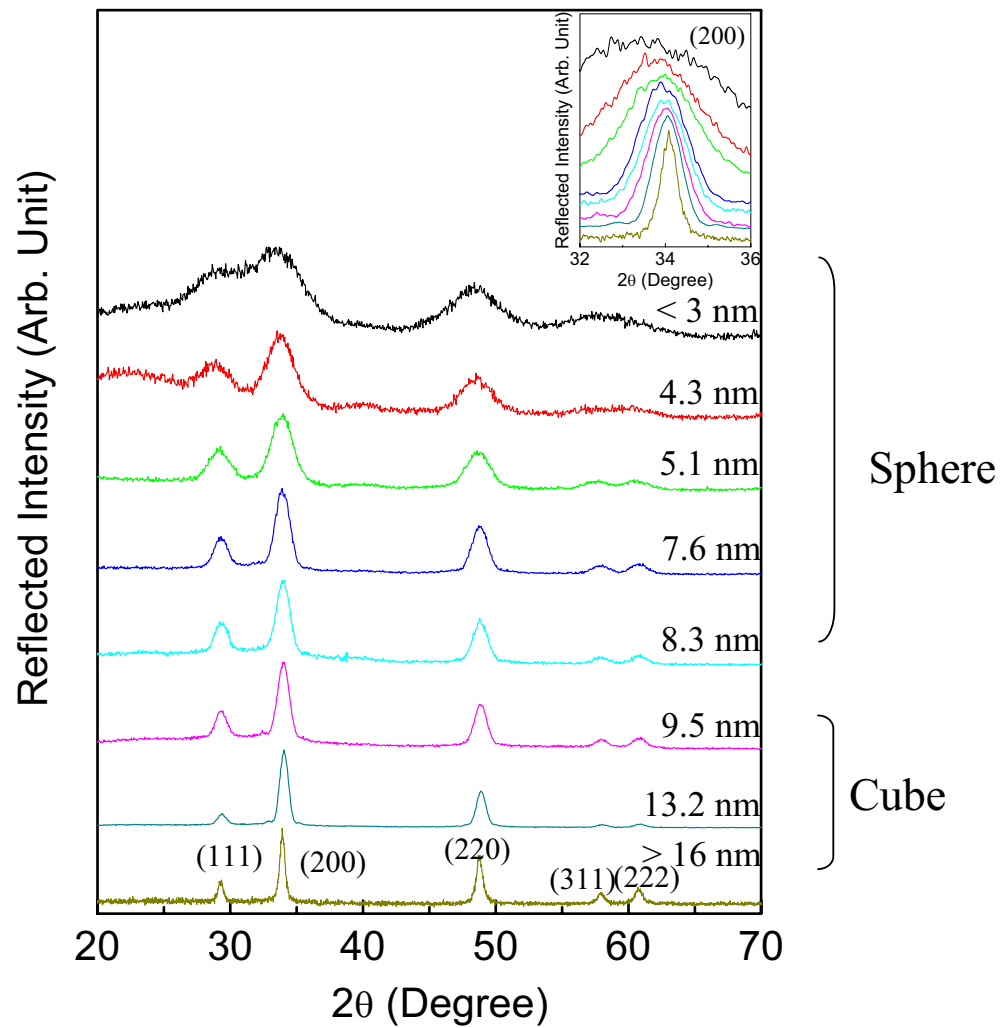
PbS nanorods are more Continuous and single-crystalline

Shape Change from Sphere to Cubic and SAXS in Polymer Matrix



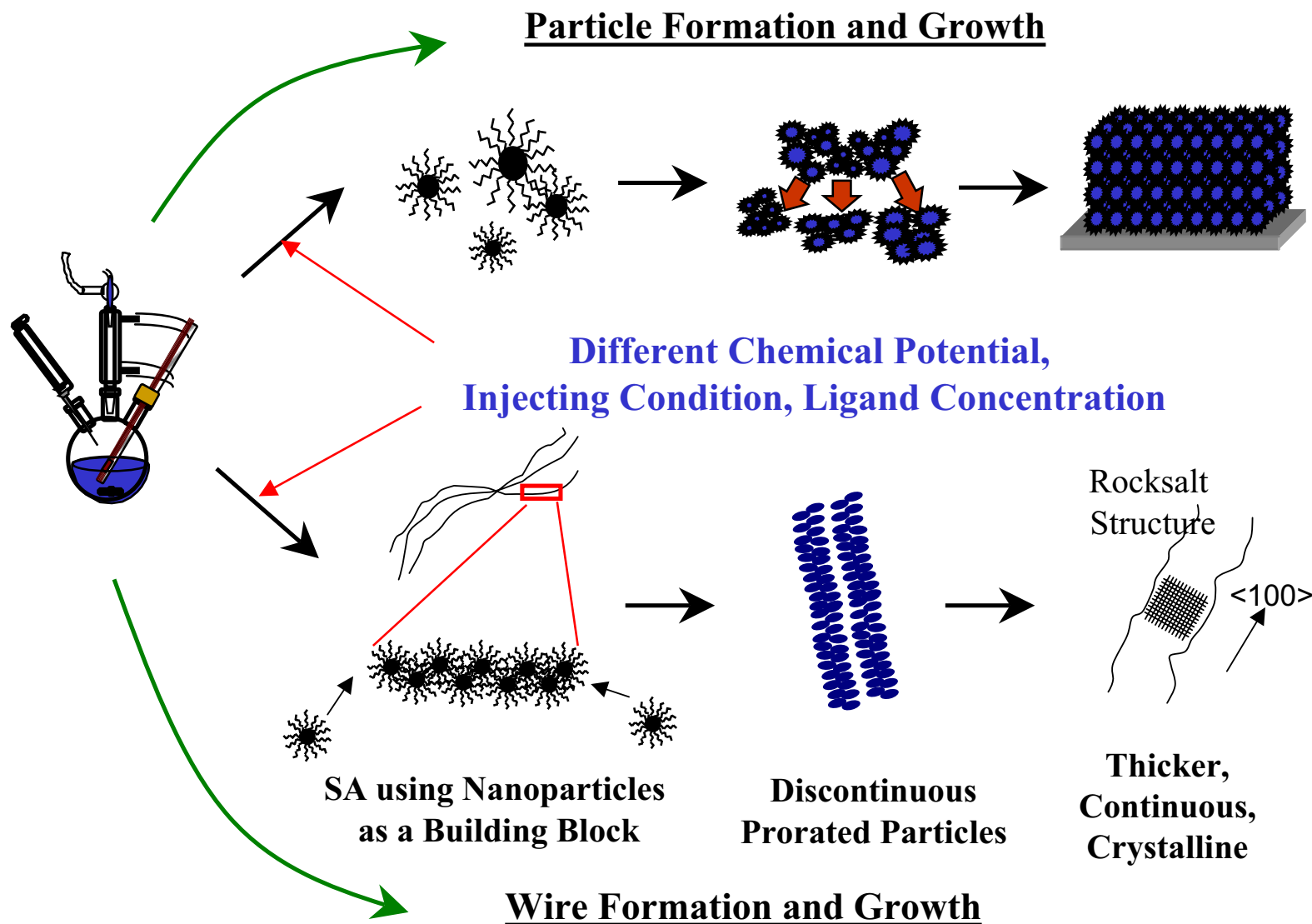
PbSe Quantum Cubes





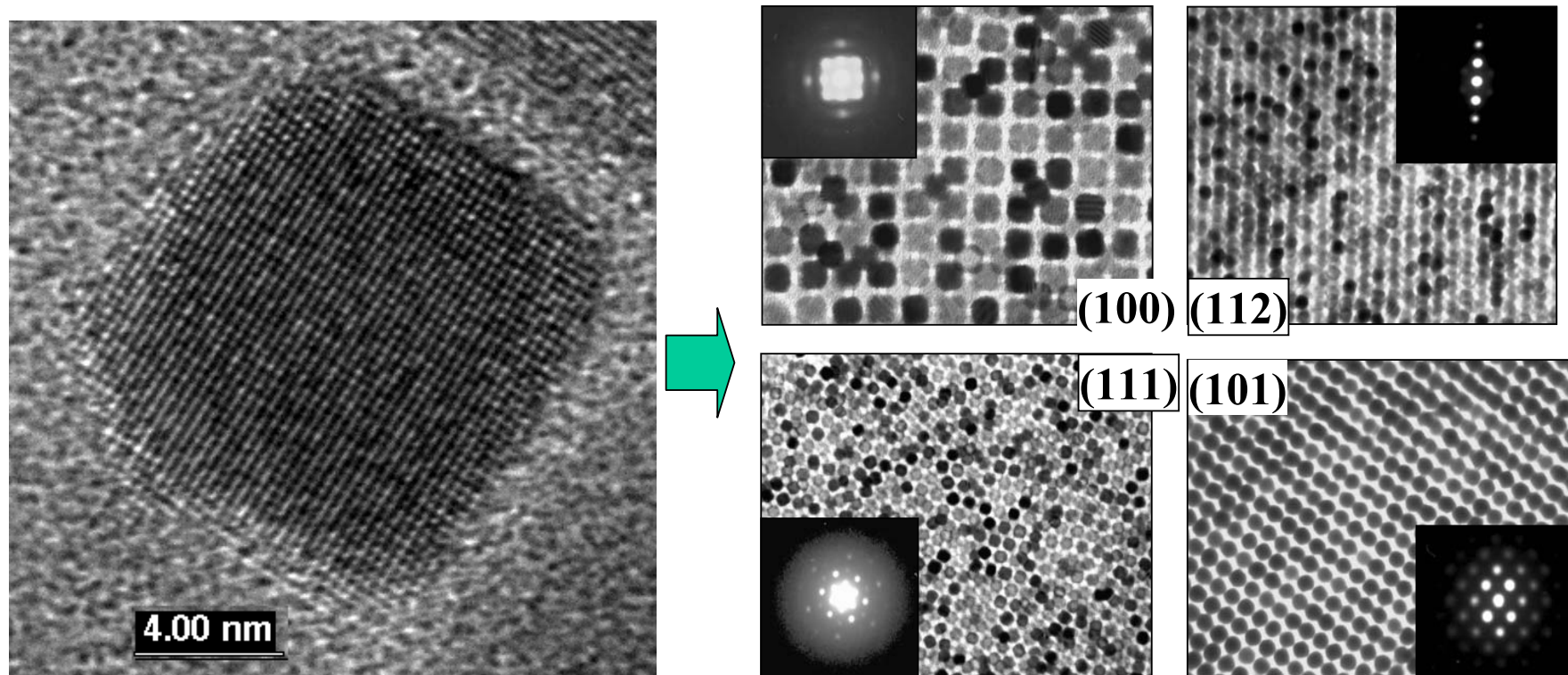
WAXS of 10 nm PbSe quantum cubes slowly deposited from toluene (top) and rapidly precipitated from methanol (bottom)

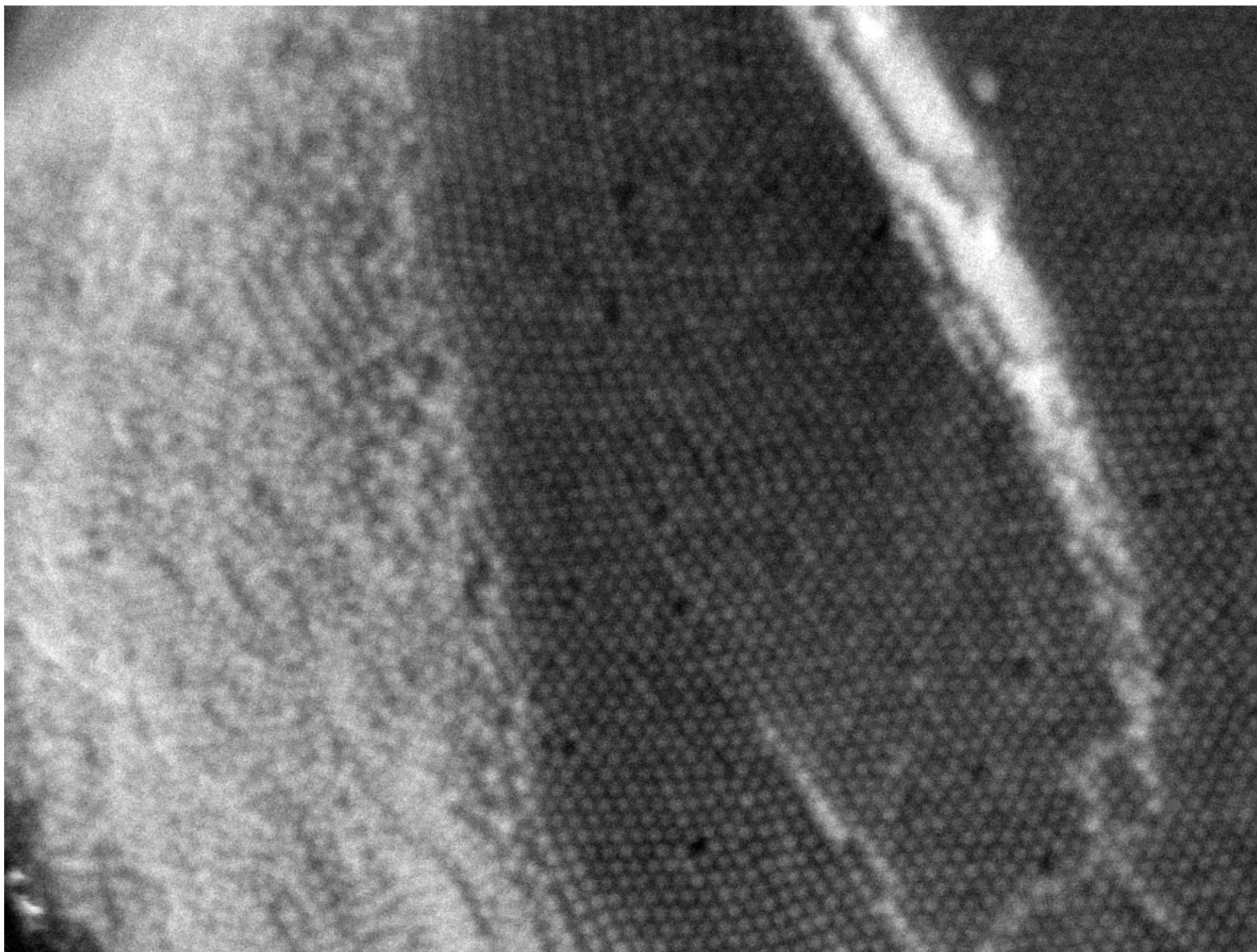
Mechanisms of Particle and Wire formation

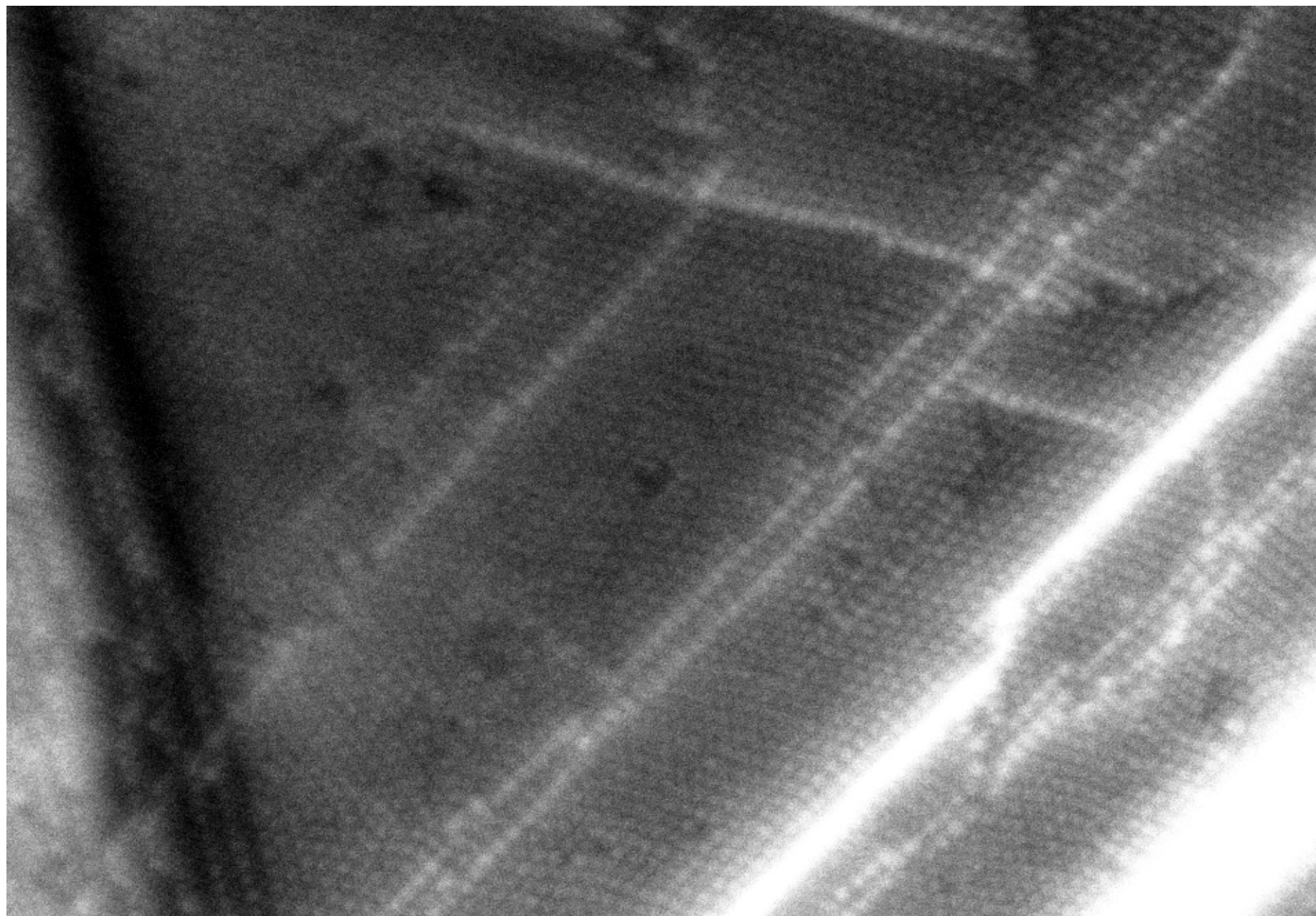


Quantum cubes:

Cubic 12 nm PbSe nanocrystals Assembling into a superlattice.







ag = 287.76 K X

200nm

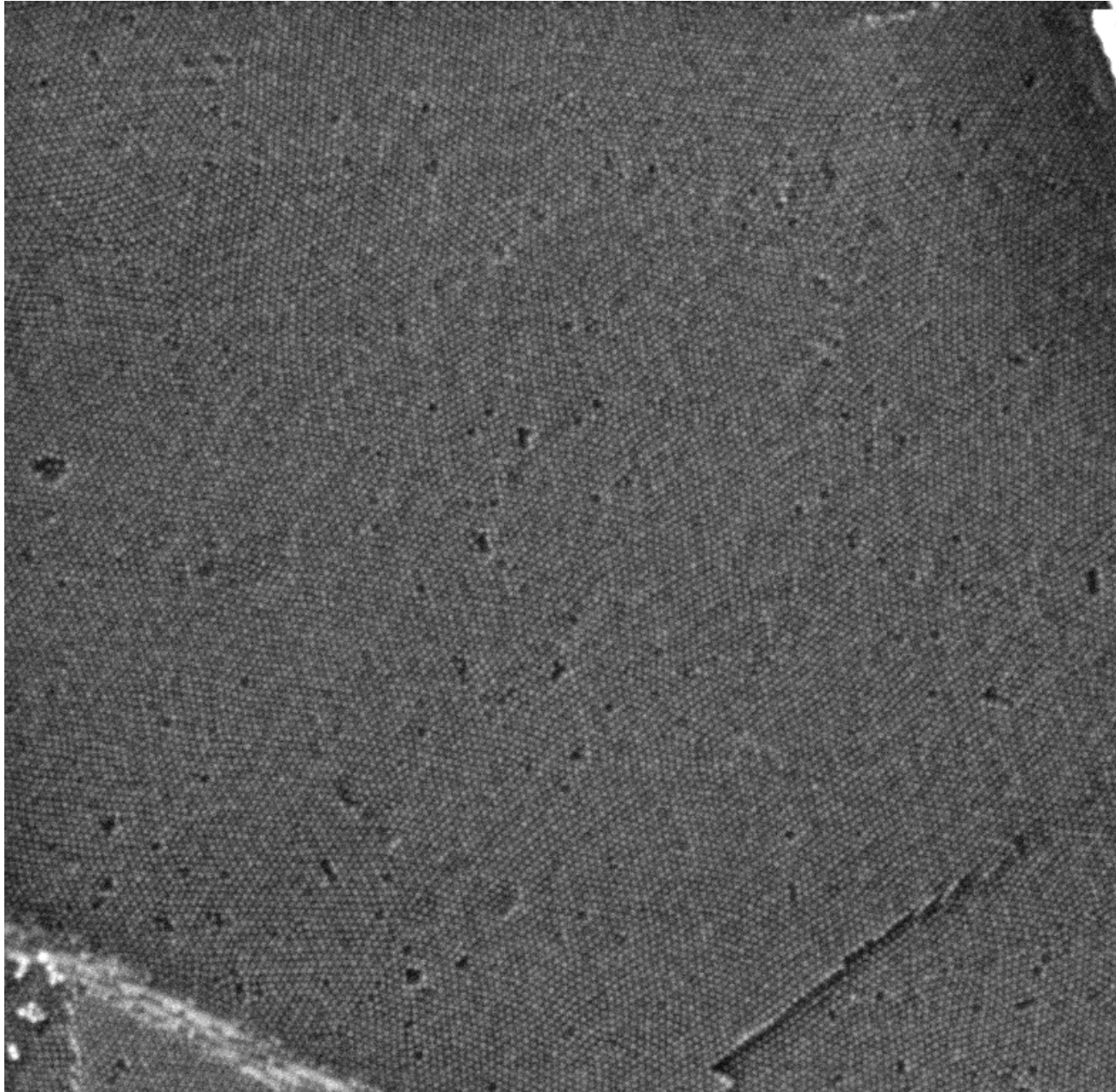


EHT = 5.00 kV
WD = 2 mm

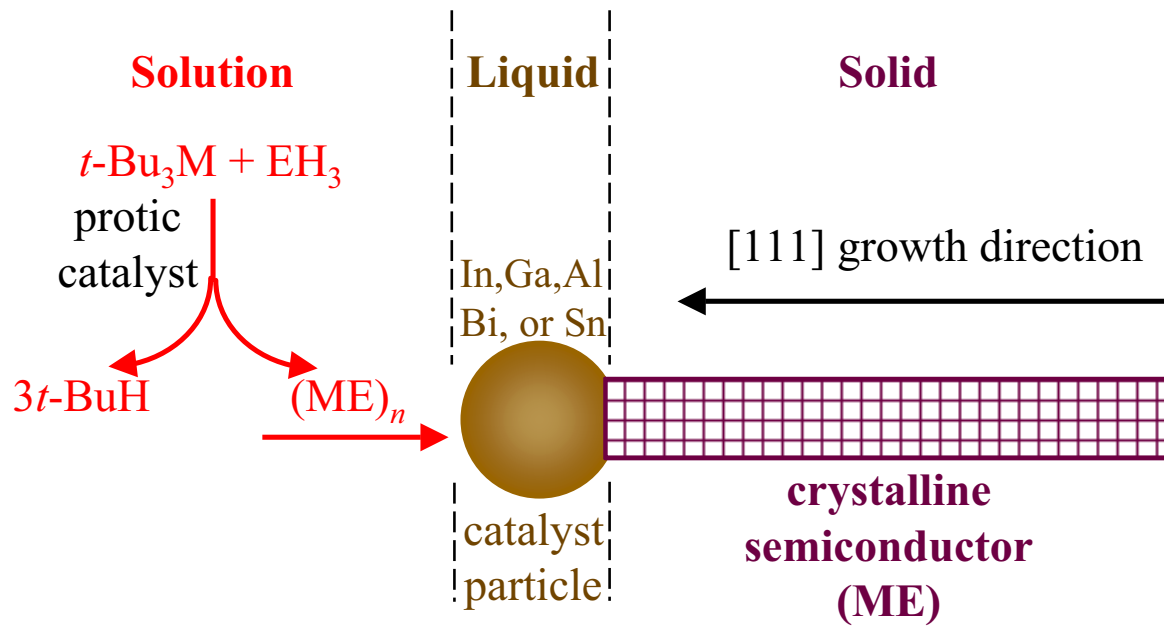
Signal A = InLens
IBM

Date :21 Jun 2000
Time :18:02

Large terrace on PbSe Superlattice of 10 nm PbSe Nanocrystals



Solution-Liquid-Solid (SLS) Growth of Semiconductors...

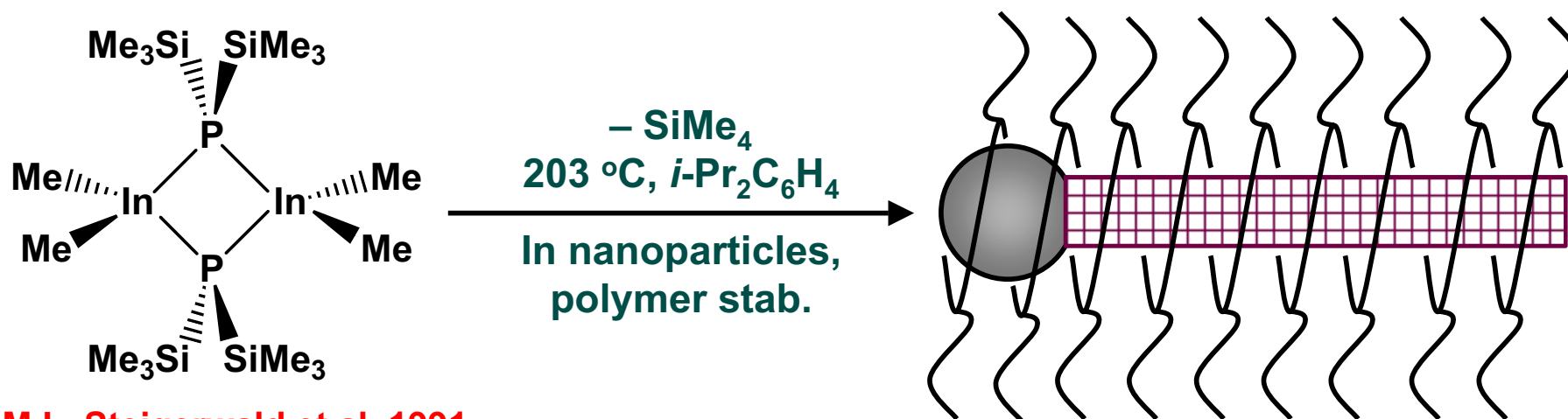


Trentler, Hickman, Goel, Viano, Gibbons,
Buhro *Science* 1995, 270, 1791



- Unsuitable for quantum-wire studies...
 - Most diameters are far too large (> 20 nm)
 - Diameter distributions are far too broad
- Require monodisperse, small-diameter, catalyst nanoparticles

SLS growth of InP nanowires from monodisperse In nanoparticles...



M.L. Steigerwald et al. 1991

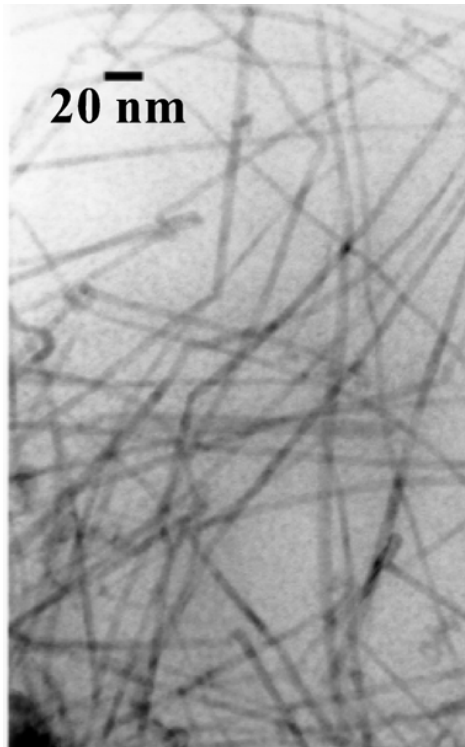
- Polyhexadecene_{0.67}-co- PVP_{0.33} was used as “surfactant” to stabilize both In nanoparticles and InP nanowires
- Nanowire samples were grown using several sizes of monodisperse In particles
- The nanowires formed dark-red dispersions that were stable indefinitely
- Nanowire samples were analyzed by TEM

H. Yu, J. Li, R.A. Loomis, L-w. Wang, W.E. Buhro *Nature Mater.* 2003, 2, 517

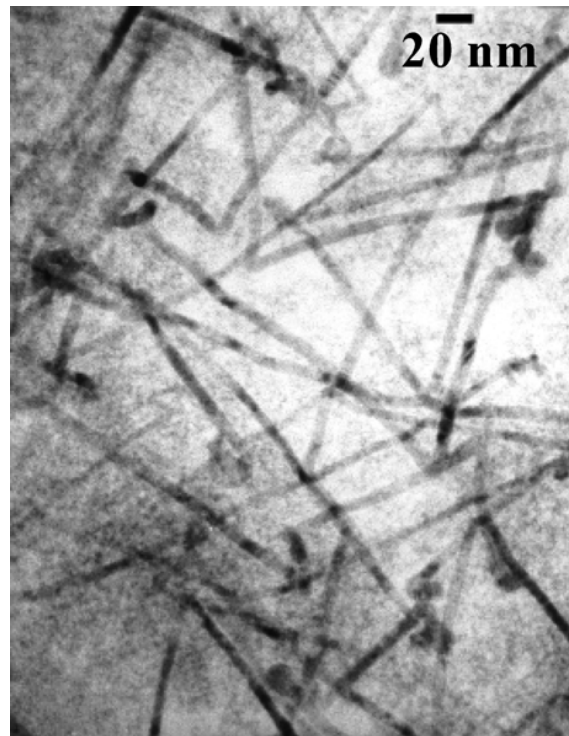


Washington University in St. Louis

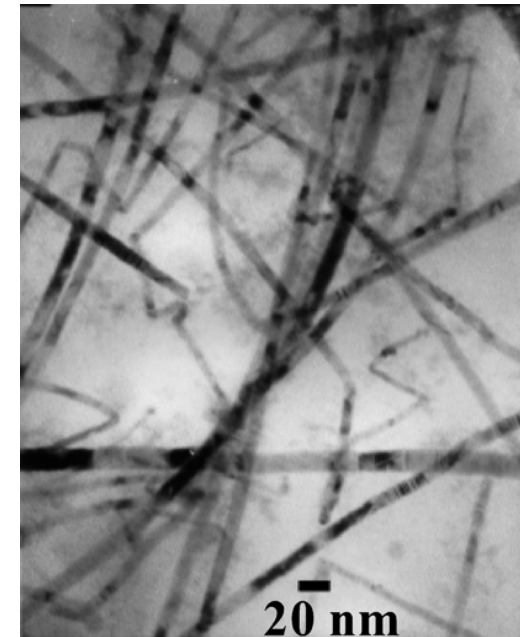
TEM images of InP nanowires: diameter control



9.9-nm In catalyst nanoparticles
4.5-nm InP nanowires



13.9-nm In
6.6-nm InP

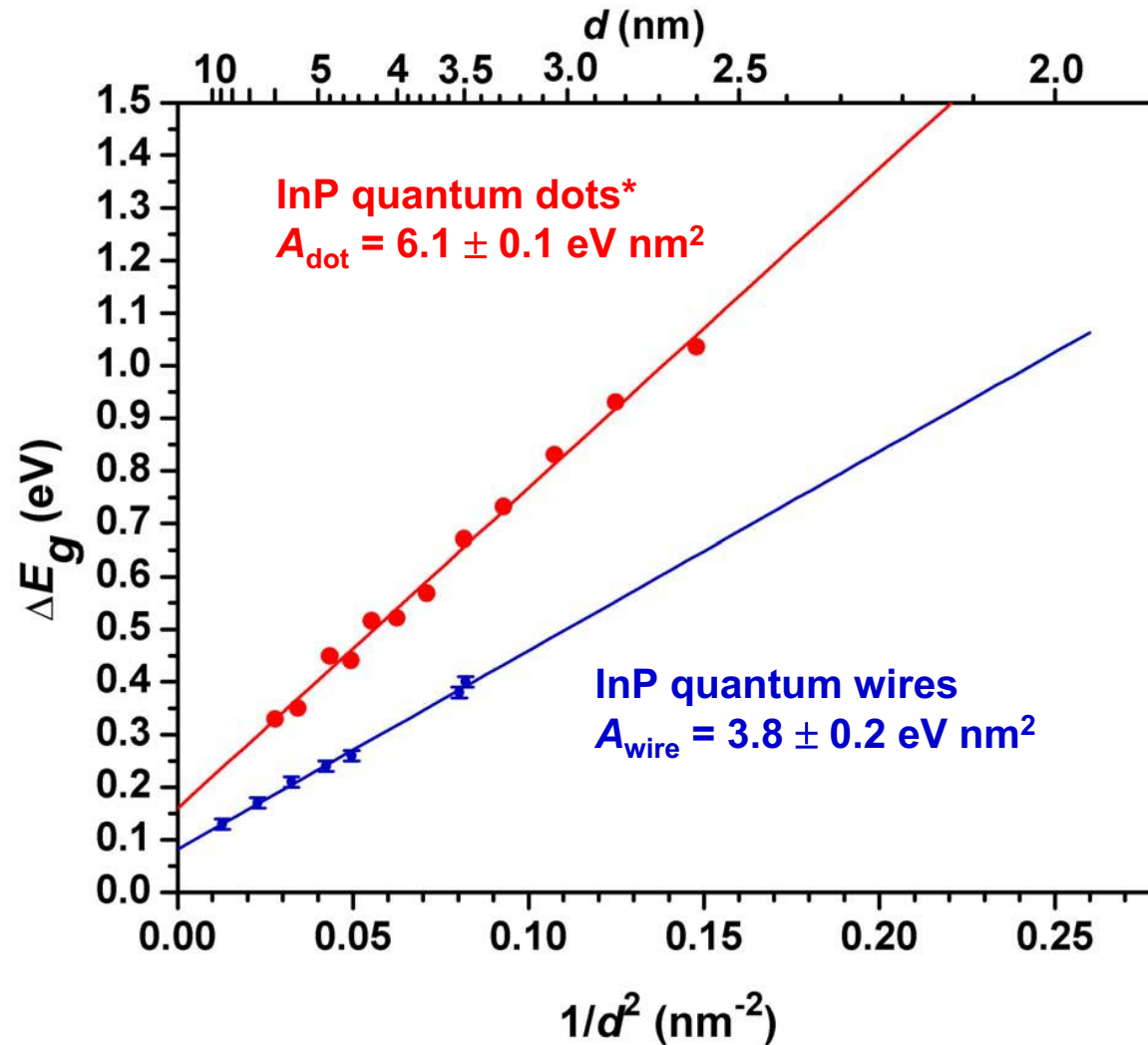


21.2-nm In
11.0-nm InP

- Nanowire diameters scale with the initial catalyst-nanoparticle diameters
- Statistical analyses confirm fairly narrow nanowire diameter distributions
- The wires are near single crystals, and are 111 oriented

Plots of ΔE_g vs. $1/d^2$ for InP quantum dots and wires...

Recall prediction for the relative slopes of the lines: $A_{\text{wire}}/A_{\text{dot}} = 0.585$

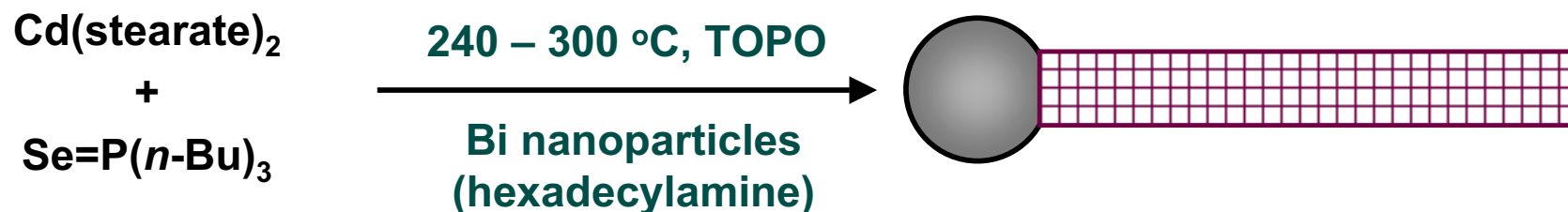


*Mičić, Nozik,
and coworkers

$$A_{\text{wire}}/A_{\text{dot}} = 0.62 \pm 0.03$$

Thus, quantum
confinement is
weakened in the wires
to the expected extent
by the loss of one
confinement dimension

SLS growth of CdSe nanowires from Bi nanoparticles...



adapted from
Xiaogang Peng
and coworkers

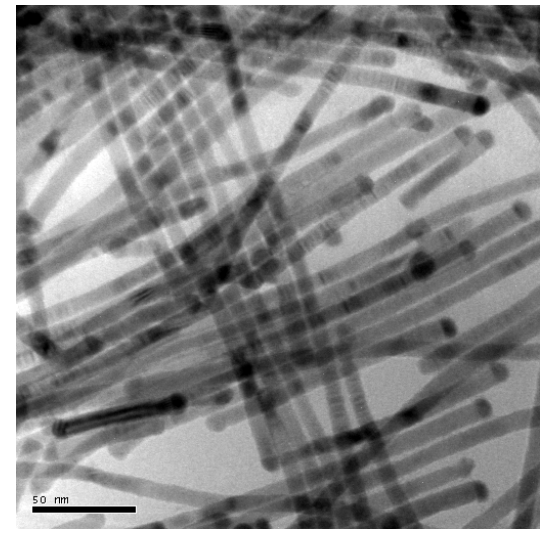
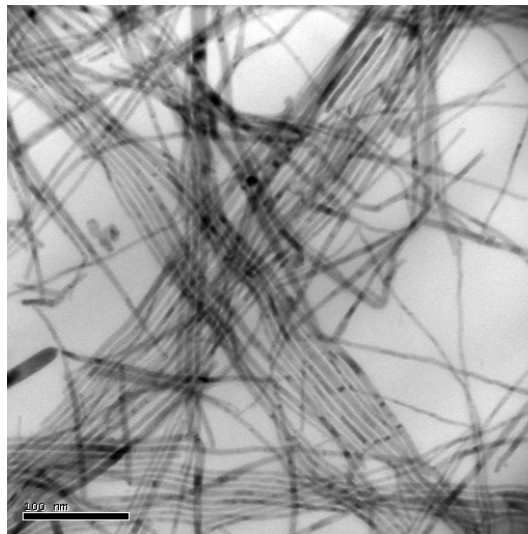
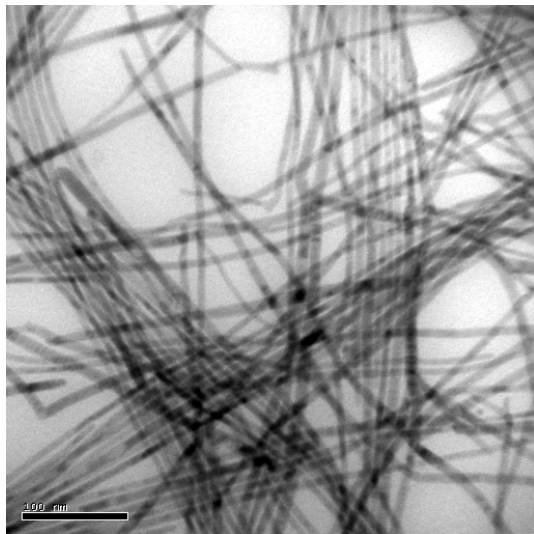
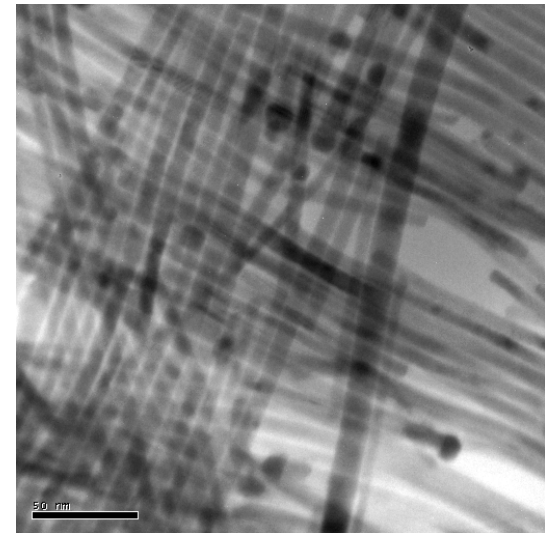
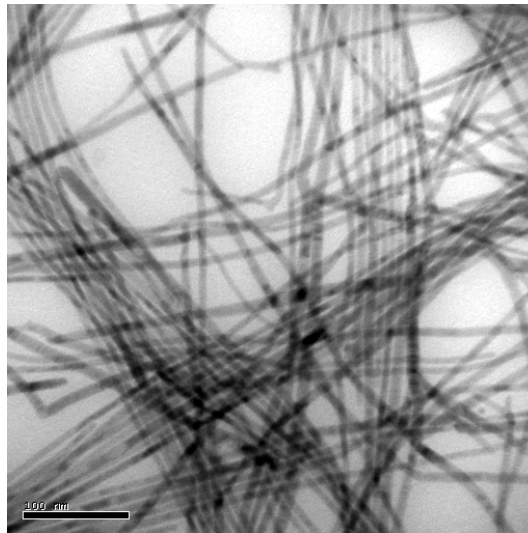
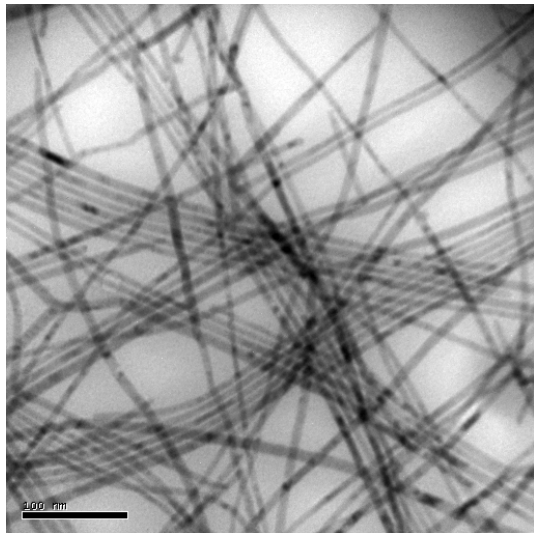
- No polymer stabilizer necessary to retain nanowire “solubility”
- Mean nanowire diameters varied with reaction temperature and catalyst nanoparticle size
- Indefinitely stable dark-red dispersions
- Nanowire specimens were analyzed by TEM; typical lengths: several μm
- Statistical analyses: diameter std. dev. = $\pm 10 - 20\%$ of mean diameter

Yu, Li, Loomis, Gibbons, Wang, Buhro *JACS* 2003, 125, 16168

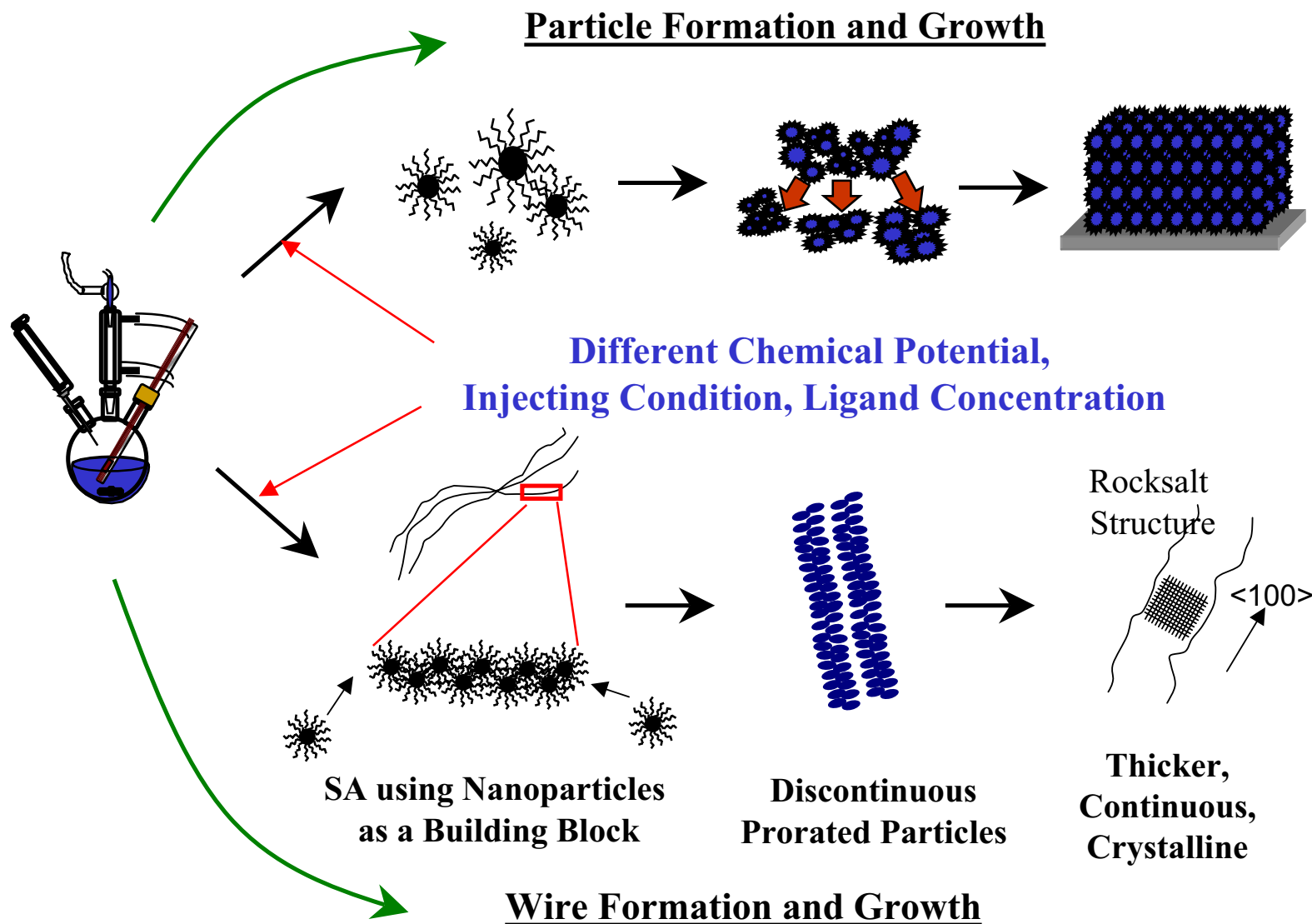


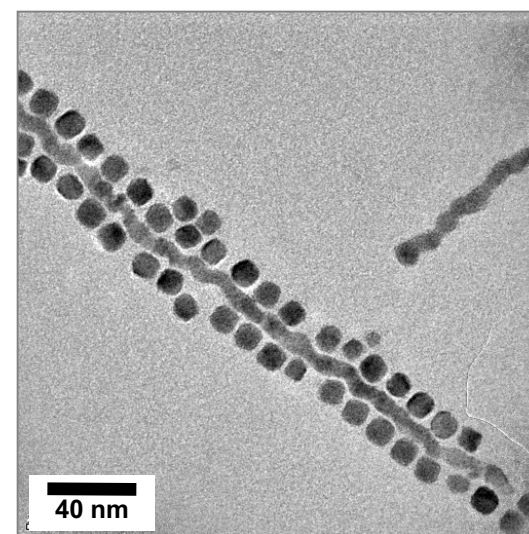
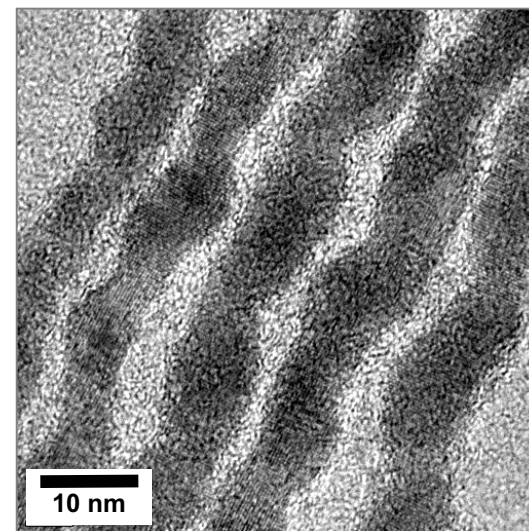
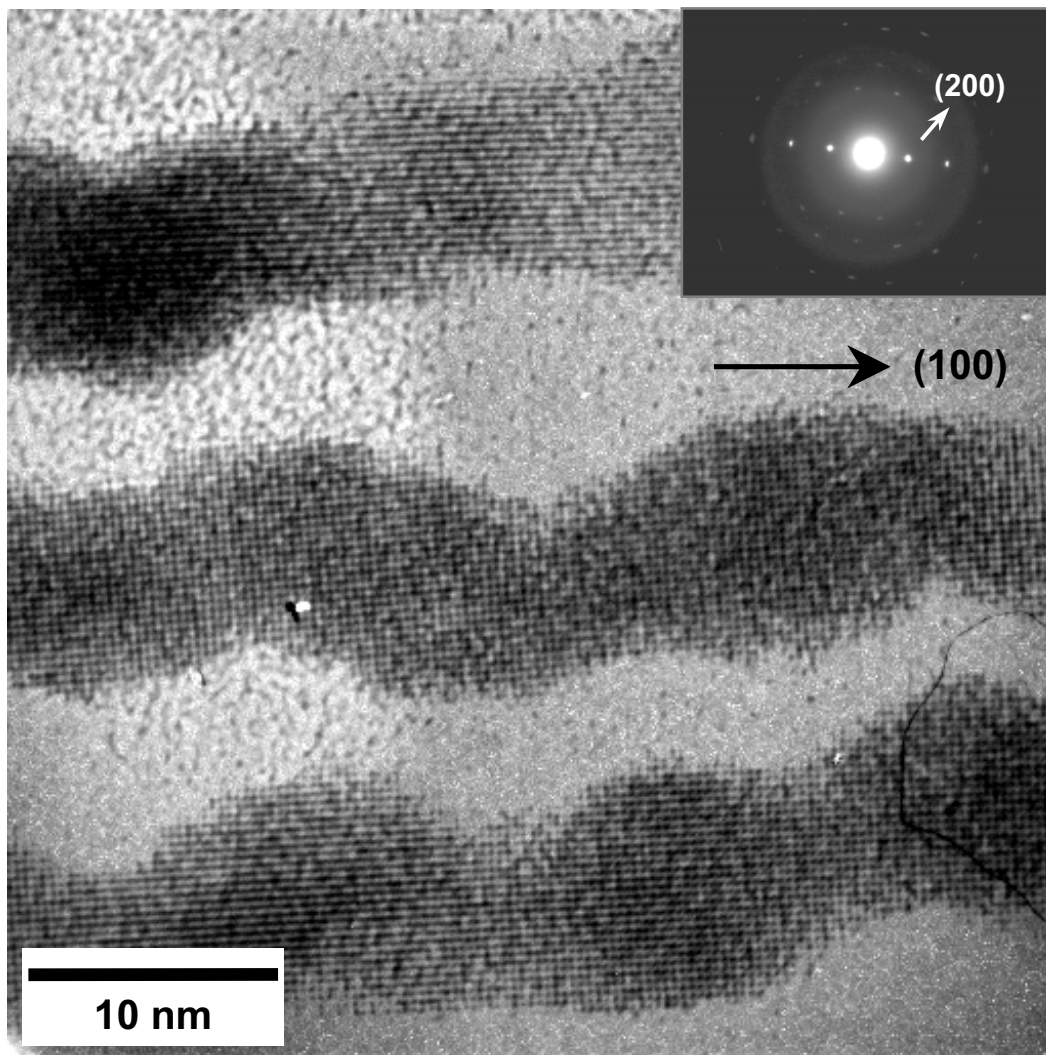
Washington University in St. Louis

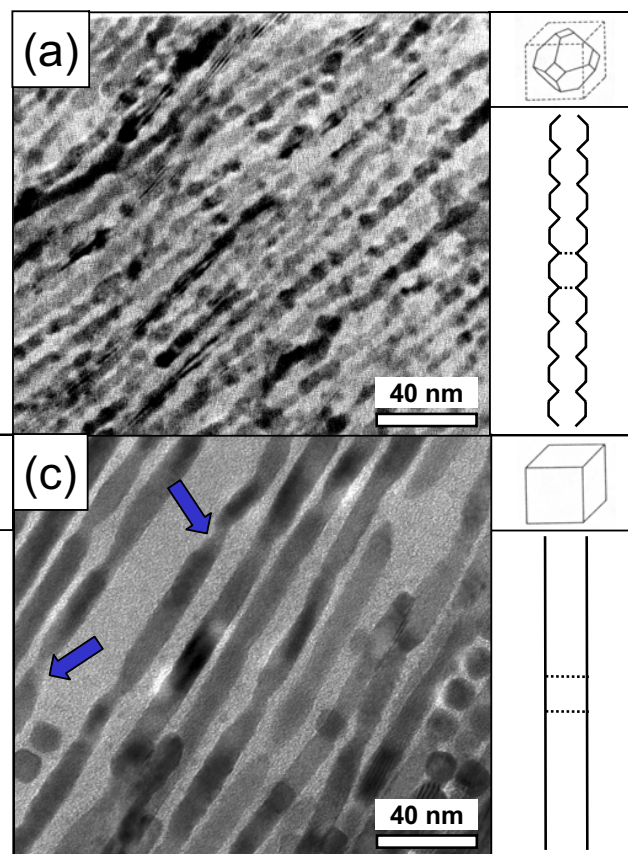
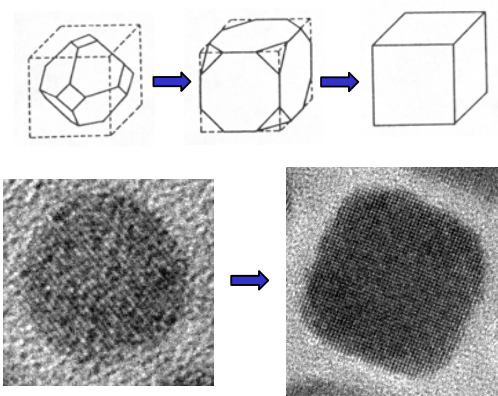
TEM images of CdSe nanowires...

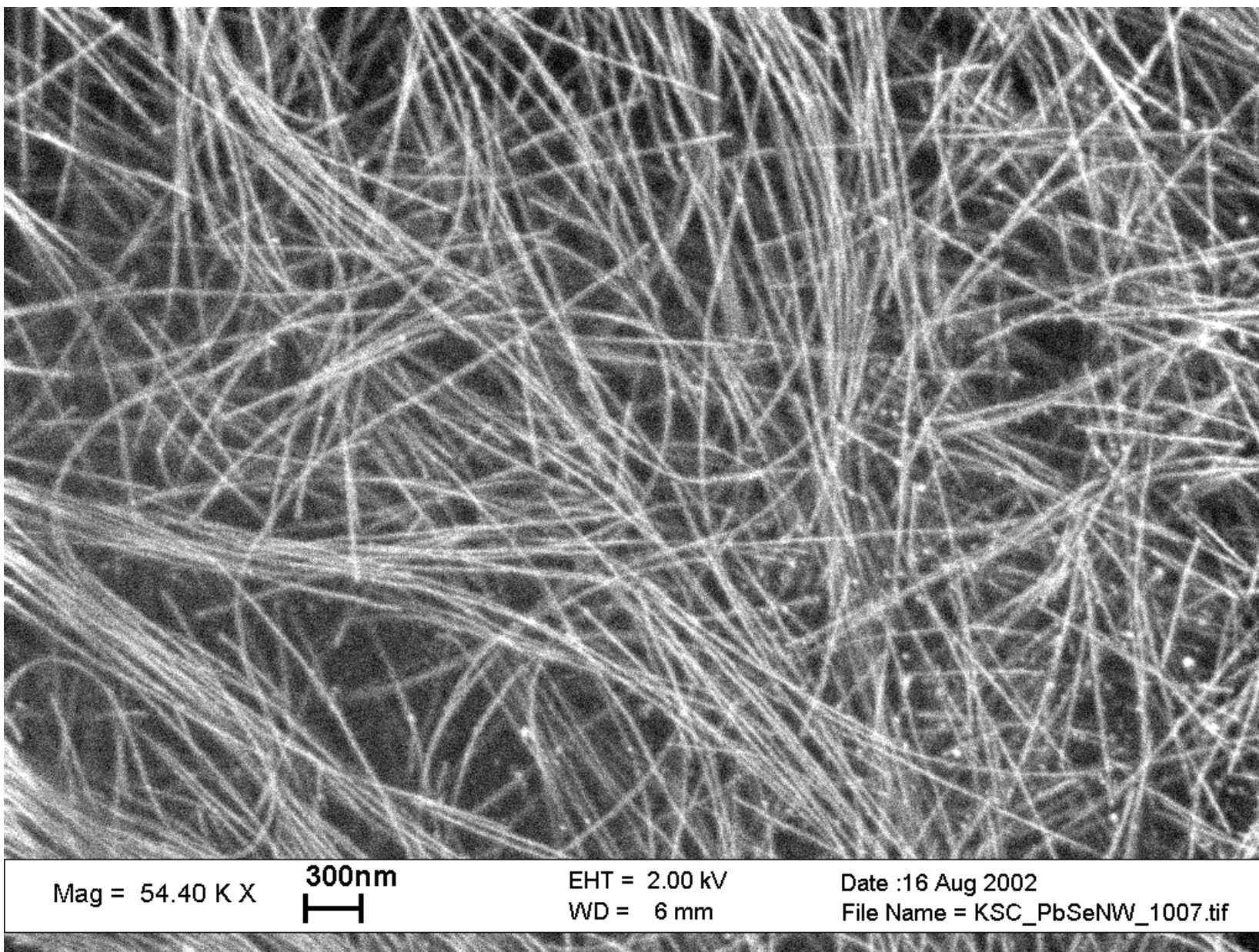


Mechanisms of Particle and Wire formation







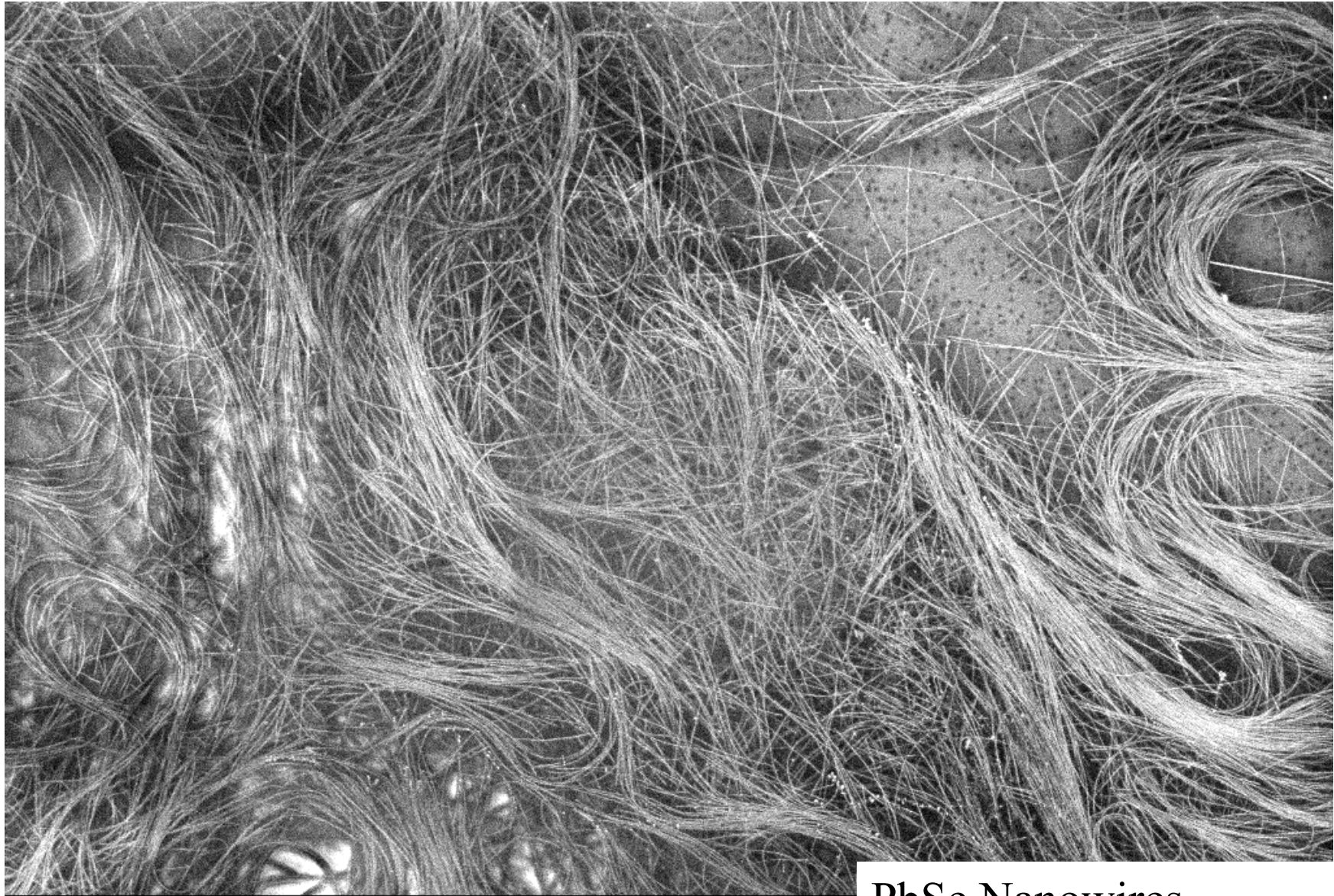


Mag = 54.40 K X

300nm
┌─┐

EHT = 2.00 kV
WD = 6 mm

Date :16 Aug 2002
File Name = KSC_PbSeNW_1007.tif



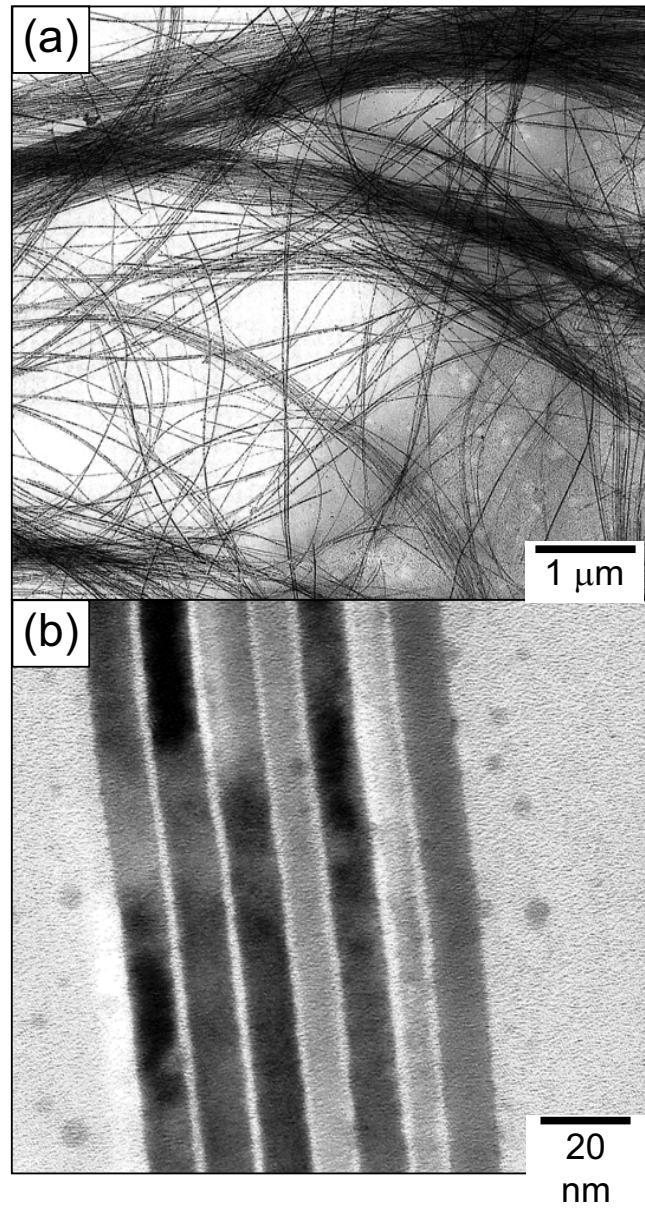
Mag = 14.92 K X

1 μ m
└──┘

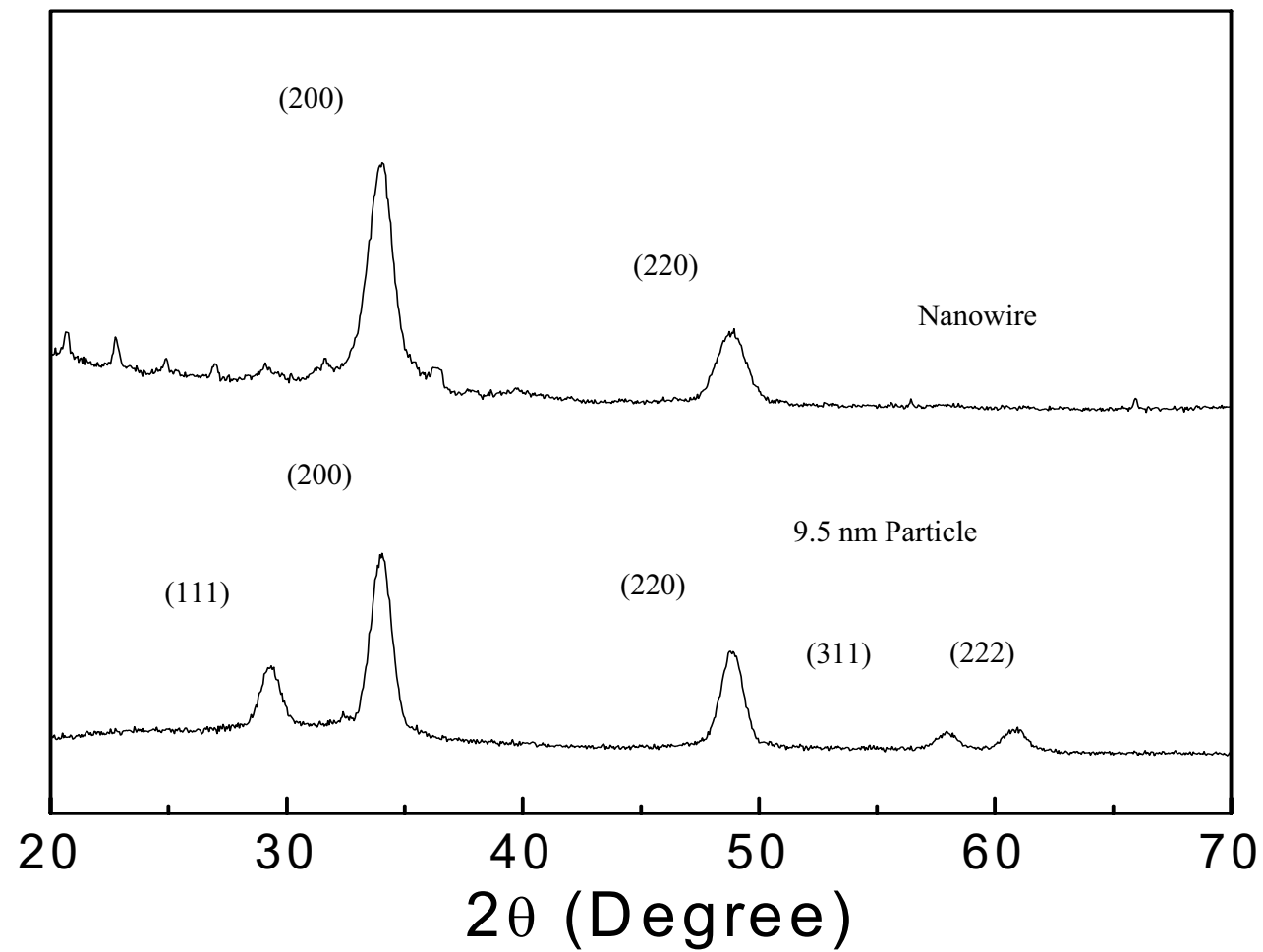
EHT = 2.00 kV
WD = 6 mm

PbSe Nanowires
20 nm Diameter

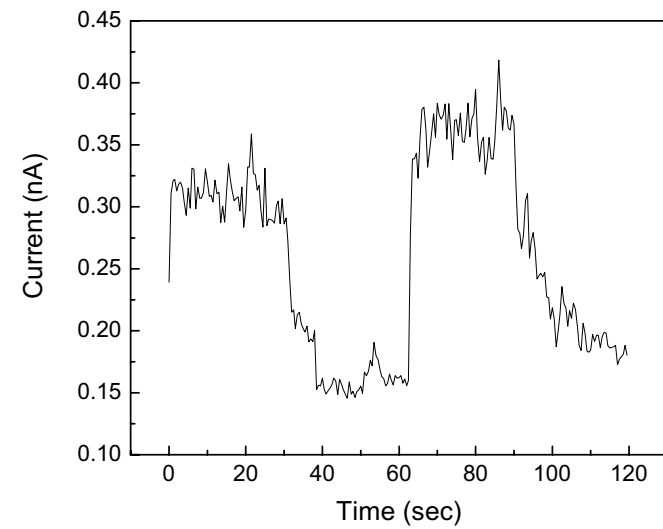
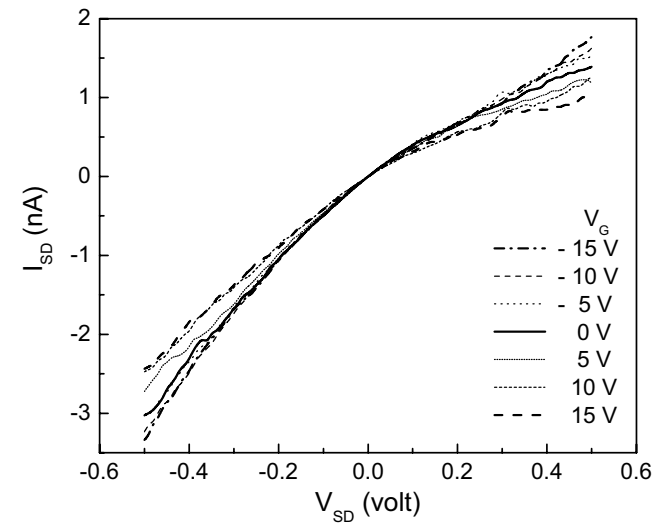
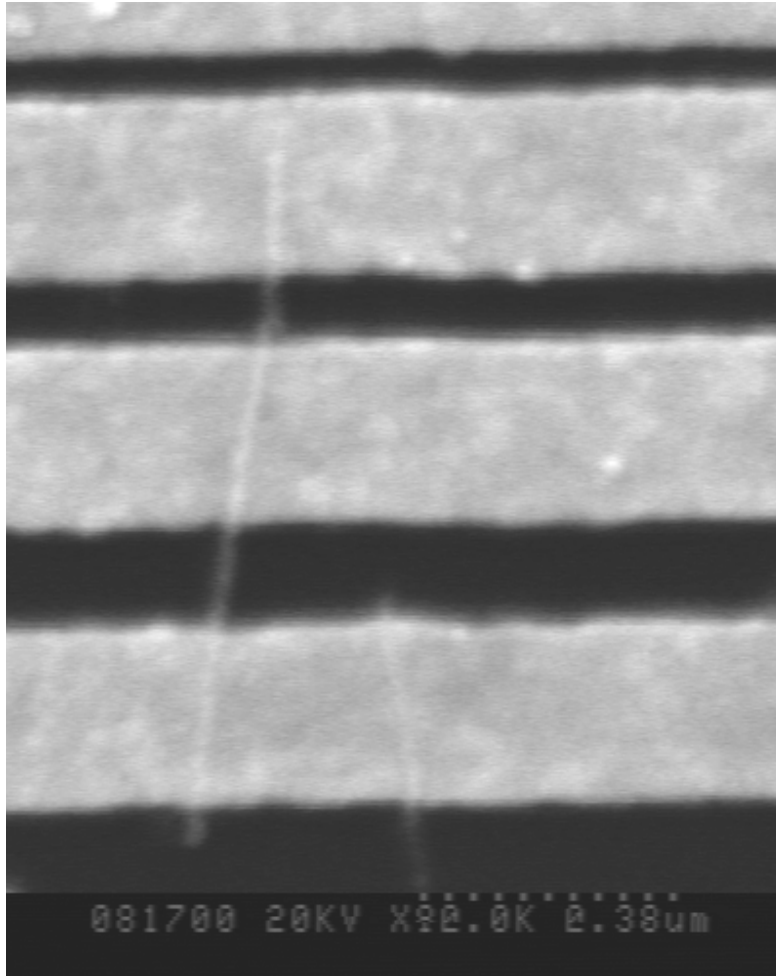
Straight PbSe NW (with Tetradecyl Phosphonic Acid)

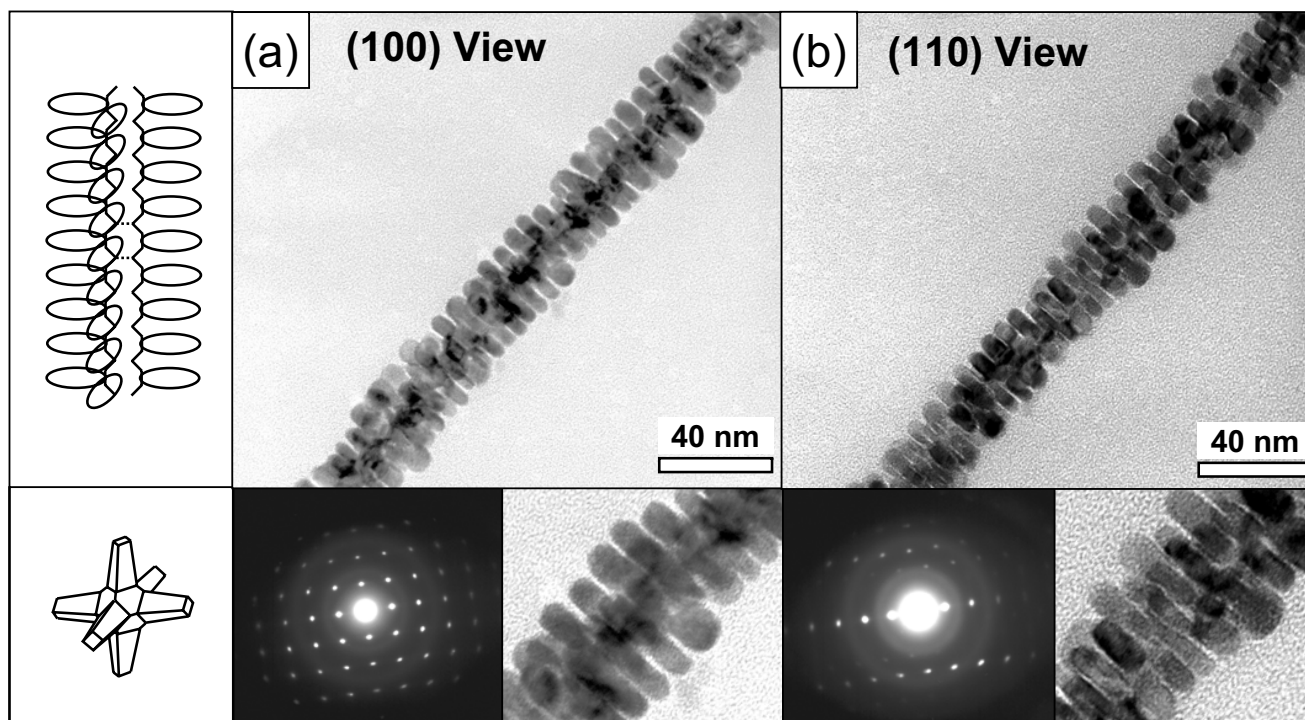
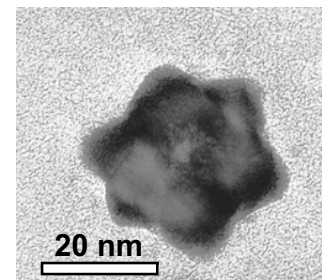
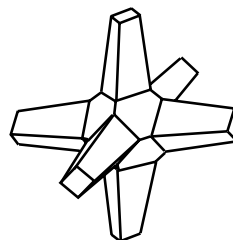
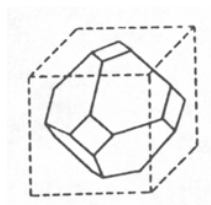
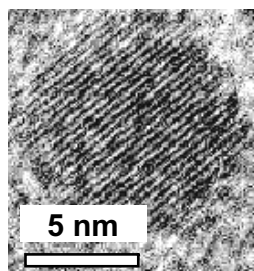


Reflected Intensity (Arb. Unit)

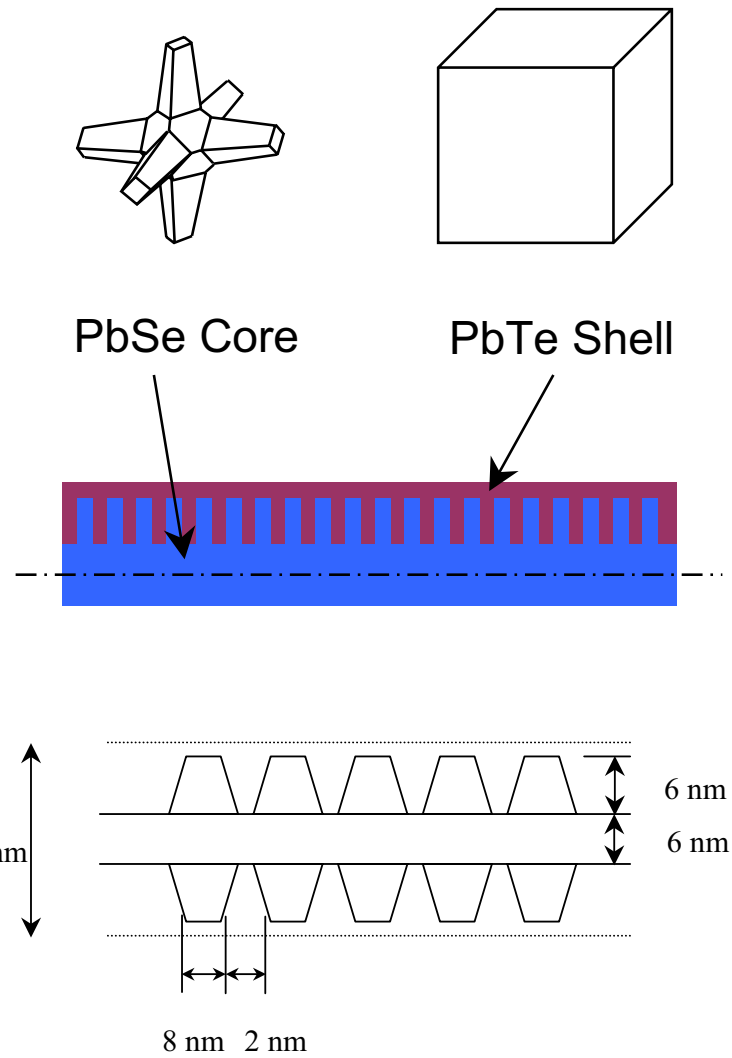
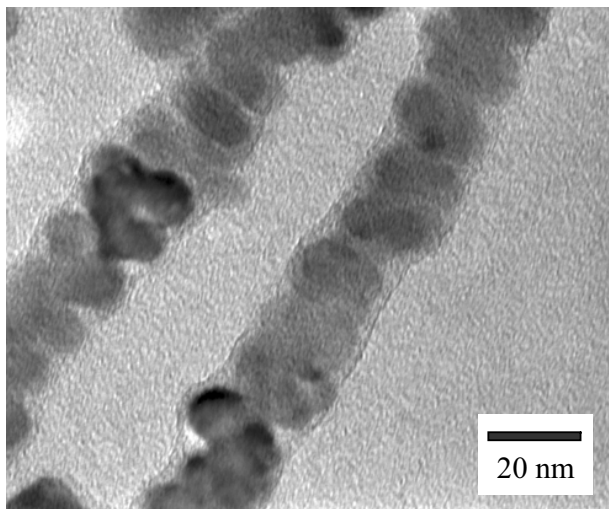
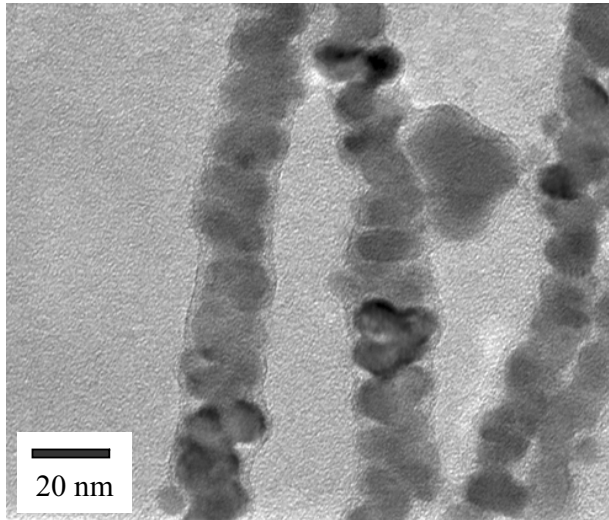


Transport in single PbSe nanowire devices.

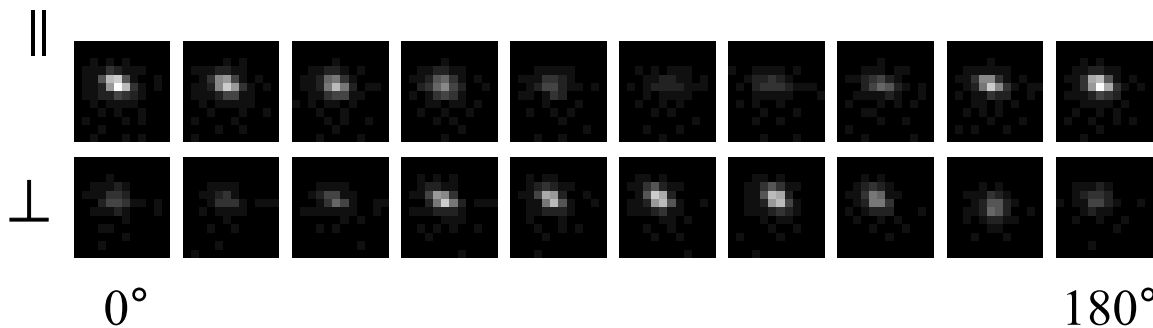
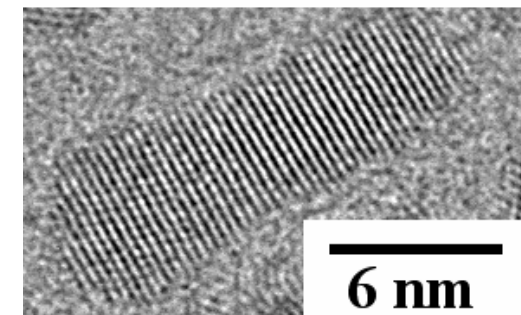
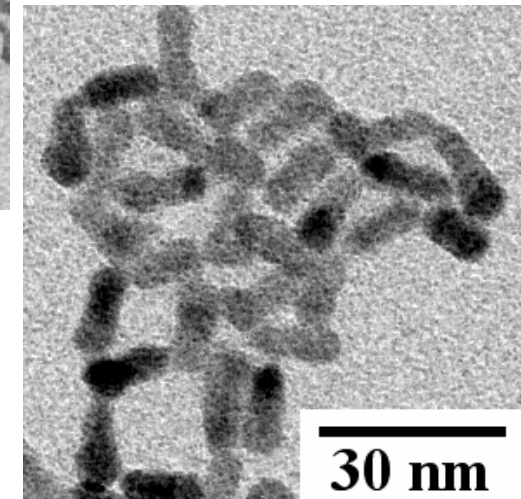
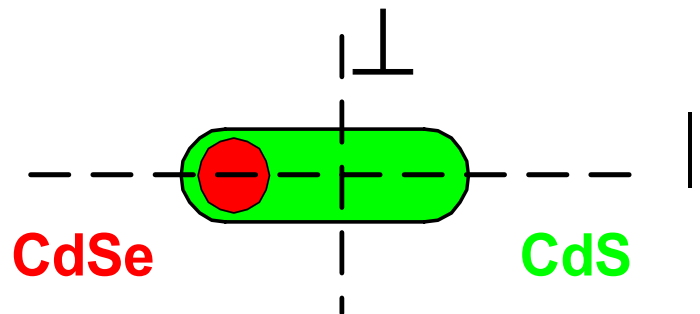
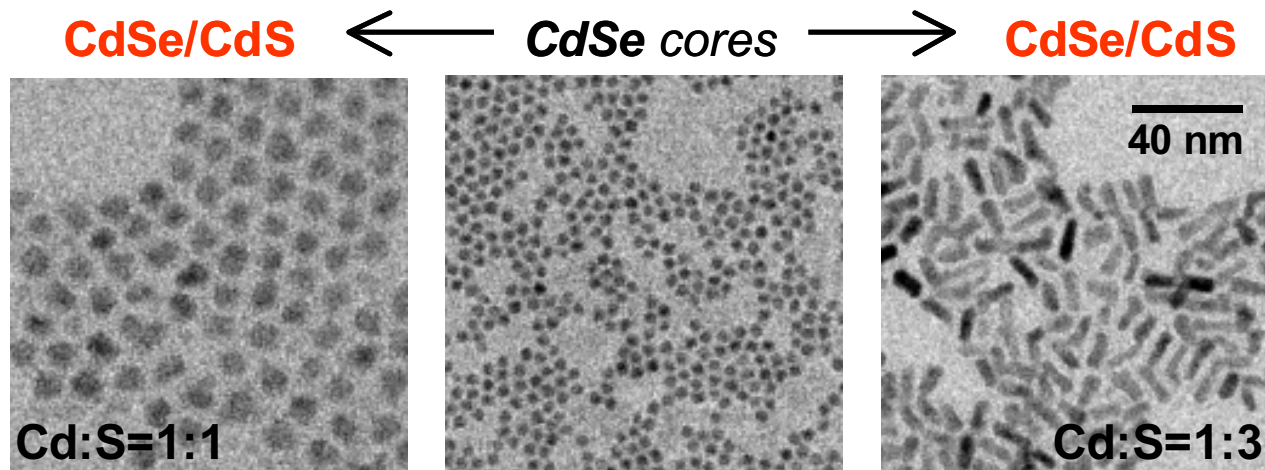




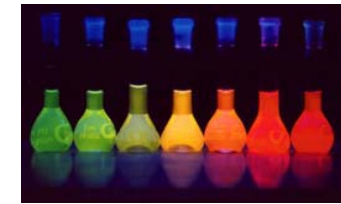
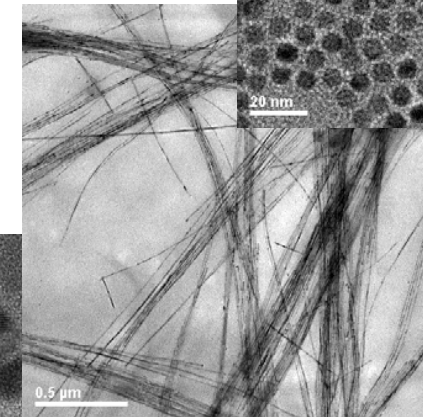
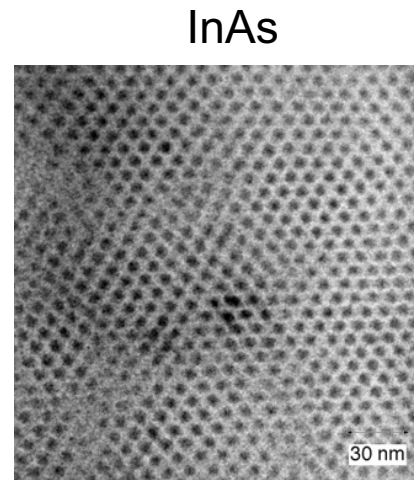
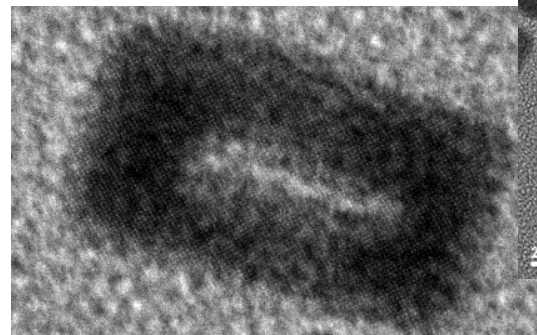
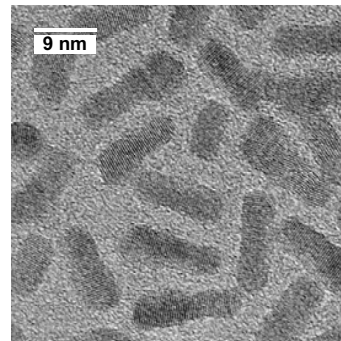
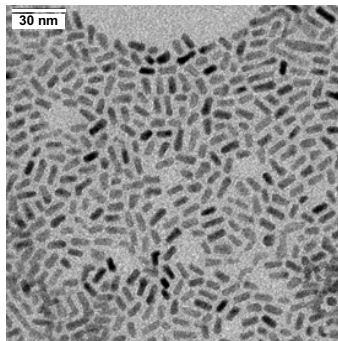
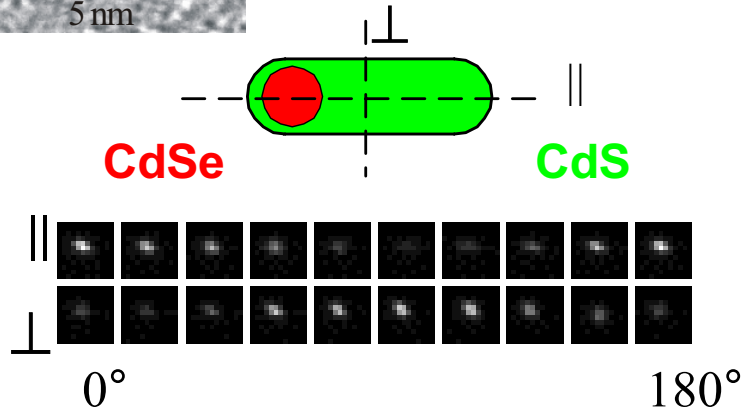
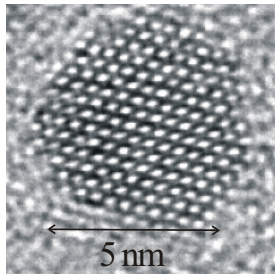
PbSe/PbTe Core/Shell NW



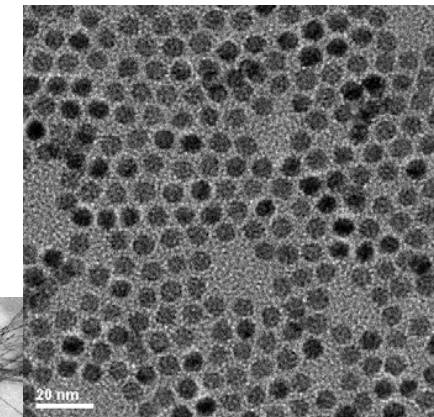
CdSe/CdS quantum dot - quantum rods



Semiconductor nanomaterials



CdTe (aqueous)



CdSe/ZnS



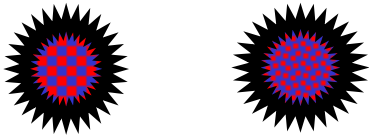
InP



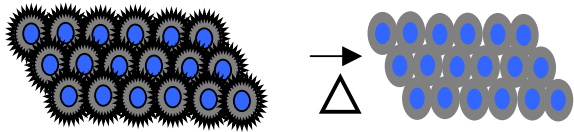
Complex Compositions and Multi-Component Structures

Simultaneous Reaction

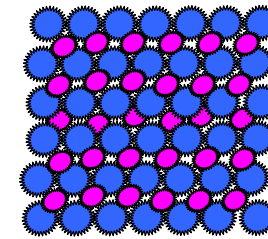
A & B Compounds & Alloys



Anneal to remove Organic



Ferromagnets,
Noble Metals,
Semiconductor QDots,
Ferroelectrics,
Superconductors

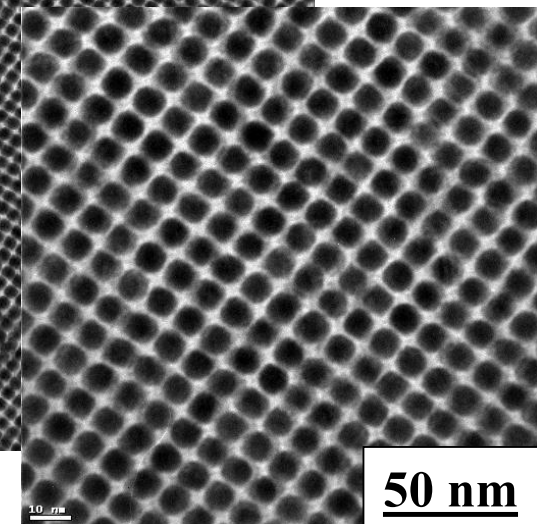
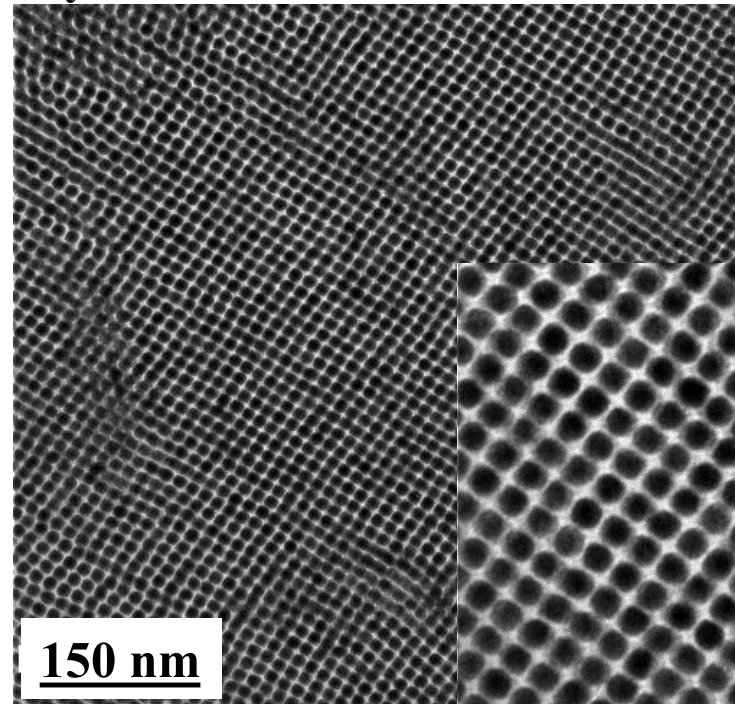
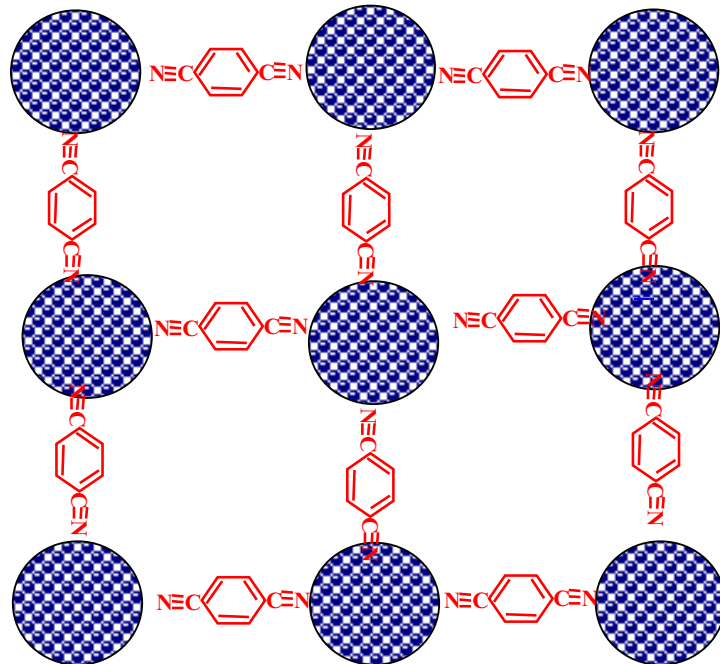


Binary Assembly
 AB_2 & AB_{13}

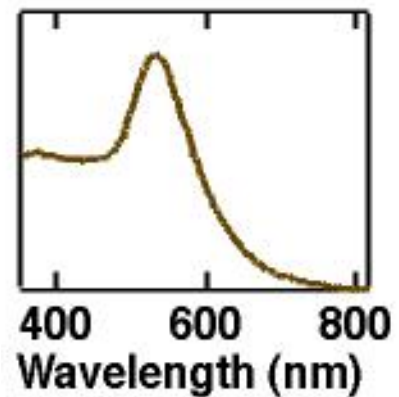
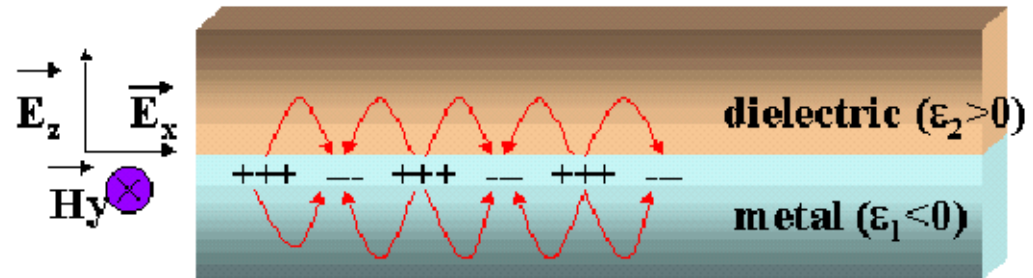
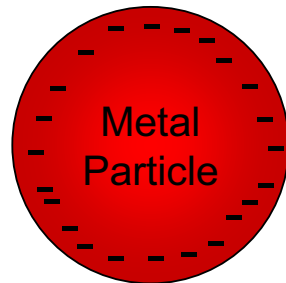


Dicyanobenzene linked Cobalt Nanocrystals

Customize organic linkers (molecular wires)



Metal Nanoparticles

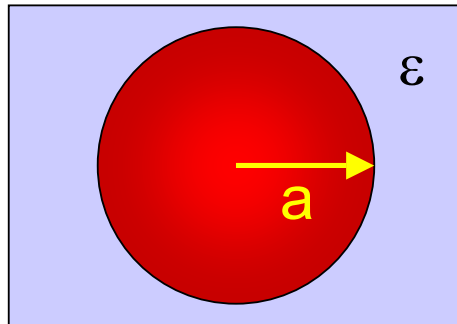


Au nanoparticle
absorption

Surface Plasmon Resonance

- dipolar, collective excitation between negatively charged free electrons and positively charged core
- energy depends on free electron density and dielectric surroundings
- resonance sharpens with increasing particle size as scattering distance to surface increases

Electronic Properties of Semiconductor and Metal Nanoparticles



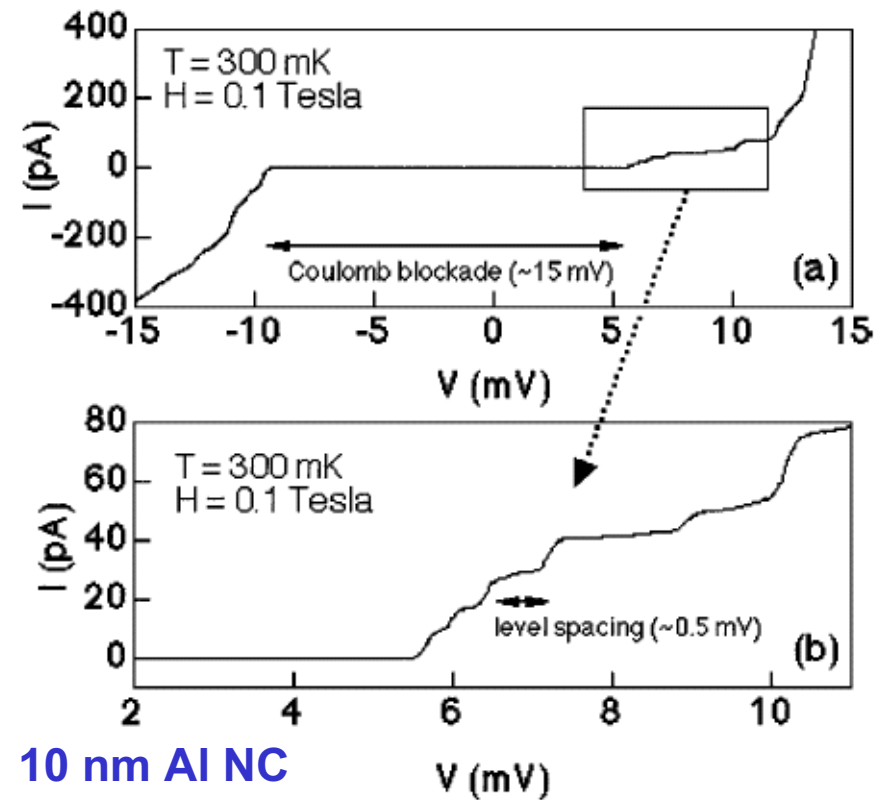
Charge not completely solvated
as in infinite solid

$$C = 4\pi\epsilon_0\epsilon a$$

$$E_c = \frac{e^2}{2C(a)}$$



Coulomb blockade at
 $k_B T < E_c$



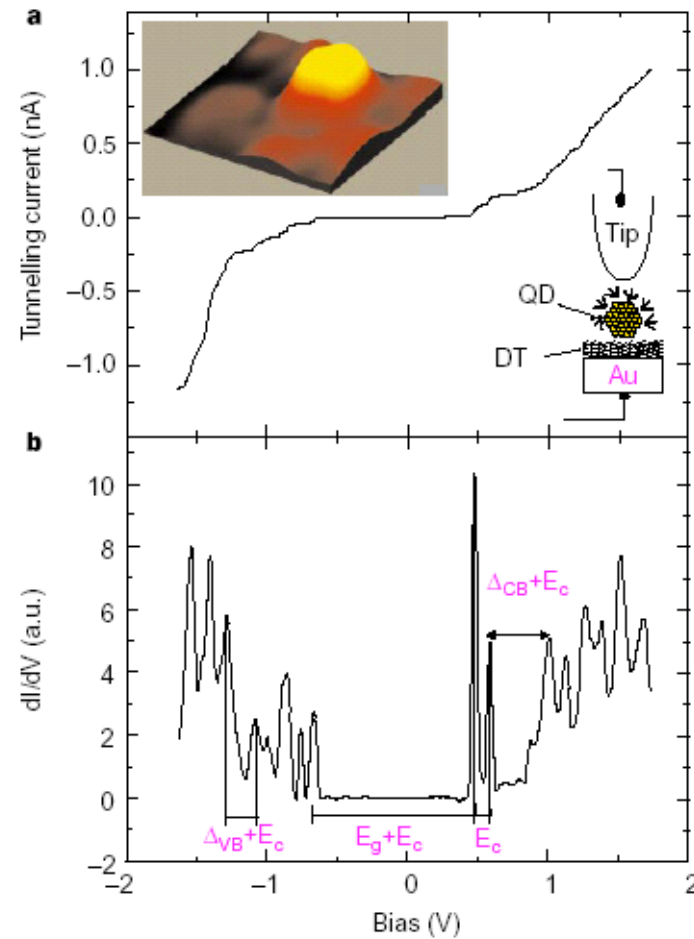
10 nm Al NC

Courtesy of C. T. Black, Thesis, Harvard U.

Structure from discrete electronic states of
metal NC

STM Measurements on Single QDs

InAs QDs



Gold COLLOIDS

Preparation of 2.5×10^{-4} M Gold Colloids (Sodium Citrate Reduction Method)

1. Make a solution of $\sim 5.0 \times 10^{-3}$ M HAuCl_4 in water. (0.1699 g HAuCl_4 in 100 mL deionized H_2O)
2. Take 1 mL of that solution and add it to another 18 mL of H_2O .
3. Make a solution of 0.5% sodium citrate (0.25g in 50 mL of H_2O).
4. Heat the 19 mL solution of HAuCl_4 until it begins to boil.
5. Add 1 mL of 0.5% sodium citrate solution, as soon as boiling commences.
6. Continue heating until colour change is evident (pale purple).
7. Remove the solution from the heating element and continue to stir until it has cooled to room temperature.
8. Top the solution up to 20 mL to account for boiling.

348

Jpn. J. Appl. Phys. Vol. 40 (2001) Pt. 1, No. 1

G. TSUTSUI *et al.*

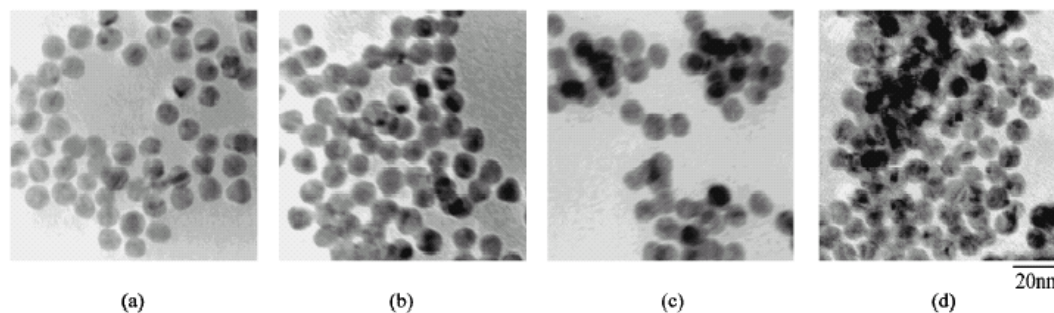


Fig. 5. TEM images of the 8.3-nm-diameter colloidal gold particles in (a) water, (b) ethanol, (c) chloroform, and (d) benzene.

This is an old method (refereed as Turkevich method) which yields fairly uniform size colloids with diameter of 15-20 nm. See reference Turkevich, J.; Stevenson, P. L.; Hillier, J. Discuss. Faraday Soc. 1951, 11, 55

Preparation of $1.0 \times 10^{-3}\text{M}$ Ag Colloids (Sodium Citrate Reduction Method)

1. Make a solution of $\sim 5.0 \times 10^{-3}\text{M}$ AgNO_3 in water. (0.0425 g in 50 mL deionized H_2O).
2. Take 25 mL of that solution and add it to another 100 mL of H_2O (now $\sim 1.0 \times 10^{-3}\text{M}$).
3. Make a solution of 1% sodium citrate (0.5 g in 50 mL of H_2O).
4. Heat the 125 mL solution of AgNO_3 until it begins to boil.
5. Add 5 mL of 1% sodium citrate solution, as soon as boiling commences.
6. Continue heating until a colour change is evident (pale yellow).
7. Remove the solution from the heating element and continue to stir until it has cooled to room temperature.
8. Top the solution up to 125 mL to account for boiling.

This method yields relatively large size silver nanocrystallites with a diameter of 60-80 nm and exhibits abs. max. ~ 420 nm. See reference *J. Phys. Chem. B*, 1998, 102, 3123

(Note: Use of Sodium Borohydride as a reductant can give smaller size silver nanoparticles with plasmon absorption around 380 nm. Presence of citric acid or polyvinyl alcohol can provide additional stability to these colloids)

Preparation of Gold Particles in Toluene:

A. Hydrogen tetrachloroaurate (30 mL of 30 mM, in water).

Mass = $393\text{g/mol} \times 0.03\text{ M} \times 30\text{mL}/1000\text{mL} = 0.3537\text{g}$ of HAuCl_4 in 30mL of H_2O

B. Tetraoctyl ammonium bromide (80 mL in 50 mM, in toluene).

Mass = $546.8\text{g/mol} \times 0.05\text{ M} \times 80\text{ml}/1000\text{mL} = 2.187\text{g}$ of TOAB in 80mL of toluene

1. Prepare 2.19 g of tetraoctyl ammonium bromide in 80 mL of toluene.

2. Add solution prepared in step 1. to a solution of hydrogen tetrachloroaurate (0.3537 g in 30 mL of H_2O).

3. Stir for 10 min.

4. Vigorously stir reaction mixture and add NaBH_4 (0.38 g in 25 mL of H_2O) dropwise over a period of ~30 min. (Ensure that organic and aqueous phases are being mixed together).

5. Stir solution for an additional 20 min.

6. Extract organic phase and wash once with diluted H_2SO_4 (for neutralization) and five times with distilled water.

7. Dry organic layer with Na_2SO_4 .

For platinum particles substitute dihydrogen hexachloroplatinate (IV) ($\text{PtCl}_6 \cdot \text{H}_2\text{O}$) for HAuCl_4 and for iridium particles substitute $\text{H}_2\text{IrCl}_6 \cdot 4\text{H}_2\text{O}$ for HAuCl_4 .

Yields highly concentrated gold colloidal suspension with particle diameter in the range of 5-10 nm. Can be suspended in both polar and nonpolar solvents.

Adopted from the reference Brust, M.; Walker, M.; Bethell, D.; Schiffrin, D. J. Whyman, R., *J. Chem. Soc., Chem. Commun.*, 1994, 801-802 and George Thomas, K. Kamat, P. V. *J. Am. Chem. Soc.* 2000, 122, 2655

Thiol Stabilized Gold Nanocrystals

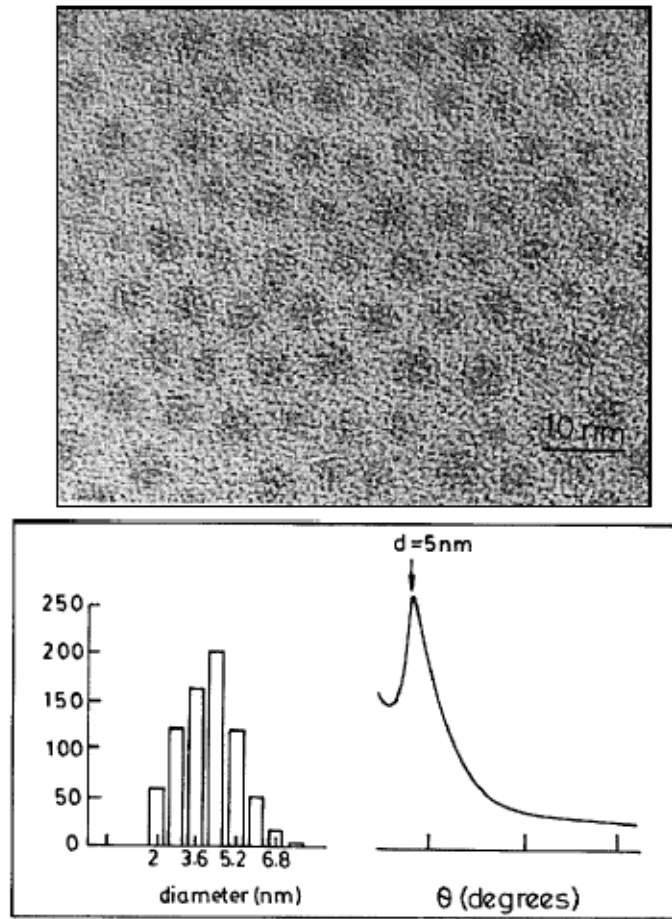


Fig. 5 2D array of thiol-derivatized Au particles of 4.2 nm mean diameter. Histograms indicating particle size distribution is given. XRD pattern from this array is also shown.

Silver Nanocrystal Preparation in Organic Medium

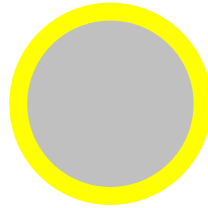
Modification of method found in source: Korgel, B.A.; Fullam, S.; Connolly, S.; Fitzmaurice, D. *J. Phys. Chem. B* **1998**, *102*, 8379-8388. (The method described in this paper yields a precipitate of AgBr in the initial extraction process)

1. Prepare ~5.0M NaNO₃ in deionized water (12.749g NaNO₃ in 30mL H₂O).
2. Prepare ~50mM TOAB in toluene (1.367g tetraoctylammonium bromide in 50mL toluene).
3. Add the TOAB/toluene solution to the NaNO₃/water solution.
4. Stir vigorously for 1 hour (to remove Br⁻ ions from solution and prevent the formation of AgBr when AgNO₃ is added).
5. Extract organic phase and set aside. Discard aqueous phase.
6. Prepare ~30mM AgNO₃ in water (0.0764g NaNO₃ in 14mL H₂O).
7. Add 7.5mL of 30mM AgNO₃ solution to the organic solution.
8. Stir vigorously for 45 minutes.

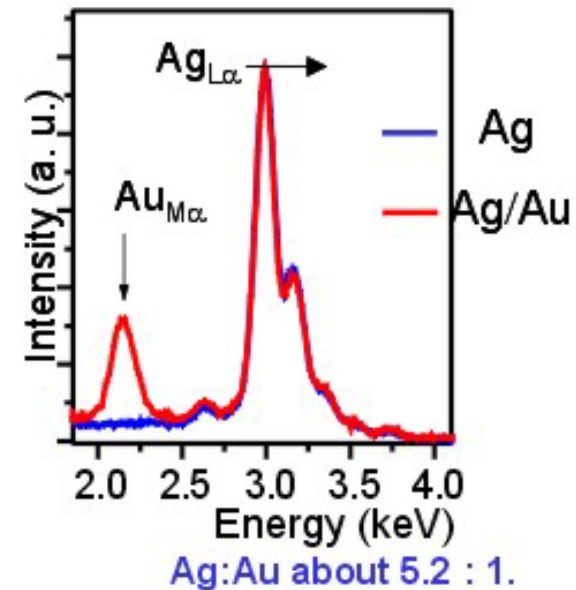
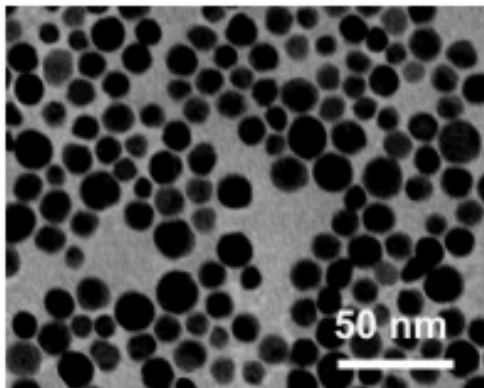
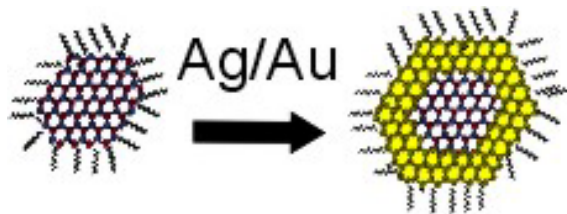
Part 2 of Silver Nanocrystals Synthesis.

9. Extract organic phase (discard aqueous layer).
10. Add 0.16mg (~0.189mL) of 1-dodecanethiol to organic solution (to cap the silver)
11. Stir vigorously for 15 minutes.
12. Meanwhile, prepare ~0.4M NaBH_4 in water (0.3783g NaBH_4 in 24mL H_2O).
13. Add 6.25mL of the NaBH_4 , dropwise over a 35min. period, to the solution containing the silver (organic layer), while stirring vigorously.
14. Stir for ~15 hours (overnight).
15. Extract organic layer (discard aqueous layer).
16. Wash organic layer 3 times with dilute ethanol.
17. Allow to settle, and extract organic layer.
18. Store in closed container.

Preparation of Au Capped Ag



1. Take 125 mL of $1.0 \times 10^{-3}\text{M}$ solution of Ag colloids and add 12,5 mL H_2O .
2. Heat this solution until it comes to a boil and then add the appropriate amount of $5.0 \times 10^{-3}\text{M}$ HAuCl_4 . (For example: $50\mu\text{L}$, $100\mu\text{L}$, $150\mu\text{L}$, $300\mu\text{L}$, and $500\mu\text{L}$)

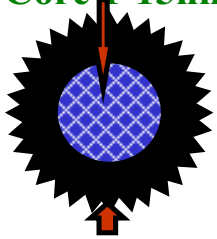


Magnetic Nanocrystals and Nanocrystal Superlattices

C.B. Murray, S. Sun, F. X. Redl, K. S. Cho and W. Gaschler.

IBM T. J. Watson Research Center; Yorktown Heights, NY

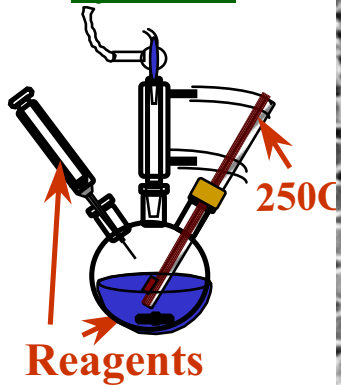
Inorganic
Core 1-15nm



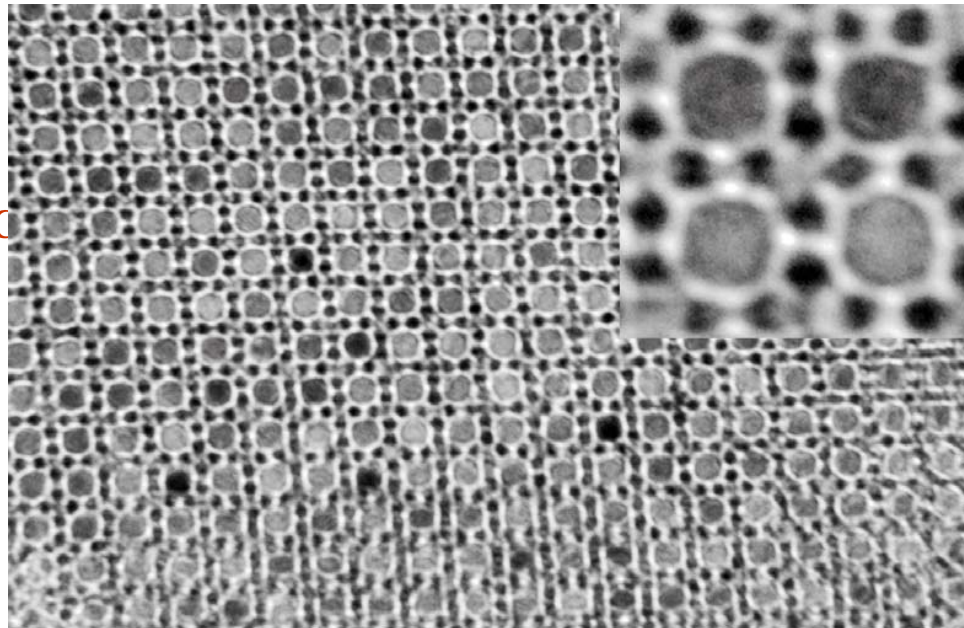
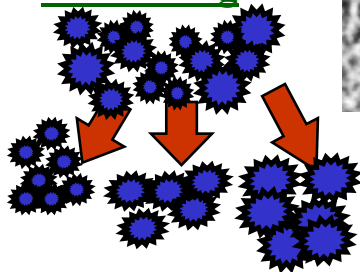
Surfactants
1-4 nm thick

- (1) Synthesize, characterize and integrate nanostructured materials.
- (2) Probe the limits conventional materials/device scaling.
- (3) Harness mesoscopic properties for future technology.
- (4) Explore the potential of self-assembly for nanofabrication.

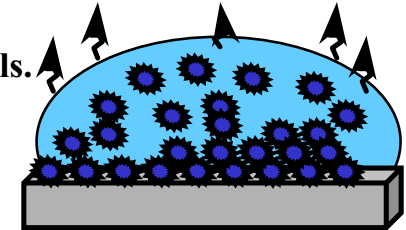
Synthesis



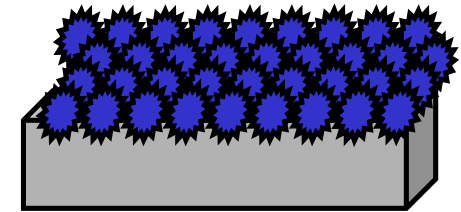
Size Selective
Processing



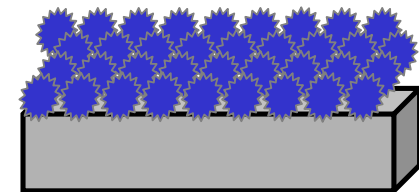
Film Growth:
Self-Assembly



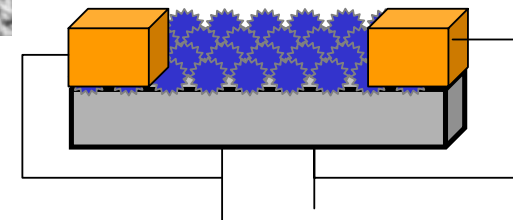
Nanocrystal Superlattice



Annealed Superlattice

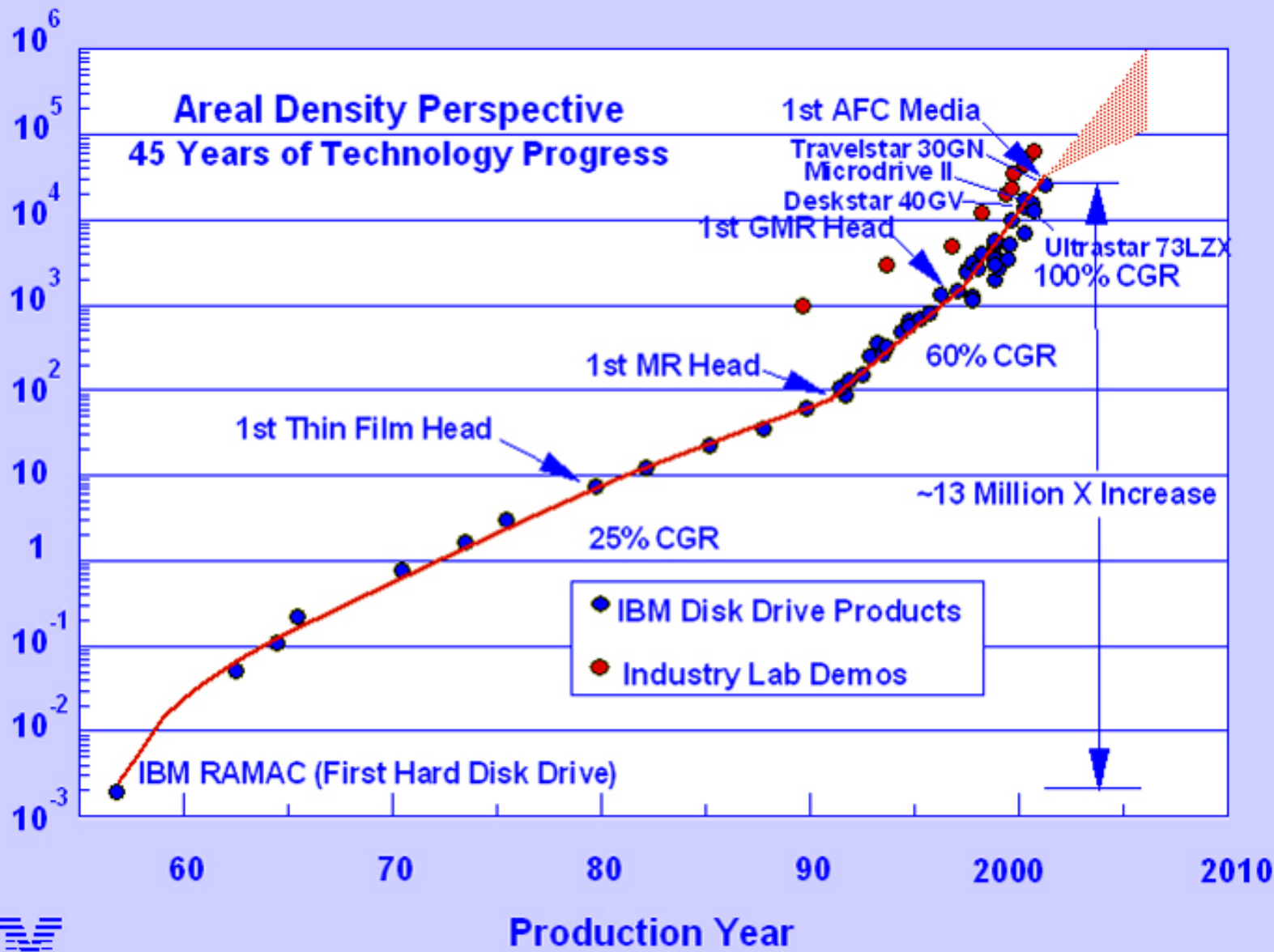


Patterning & addressing



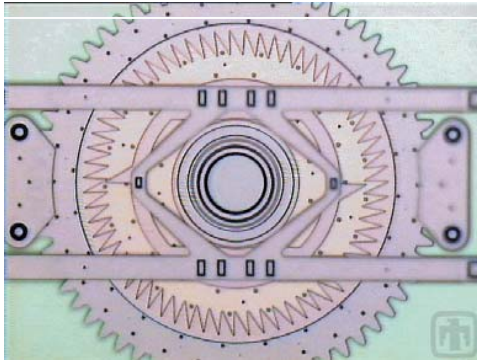
Areal Density Megabits/in²

arpers2001an.pptz



Ed Grochowski at Almaden

Applications & Opportunities for High Energy Product magnets.



Micro/Nano Devices



Automotive and Avionic Components



Medical diagnostic system



**Hard disk drives
Head actuators**

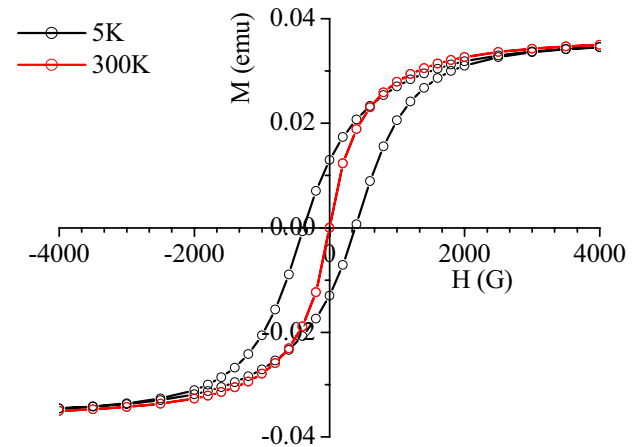
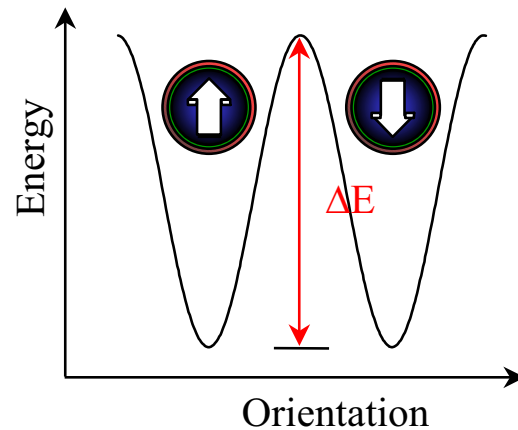


**Various actuators
in acoustic systems**

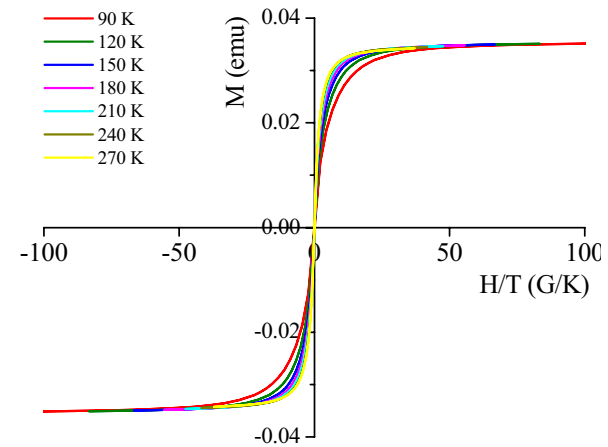
Superparamagnetism

- Single magnetic domain particles.
- Orientation determined by anisotropy energy, K .
- Energy barrier, $\Delta E = KV / k_B T$
- Remnant magnetization, M_{rem}

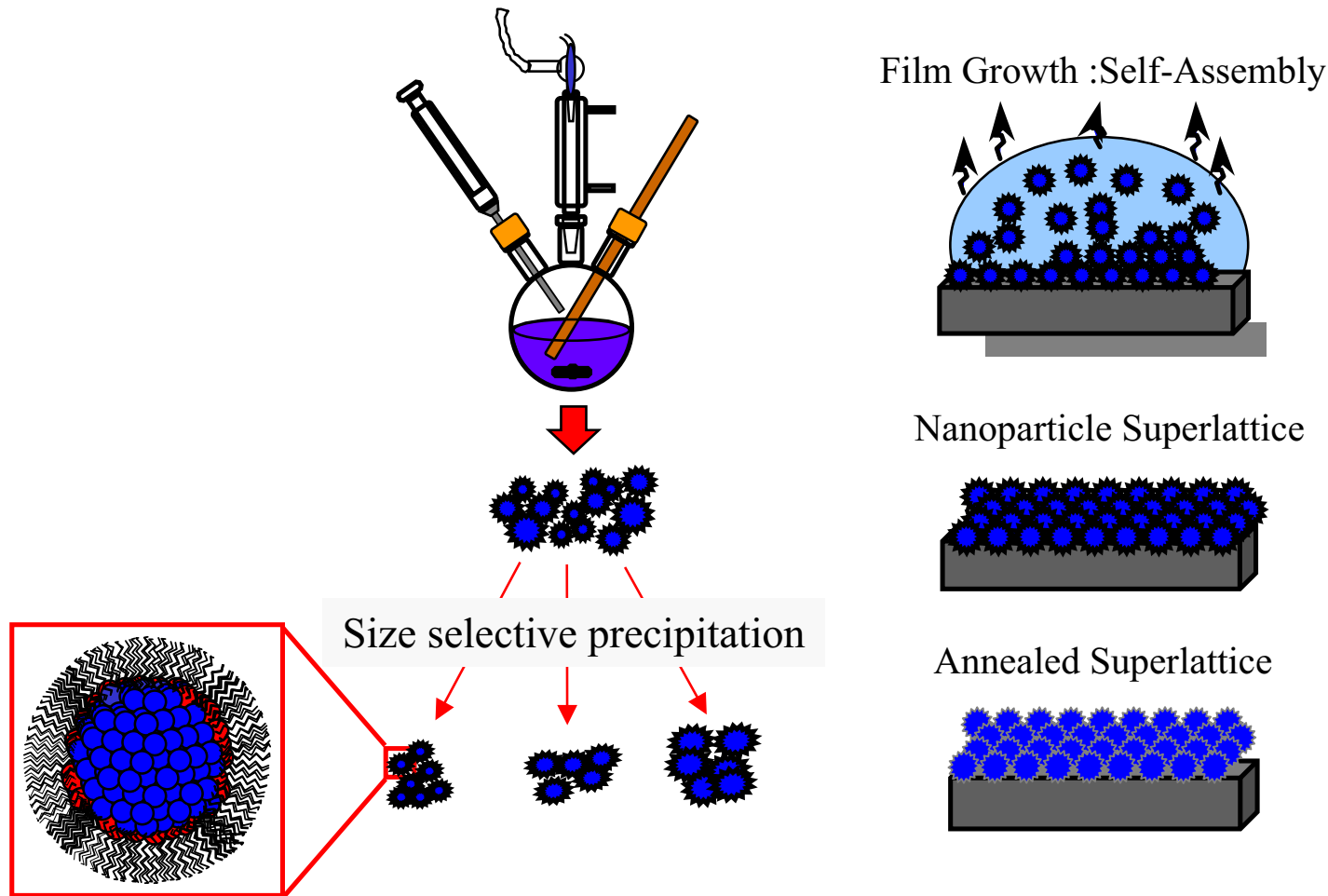
$$M_{rem}(t) = M_{sat} e^{-t/\tau} \text{ where } \tau = \tau_0 e^{-KV/k_B T}$$
- Blocking temperature, $k_B T_B \approx 25\Delta E$
- At $T \gg T_B$, particles are superparamagnetic.
- Zero hysteresis – Langevin equation
 - $M(H) = \coth(\mu H / k_B T) - k_B T / \mu H$
- At $T \ll T_B$, particles are ferromagnetic.



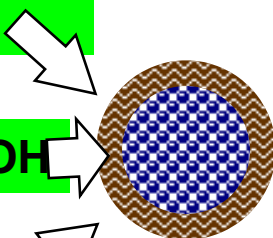
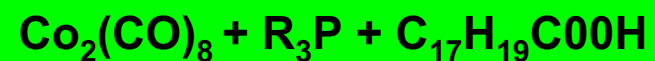
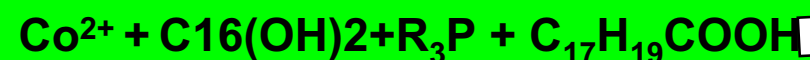
8nm MT Co



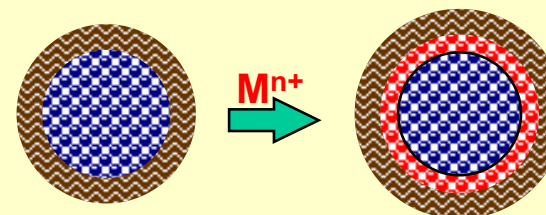
Magnetic Nanoparticles synthesis and self-assembly into thin-films



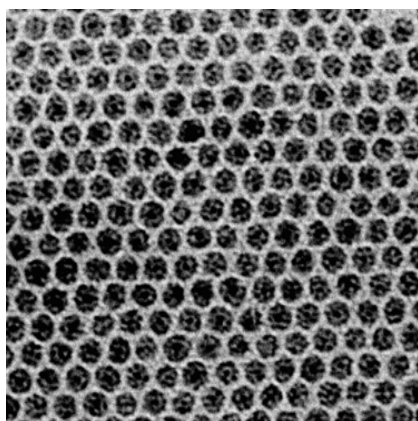
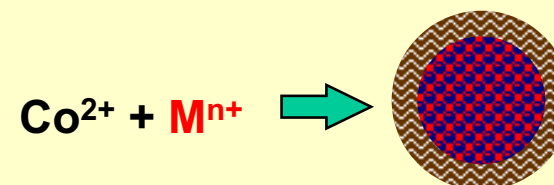
Synthesis of Transition Metal Nanocrystals



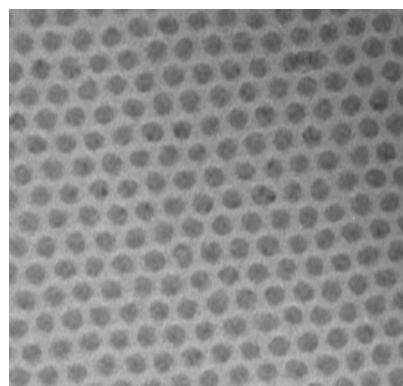
Sequential reduction of metals Core/Shell



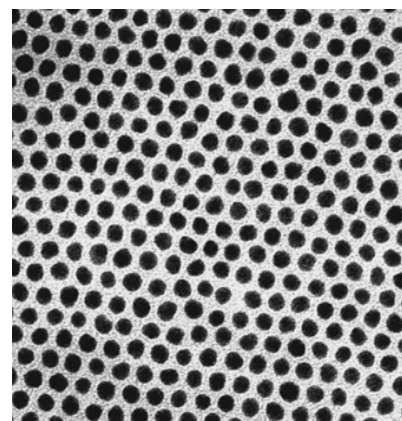
Simultaneous reduction of metals alloys



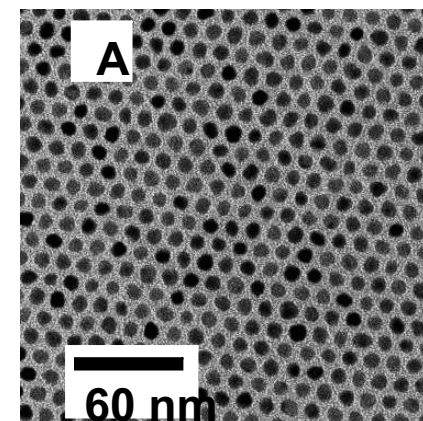
Co 8 nm



Ni 9 nm

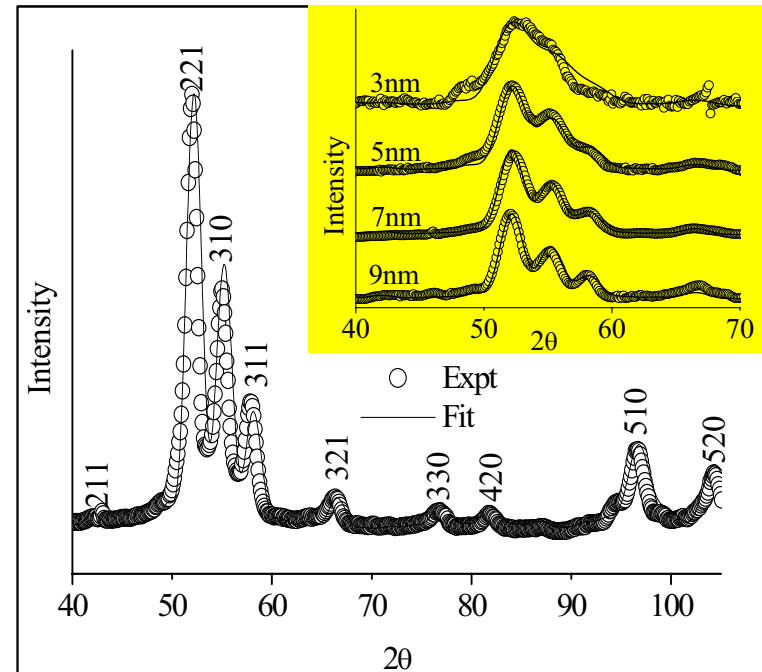
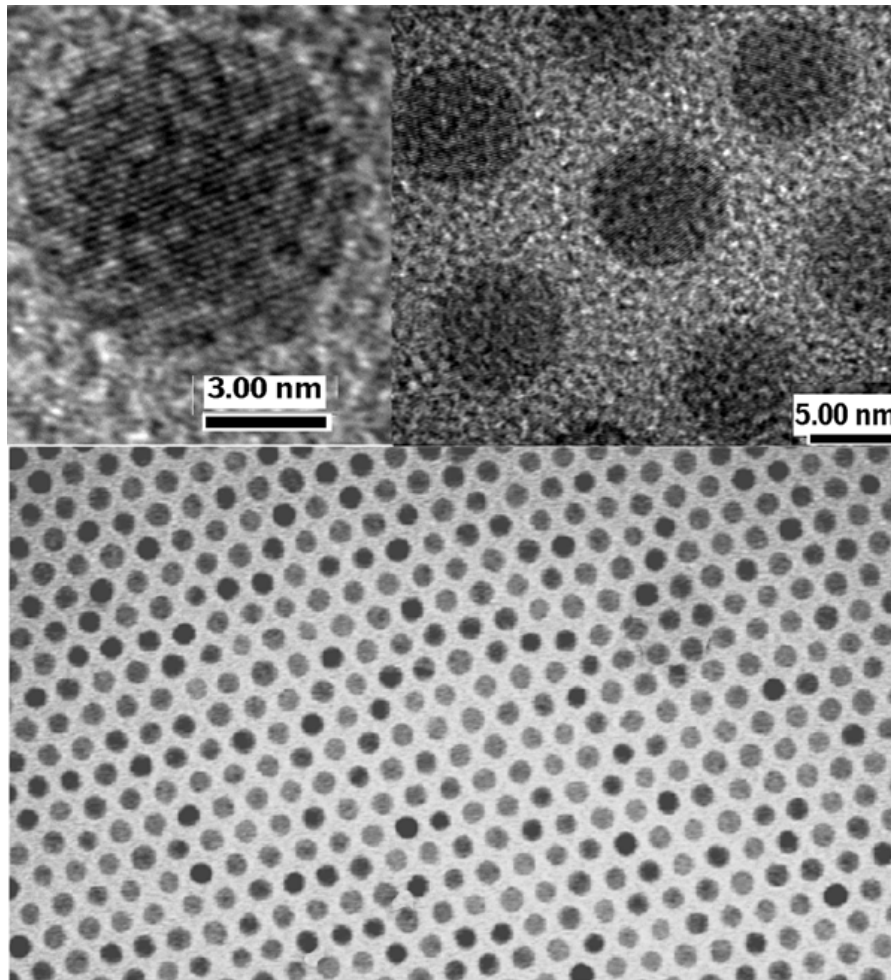


Co/Ni 9 nm

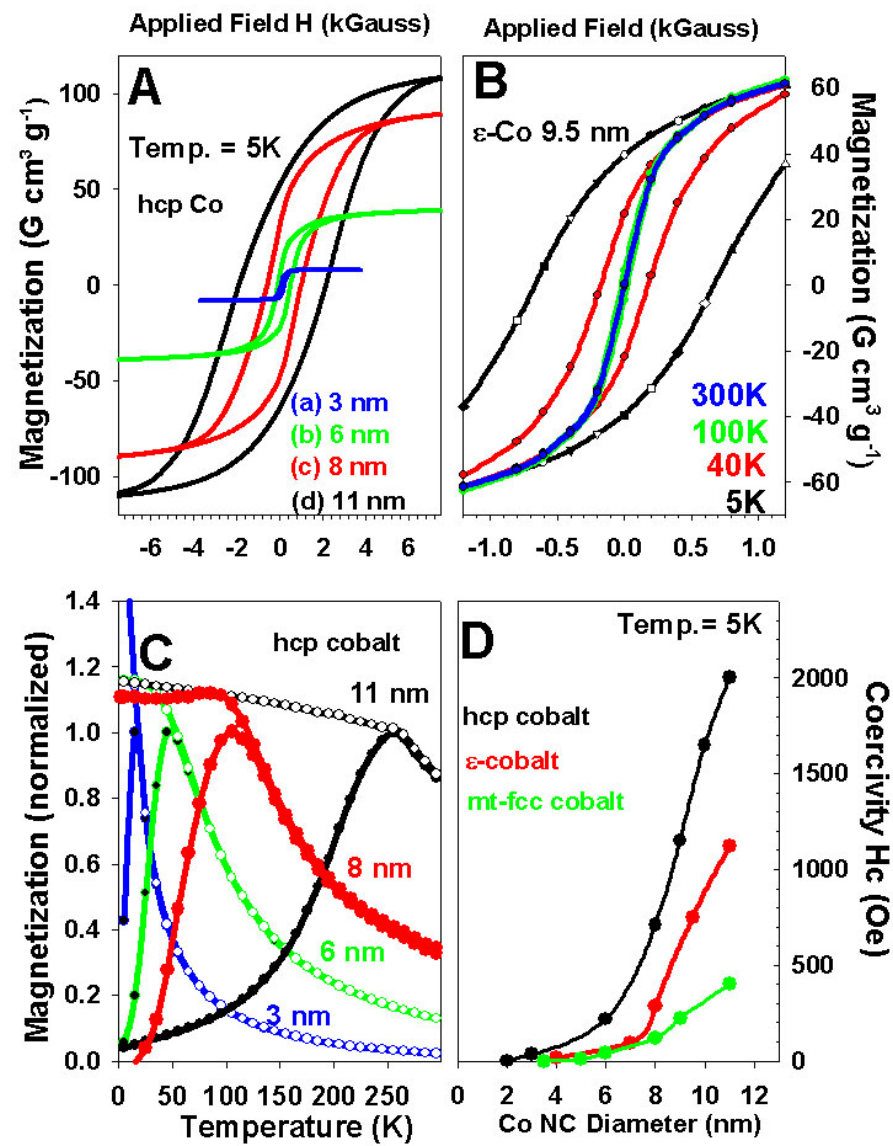


FePt 4 nm

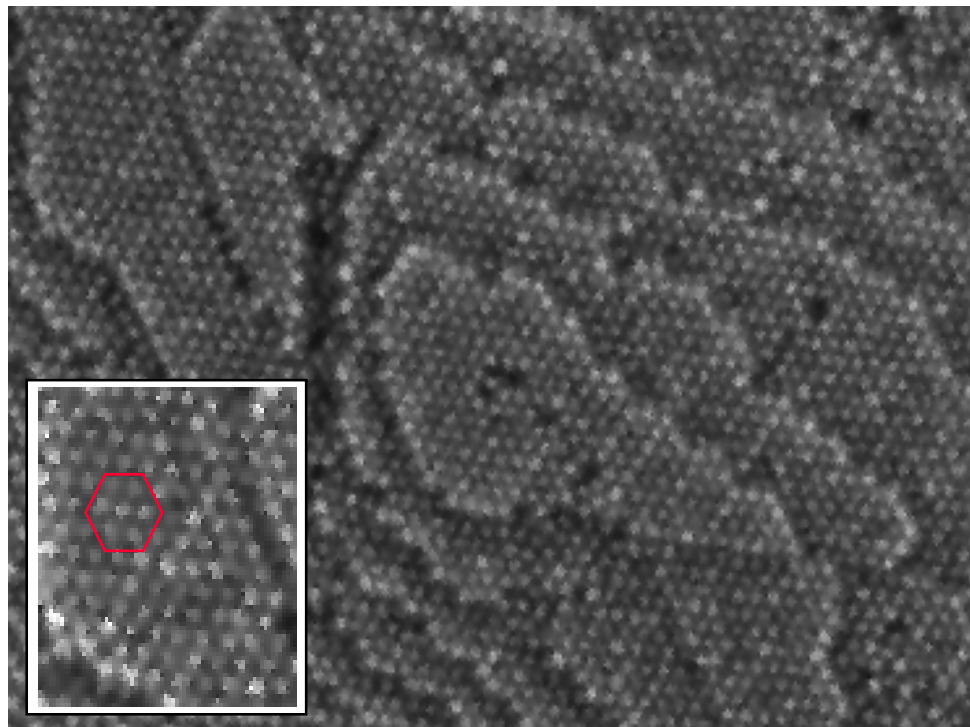
XRD Modeling of ϵ -Co nanoparticles



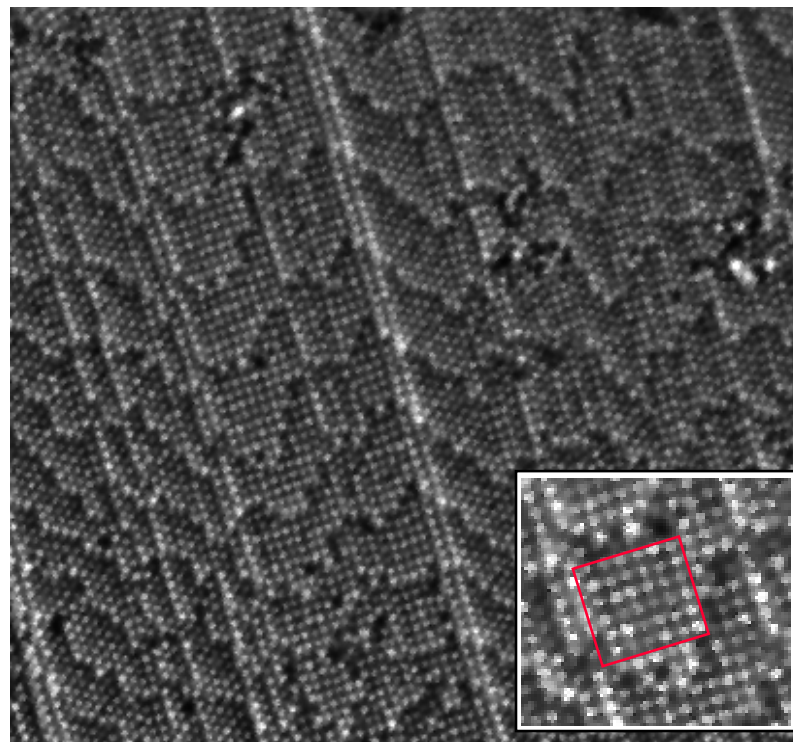
- TEM images show that ϵ -Co forms as spherical nanoparticles with narrow size distributions.
- XRD fits - perfect crystalline internal structure.
- Supported by HR-TEM images of individual nanoparticles.



Cobalt Nanocrystal Superlattices (T. Betley et al)

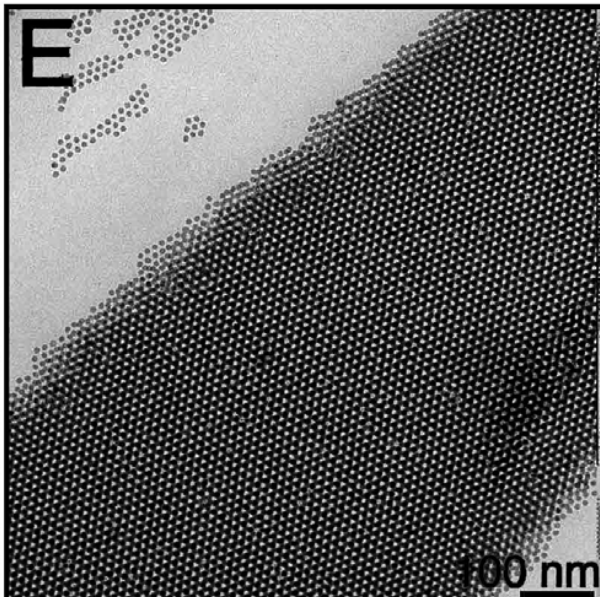
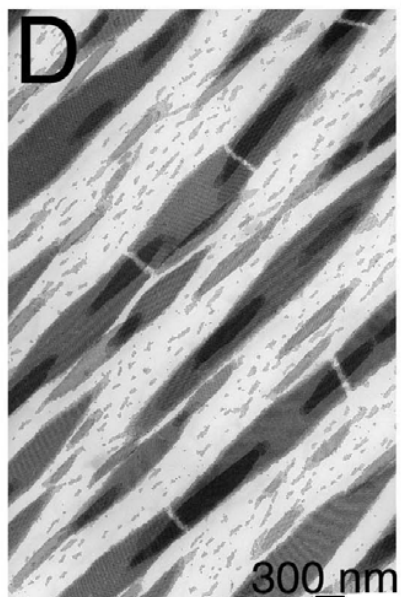
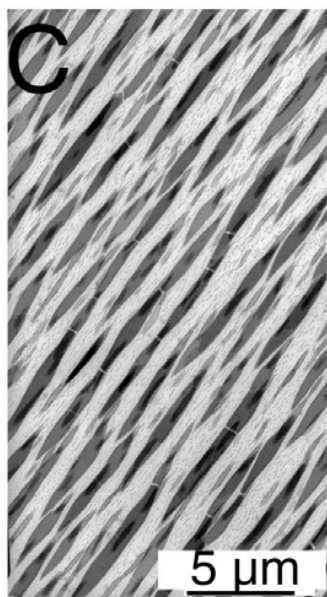
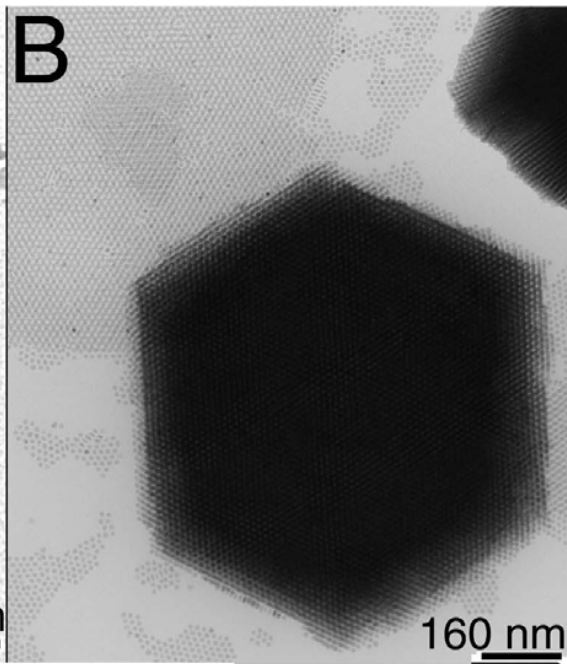
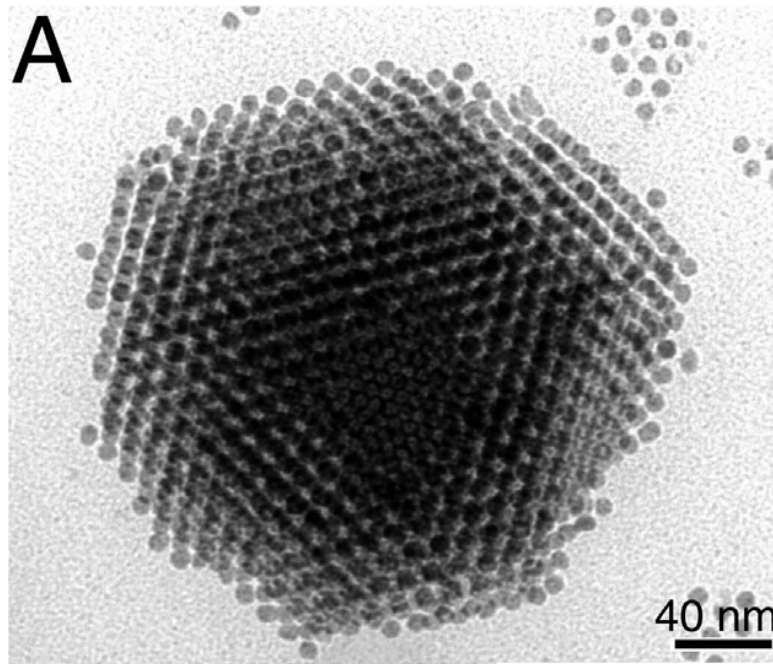


Hexagonal packing

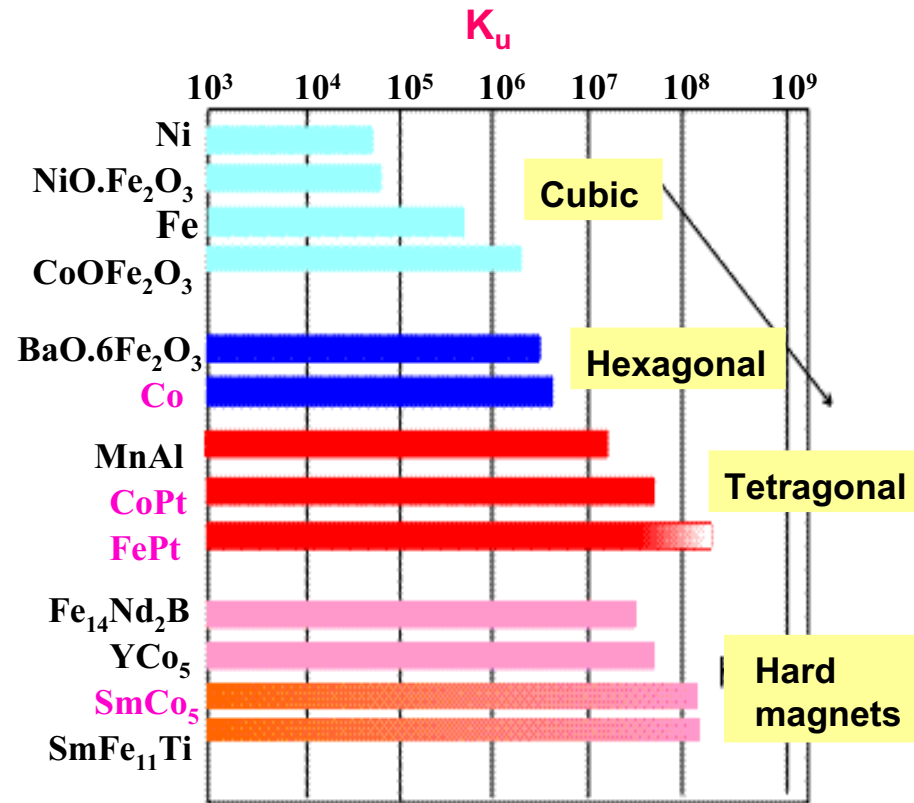


Cubic packing

10 nm Cobalt NCs



Materials Selection: $K_u V \gg kT$

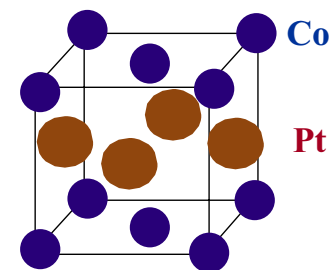


$K_u V \gg kT$

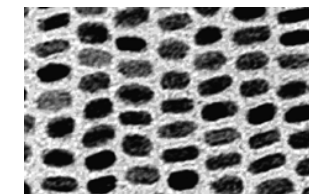


$K_u V < kT$

Crystal Anisotropy
Shape Anisotropy
Exchange Anisotropy
Strain Anisotropy



CoPt L₁₀ structure
(tetragonal)

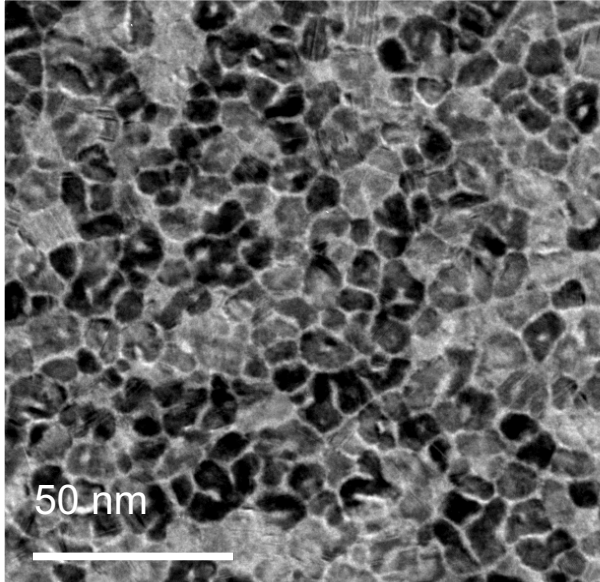


Shape ?

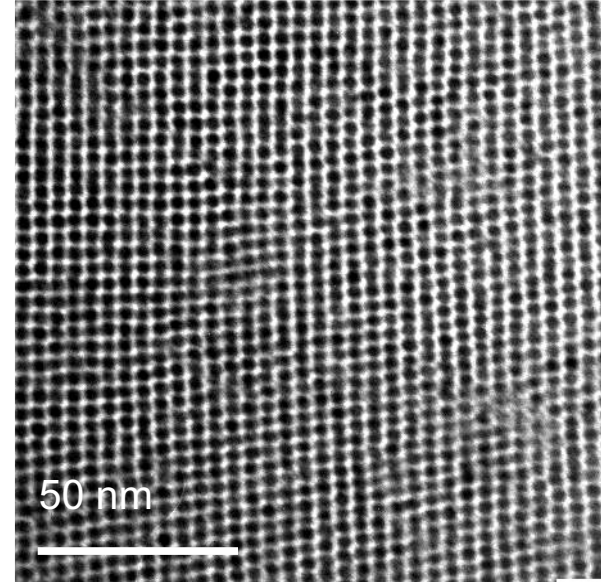
Nanoparticles for magnetic storage

- Narrow size distribution \rightarrow higher thermal stability
- Smaller particles \rightarrow narrower transition widths

35 GBit/in² prototype media
8.5 nm grains
 $\sigma_{\text{area}} \cong 0.6$

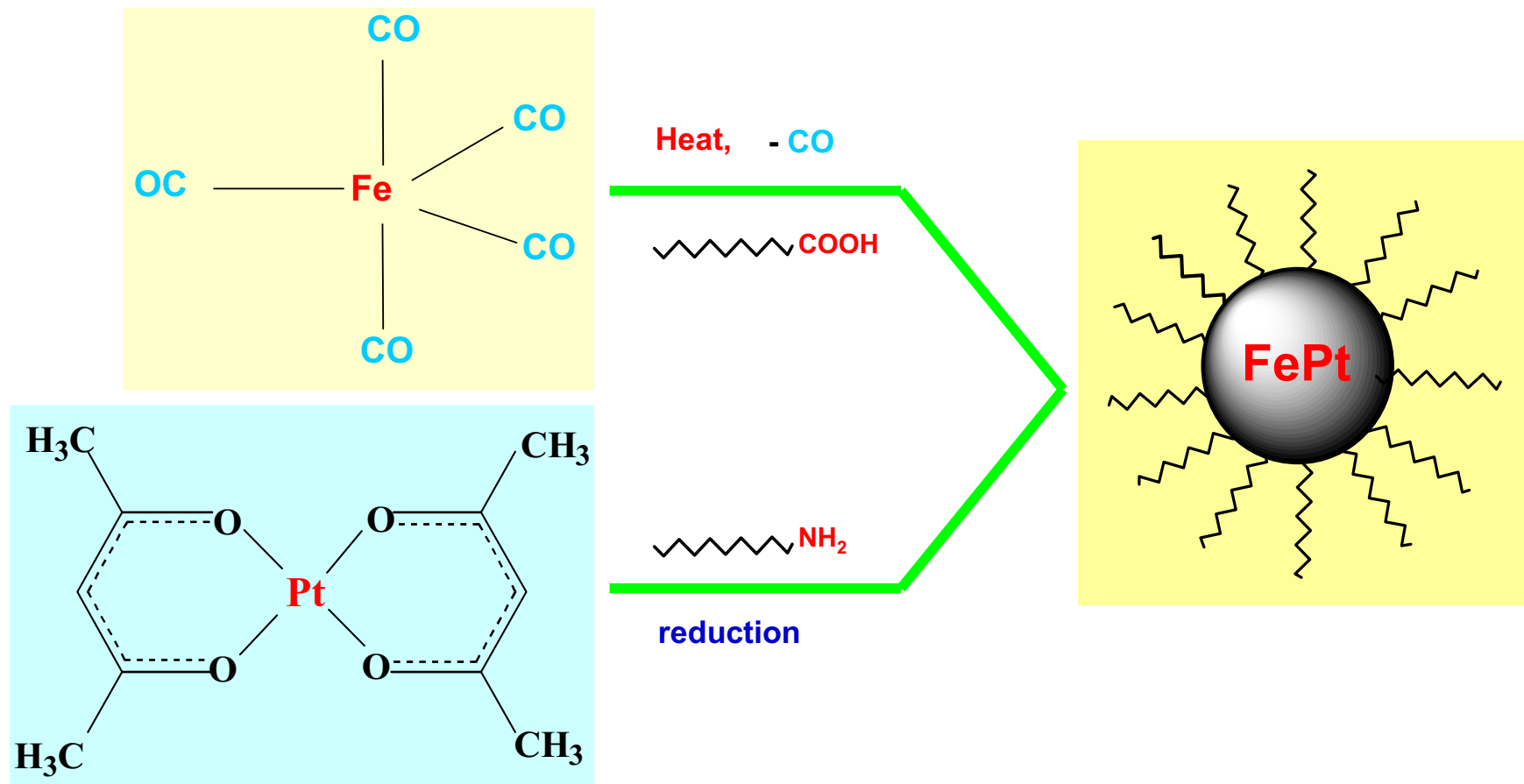


Nanoparticle arrays
4 nm FePt particles
 $\sigma_{\text{area}} \cong 0.05$

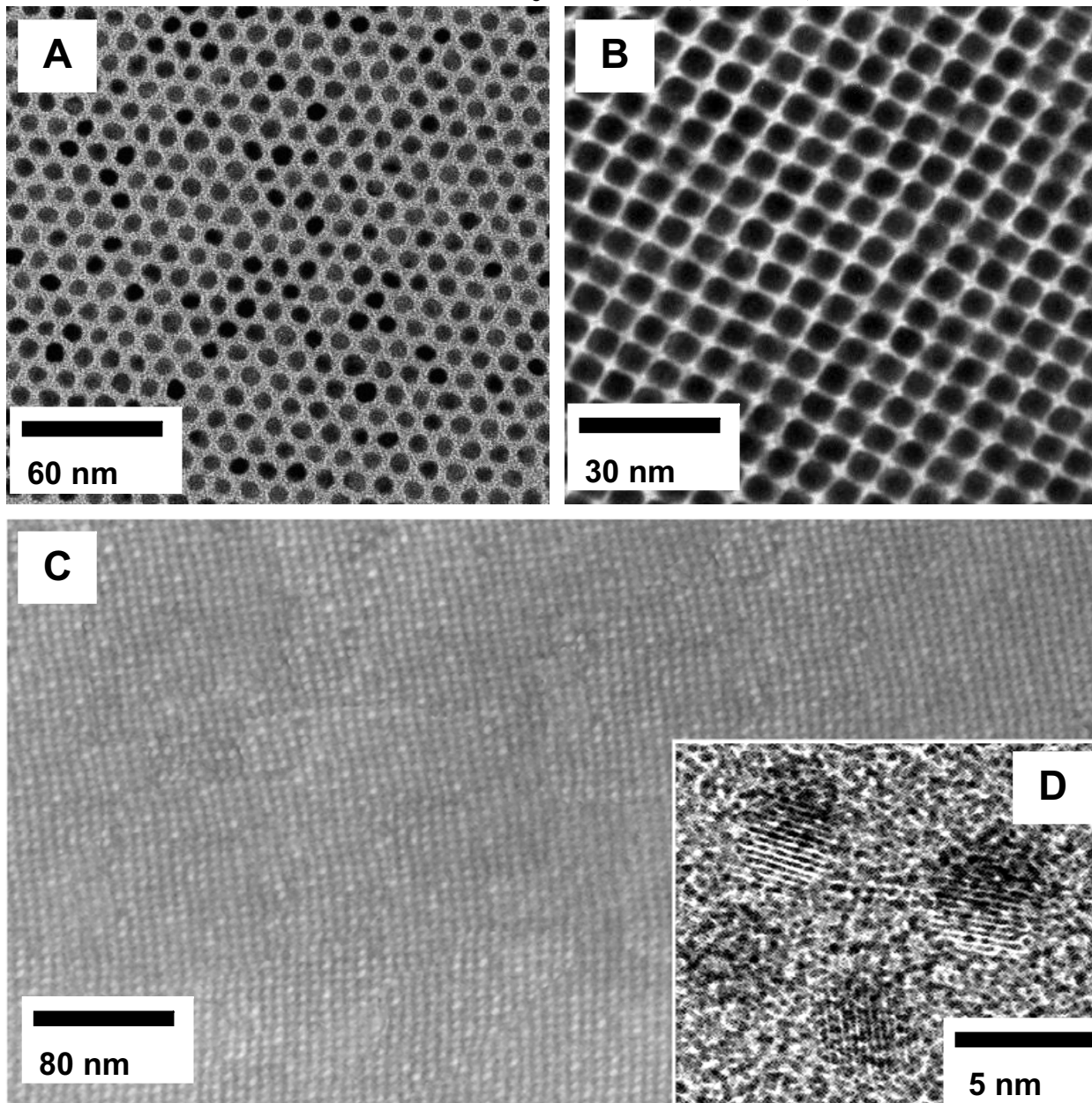


S. Sun, Ch. Murray, D. Weller, L. Folks, A. Moser,
Science, 287 (2000) 1989

FePt Nanoparticle Synthesis

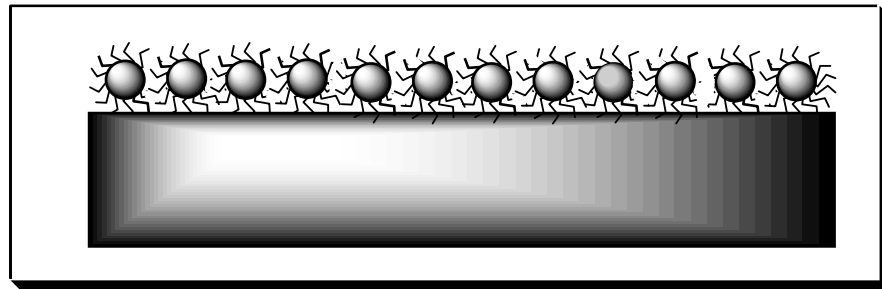


FePt Nanocrystals (4 nm)

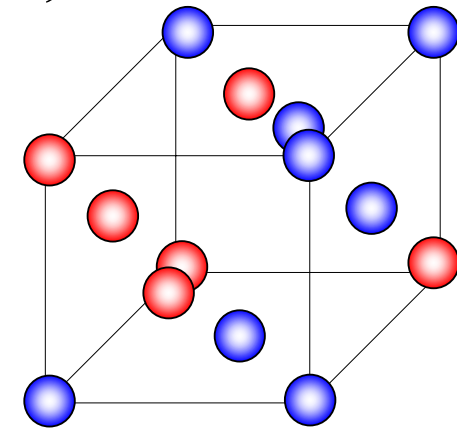


Magnetic properties

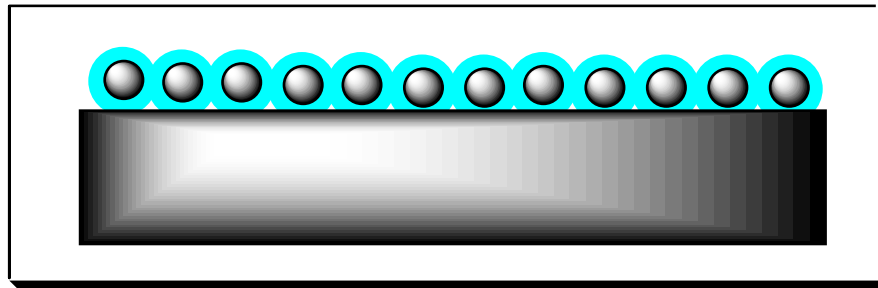
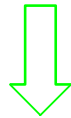
- Annealing leads to formation of ordered, ferromagnetic phase



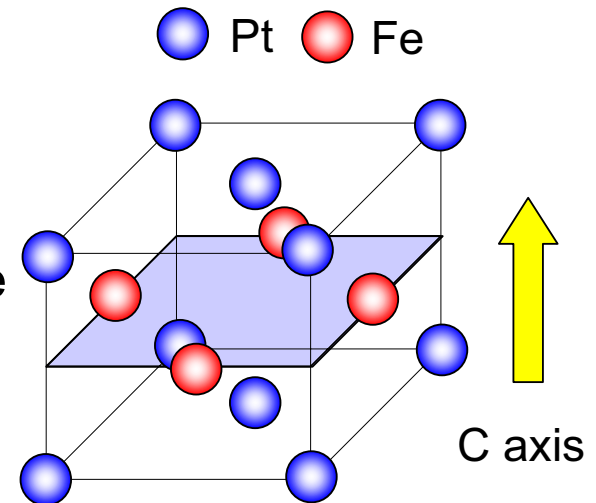
Chemically disordered
fcc structure
Superpara-
magnetic



Annealing at 550C



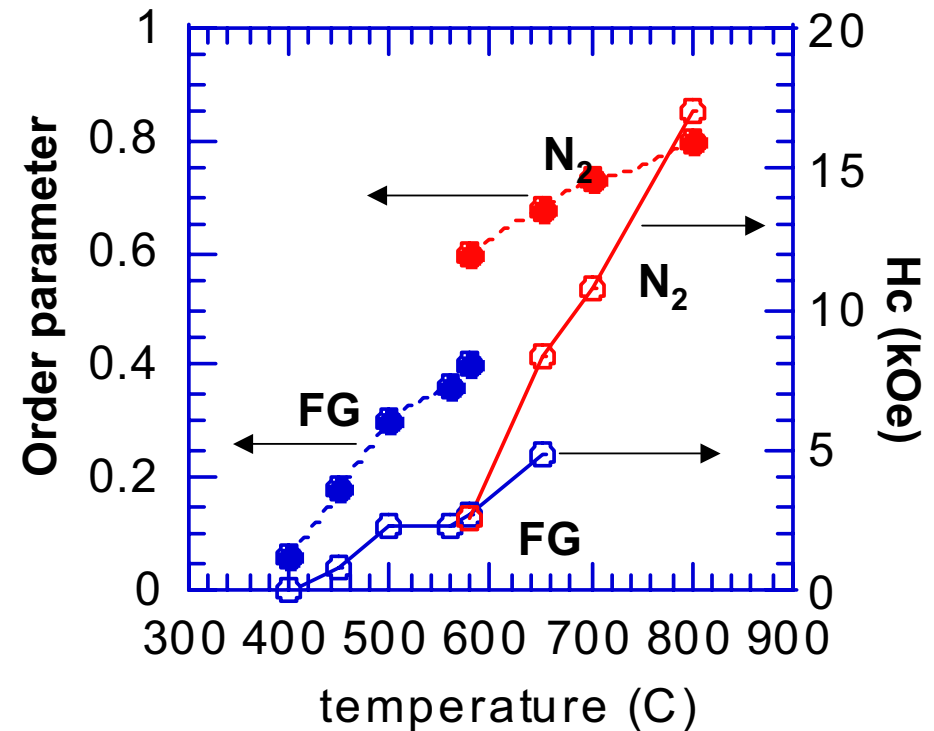
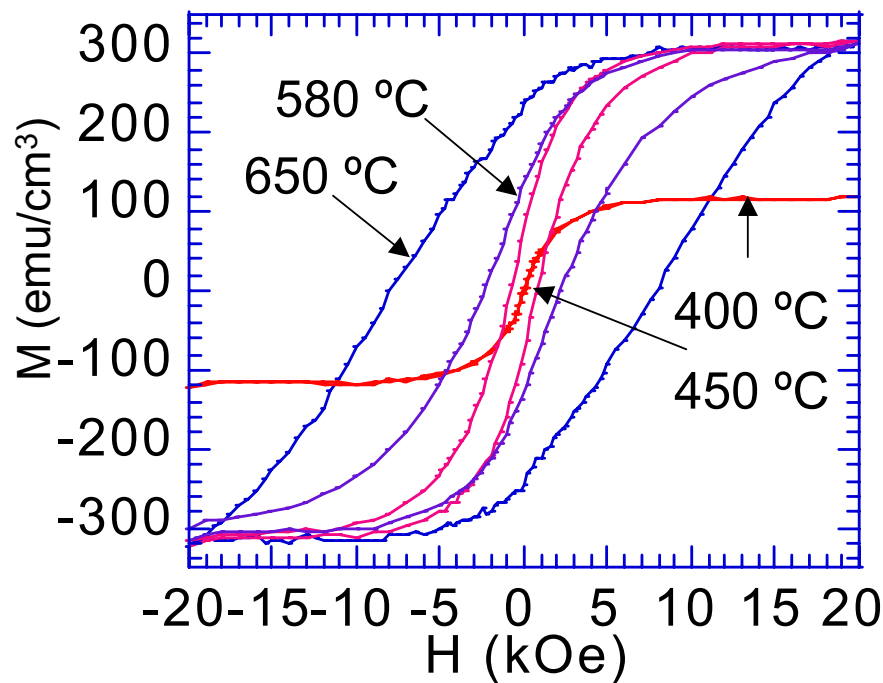
Chemically
ordered
fct structure
Ferro-
magnetic



Magnetic properties

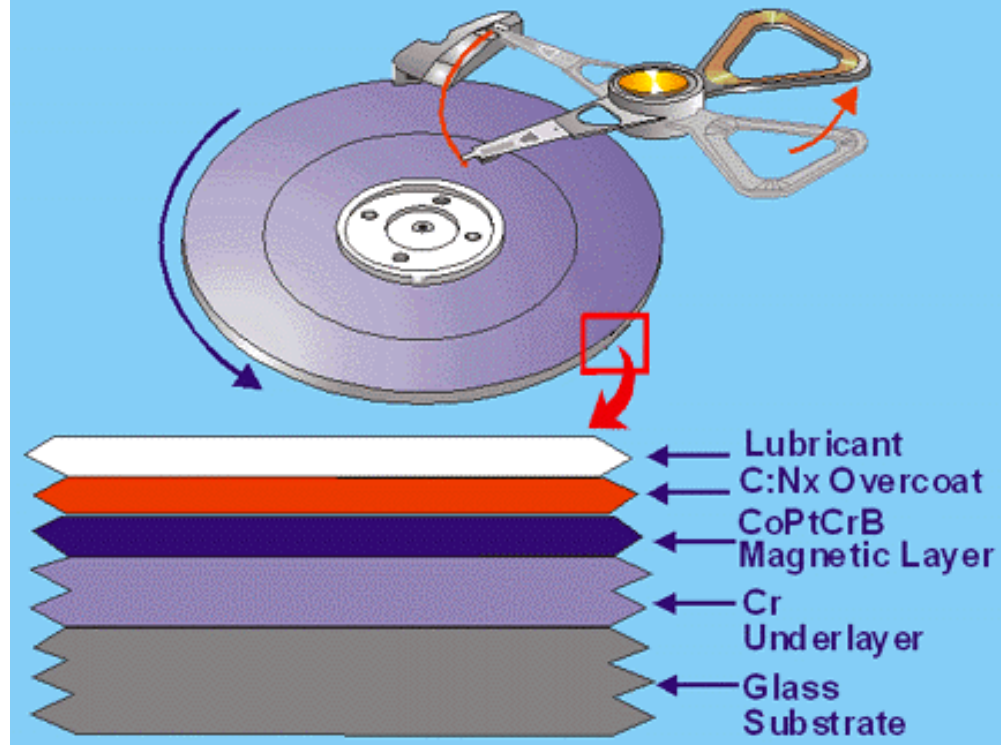
- Order parameter and coercivity increase with annealing temperature and duration

3 layer samples of 6 nm FePt particles



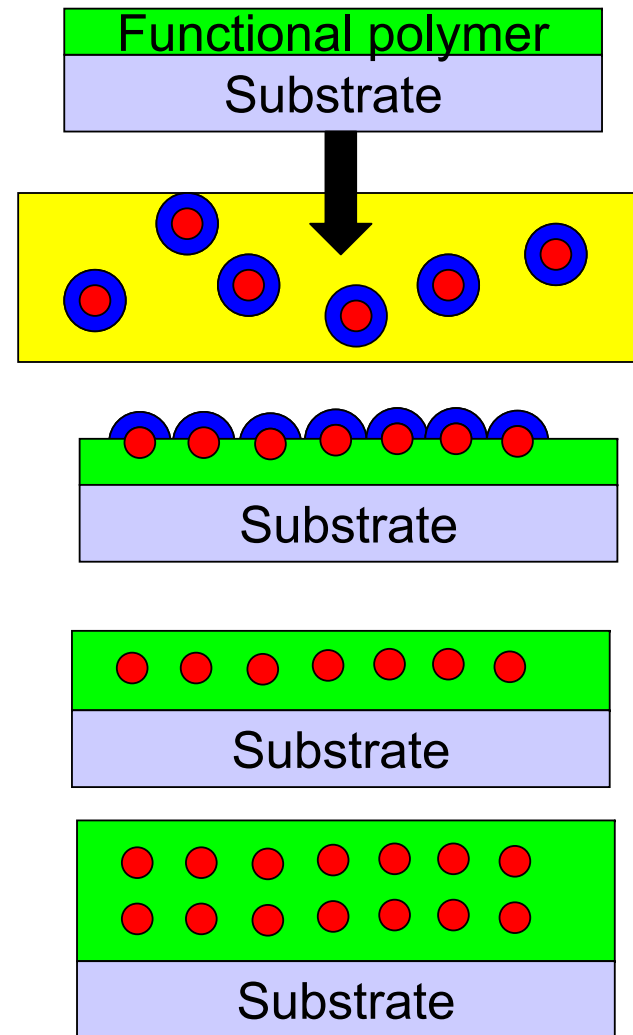
XRD data M. Toney, IBM Almaden

Disk Technology

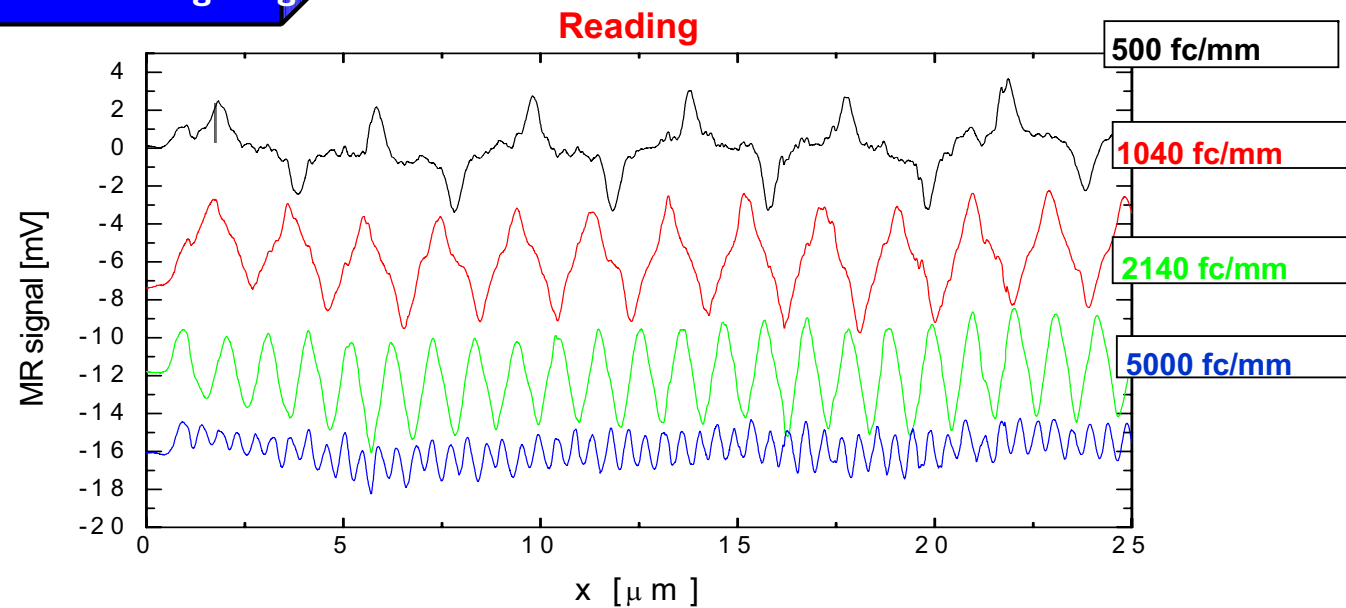
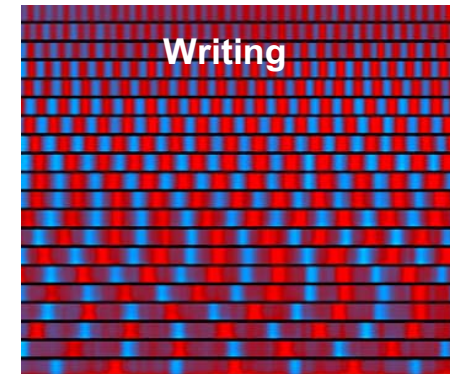
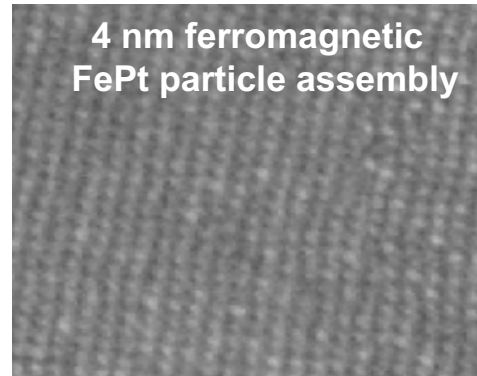
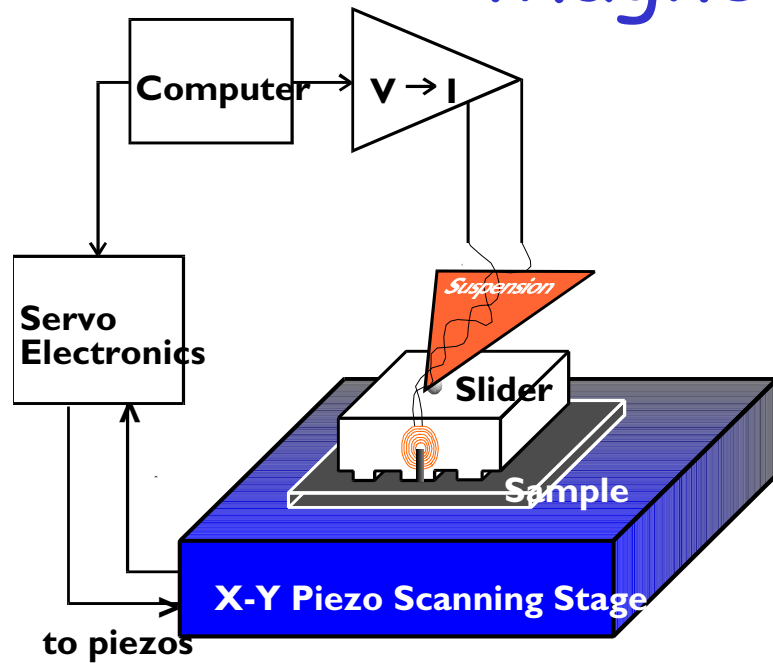


Polymer-mediated self assembly

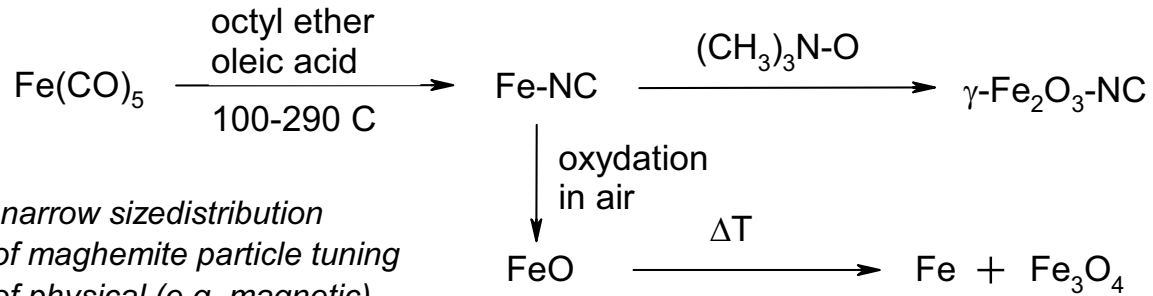
- Substrate surface is functionalized
- Dipped into dispersion of stabilized nanoparticles
- Ligand exchange leads to formation of strongly bound layer of nanoparticles



Magnetic recording

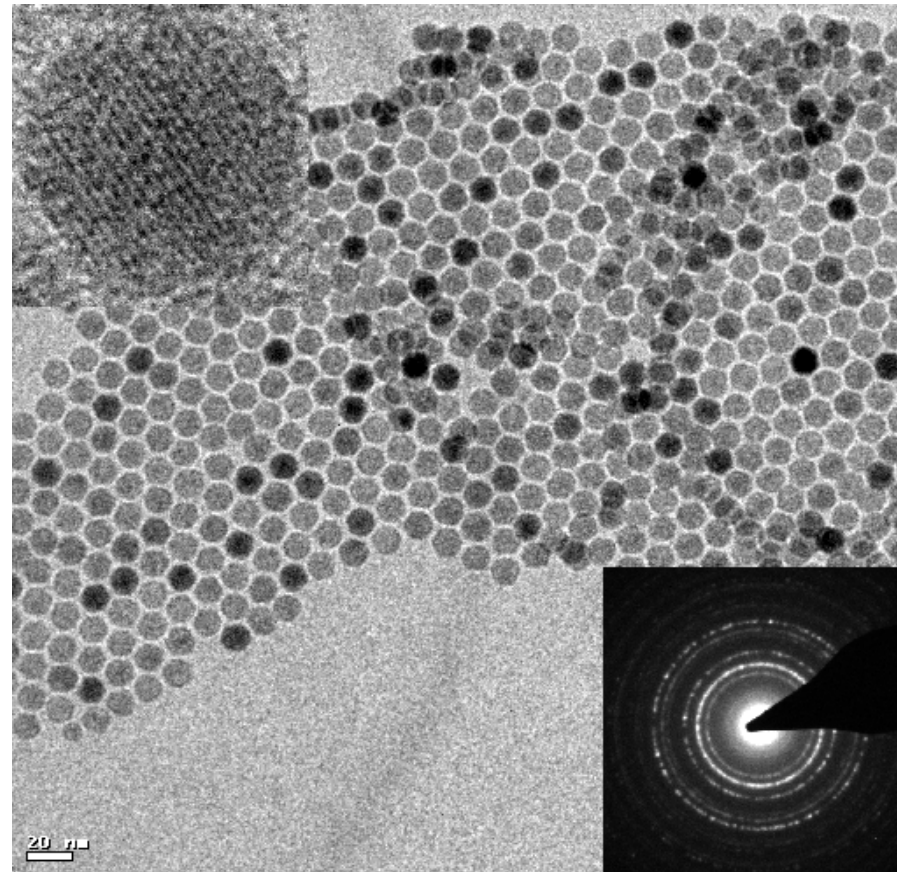
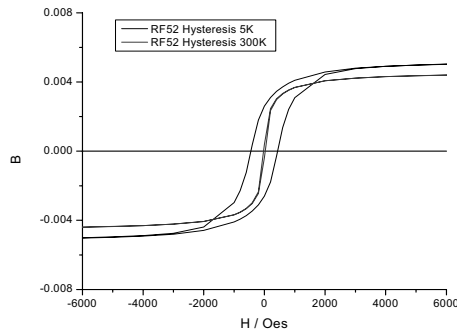
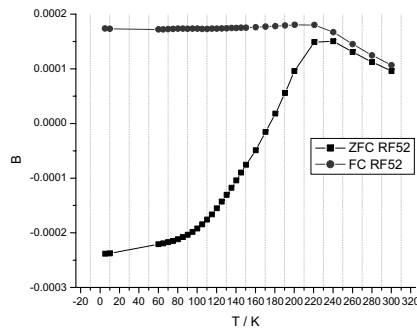


Synthesis and Characterization of Iron Oxide Nanoparticle



*narrow sizedistribution
of maghemite particle tuning
of physical (e.g. magnetic)
properties.*

*RF & Microwave
Bio applications.*



Fe₃O₄ Nanocrystals

(Sun and Zeng)

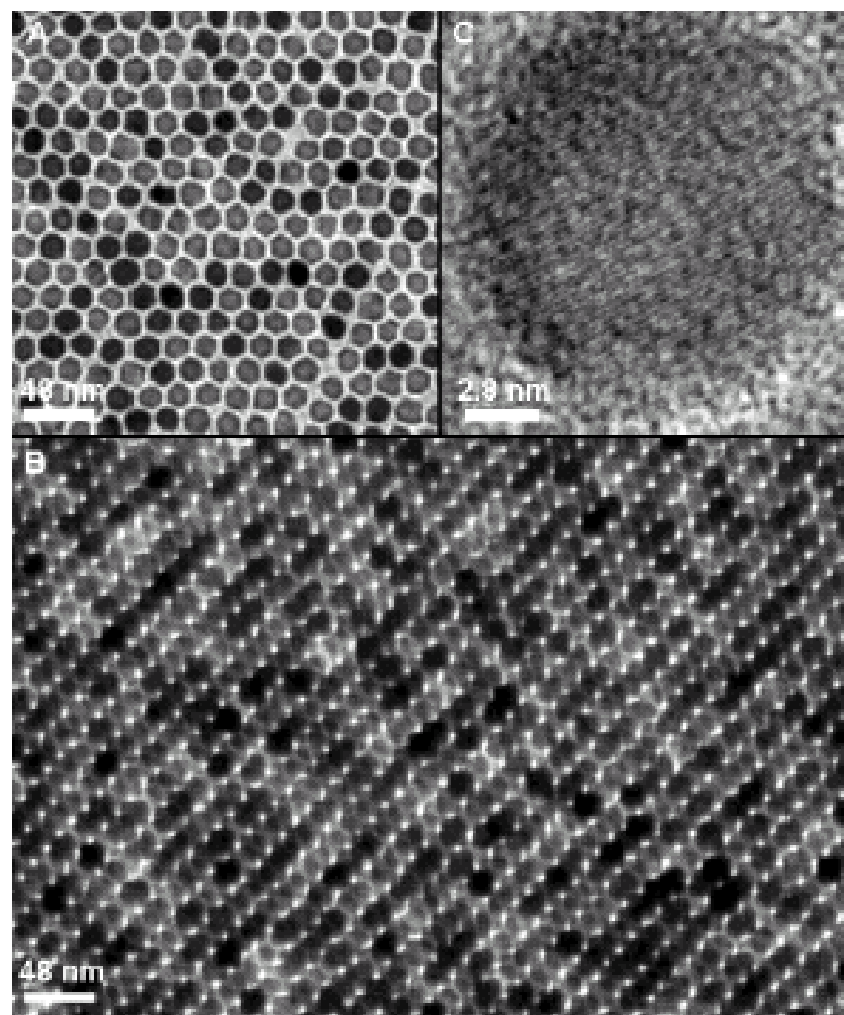
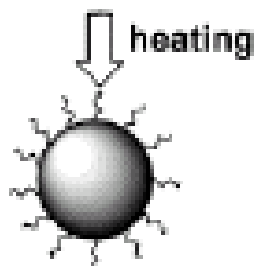
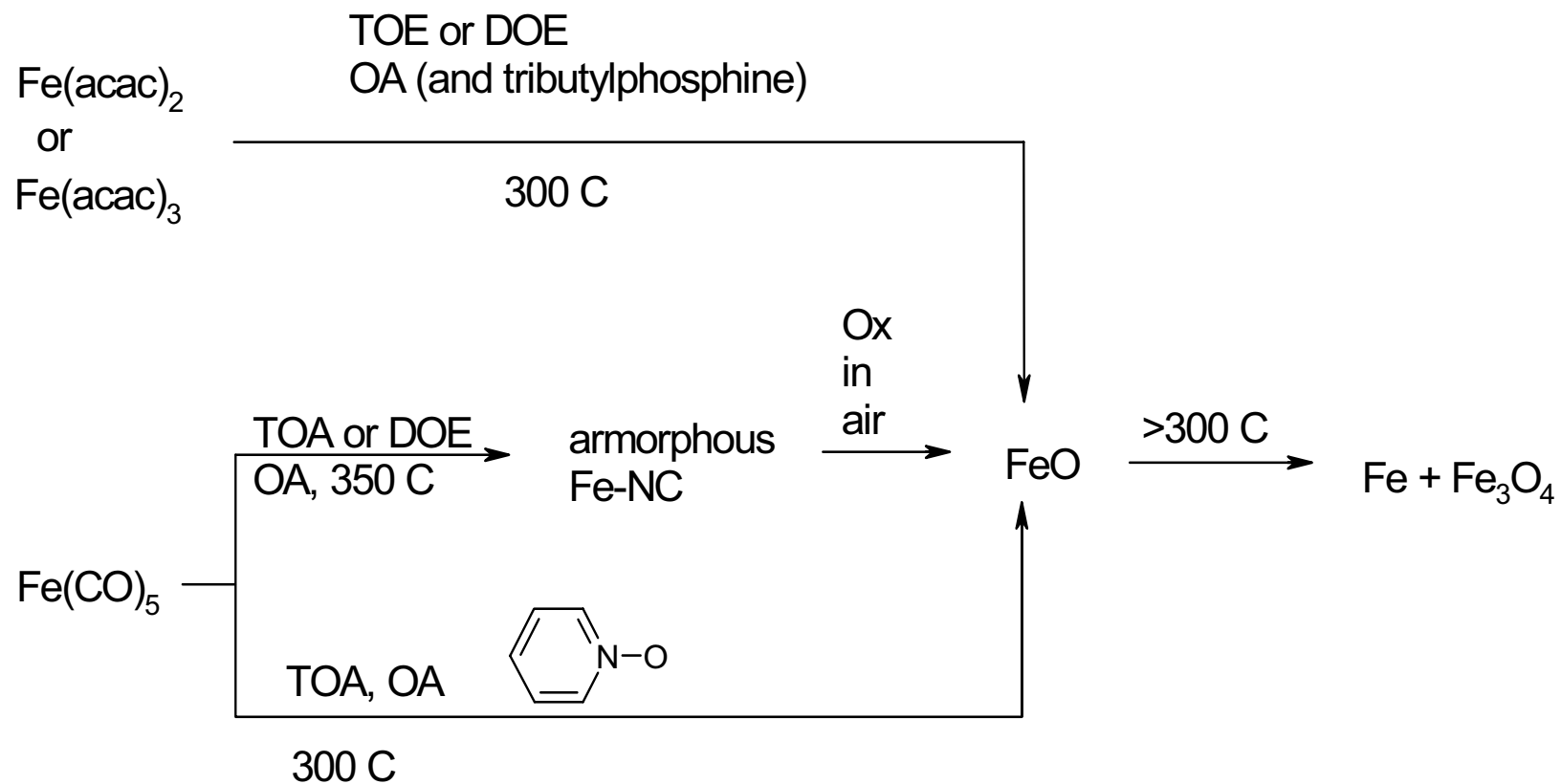


Figure 1. TEM bright field image of 16-nm Fe₃O₄ nanoparticles deposited from their dodecane dispersion on amorphous carbon surface and dried at 60 °C for 30 min: (A) a monolayer assembly, (B) a multilayer assembly, (C) HRTEM image of a single Fe₃O₄ nanoparticle. The images were acquired from a Philips EM 430 at 300 KV.



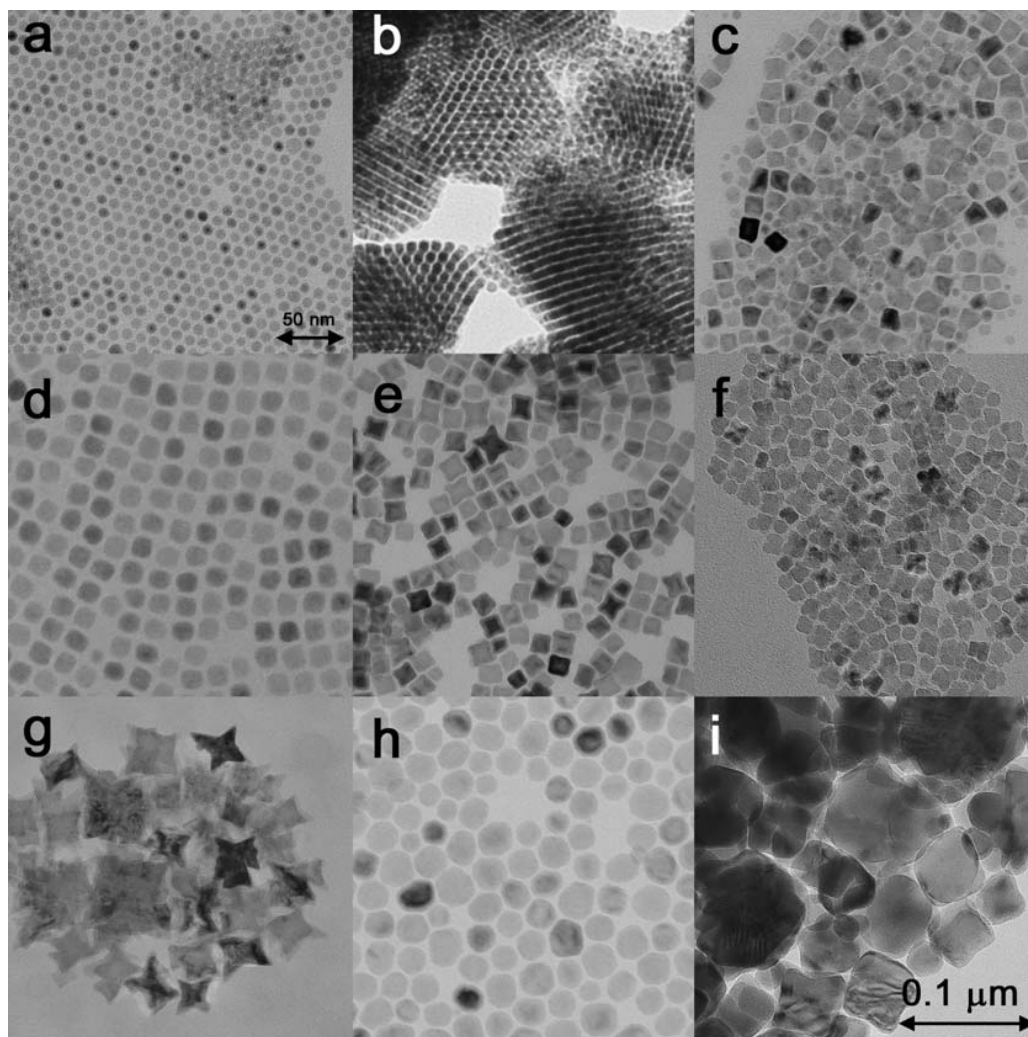
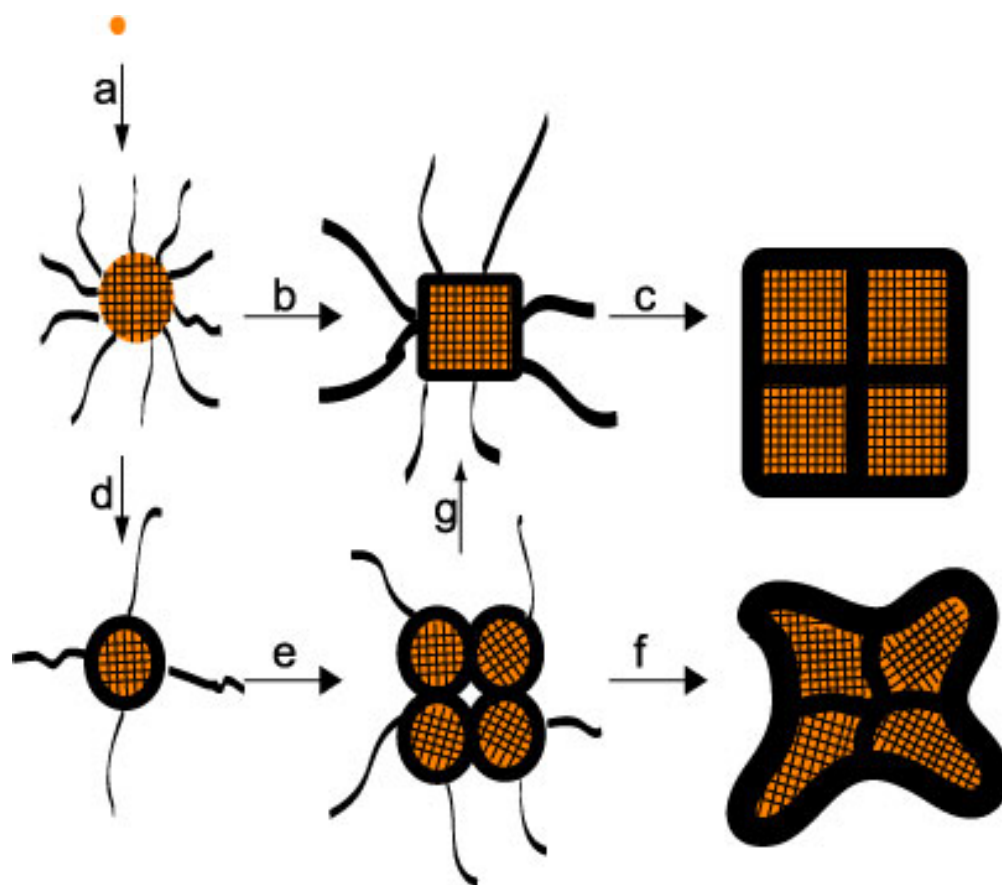


Figure 2: TEM images of nanoparticle produced by the decomposition of iron pentacarbonyl in DOE or TOA in presence of LA and PYO. a) Spherical particle of 8 nm size. b) Superlattices of 8 nm nanoparticles. c) Mixture of spherical and cubic particle, which have a diagonal length of roughly twice of the size of the spherical particles. d) Cubic particles of 13 nm edge length and 18 nm diagonal length. e) Cubic and “star-shaped” particles. f) Aggregates of spherical particles forming “cubic” particles. g) Larger “star-shaped” particles. h) Larger strongly faceted particles. d) Large cubic particles composed of α -Fe and Fe_3O_4 .



Scheme 3: Suggested model for growth of FeO particles and observed sizes. a) Particle growth after nucleation. b) Under stabilizing conditions spherical particles grow to cubes ($\{100\}$ -surfaces), the preferred shape of the rocksalt structured phase. c) Partial phase-transition of the cubic FeO particle leads to aggregation under ongoing phase transition. Larger cubes or rectangles are formed. d) Phase transition leads to a change in surface chemistry and destabilizes surfactants. e) Because of less tightly bound surfactant spherical particles aggregate. f) Annealing at high temperature leads to ongoing phase-transition and structural transformation to the star-shaped particles. g) Alternative formation mechanism of cubes by aggregation of small particles. According to particle size (crystal size) the aggregation happens randomly. The crystal size of aggregating cubes is limited by separating iron layers.

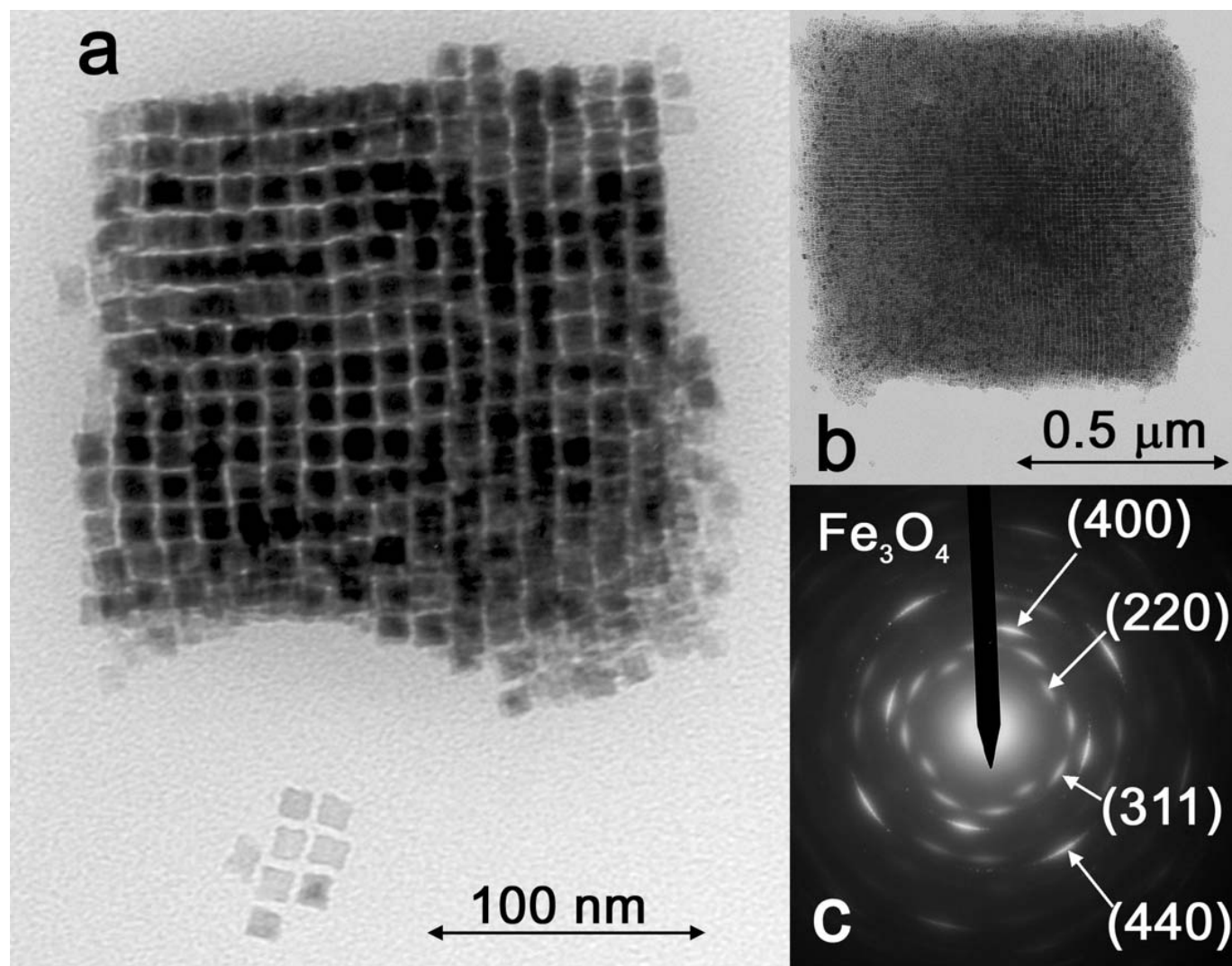


Figure 8: a) TEM image of a single cubic superlattice built of cubic FeO nanocrystals with 11 nm edge length. b) TEM image of a larger superlattice oxidized or decomposed after storage. c) SAED of the cubic superlattice in b) showing reflections for magnetite and orientational ordering in the superlattice.

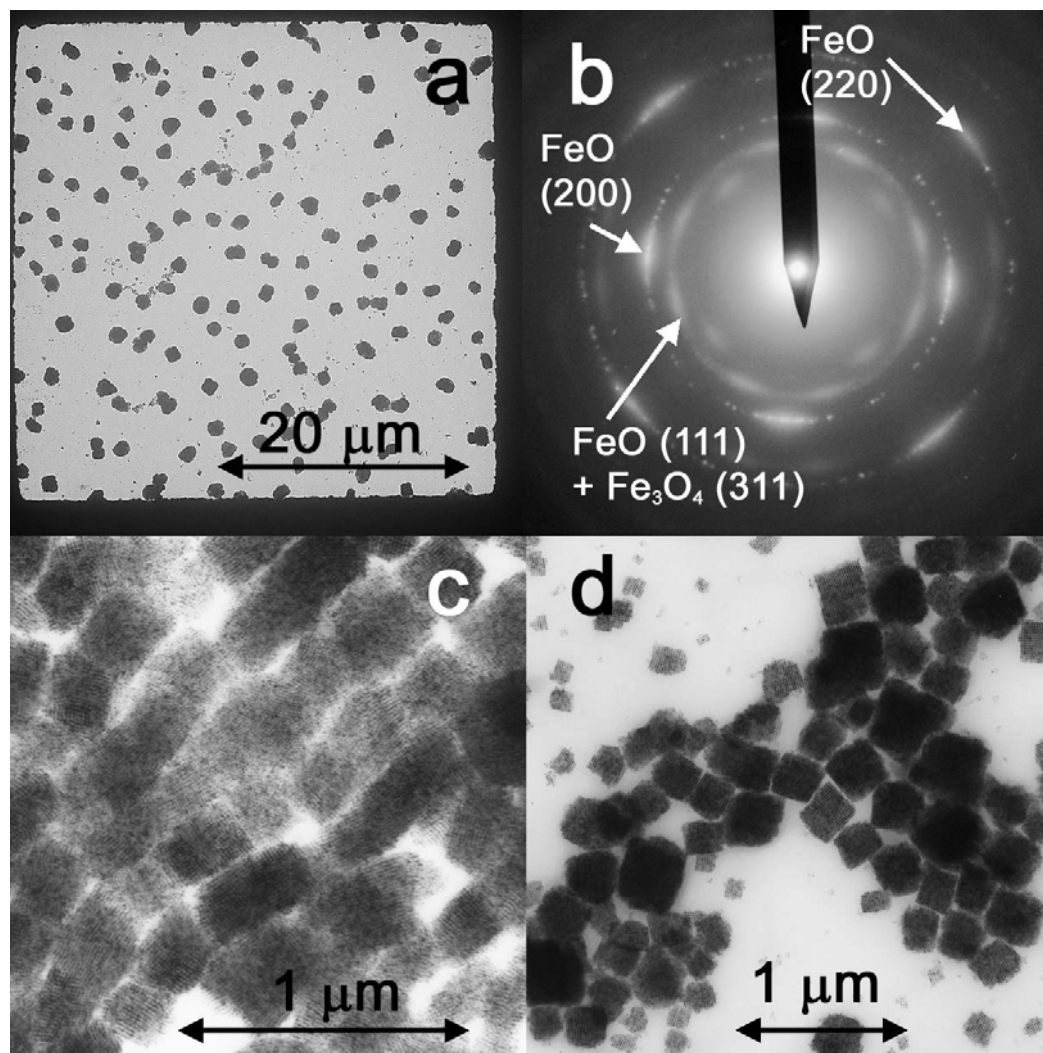


Figure 4: a) LRTEM image of a quadratic subunit of a TEM grid showing nearly cubic superlattice built up of cubic wuestite nanocrystals. b) SAED of a selected superlattice with uneven but symmetric intensity distribution caused by preferred alignment of the particles (orientational ordering). c) TEM image of aligned superlattices arising during deposition of cubic FeO nanocrystals in a magnetic field parallel to the substrate. d) TEM image of aggregated superlattices deposited without external magnetic field.

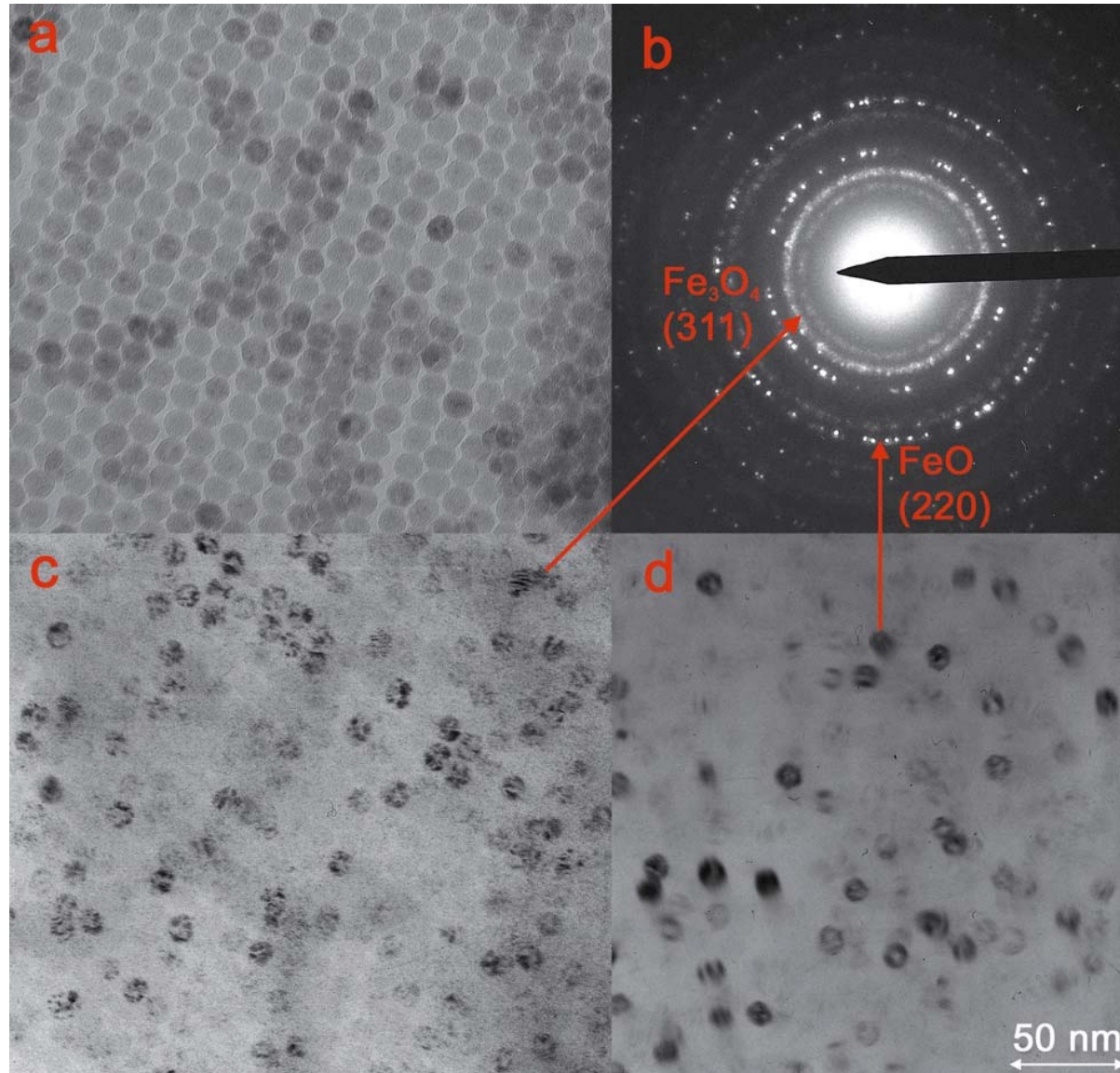
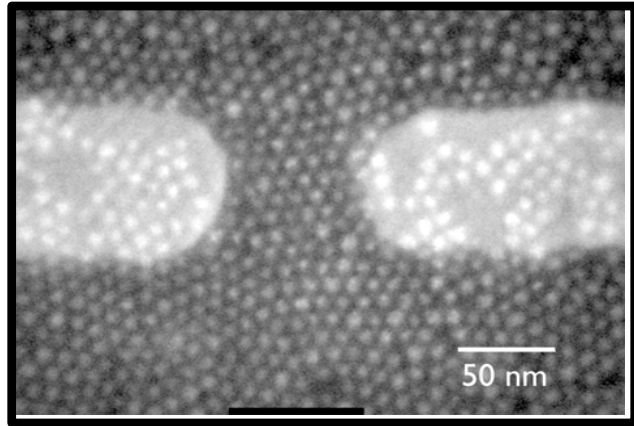


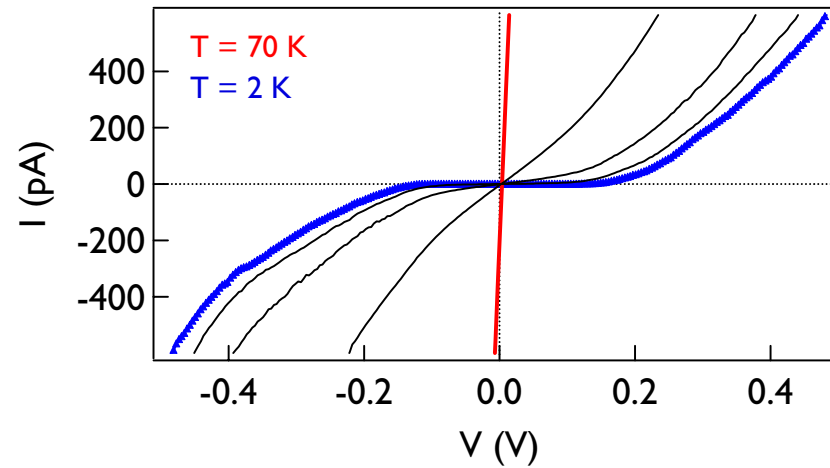
Figure 6: a) TEM image of wuestite nanocrystals with seeds of magnetite inside. b) SAED of the material showing a speckled pattern for FeO reflections and diffuse rings for magnetite reflections. c) Dark-field image of the region in Figure 5a (shown as negative); a part of the magnetite reflections were selected with the objective aperture. d) Dark-field image of the region in Figure 5a (shown as negative); a part of the wuestite reflections were selected with the objective aperture.

Spin-dependent tunneling in Nanocrystal arrays

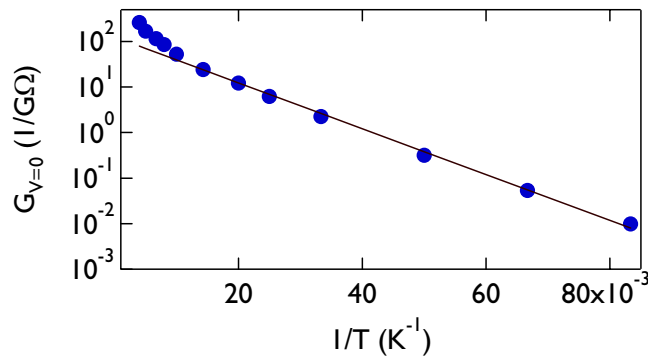
Chuck Black, Bob Sandstrom, Chris Murray, Shouheng Sun



► shortest current path ~ 8 nanocrystals



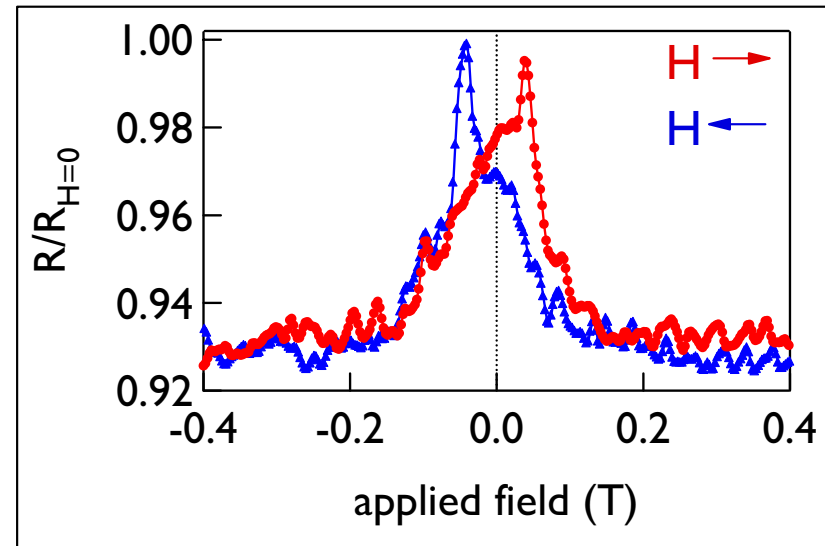
$G_{V=0}$ follows simple thermal-activation



data fit by: $\ln(G_{V=0}) = \text{const.} - E_c/k_B T$

► from fit to data, measure $E_c \sim 10 \text{ meV}$

► for all devices measured, $10 \text{ meV} < E_c < 14 \text{ meV}$



Ferroic Nanoparticles: synthesis and self-assembly into Ferroic Nanocomposites

Target ferroelectrics:

BaTiO₃

SrTiO₃

BaSrTiO₃

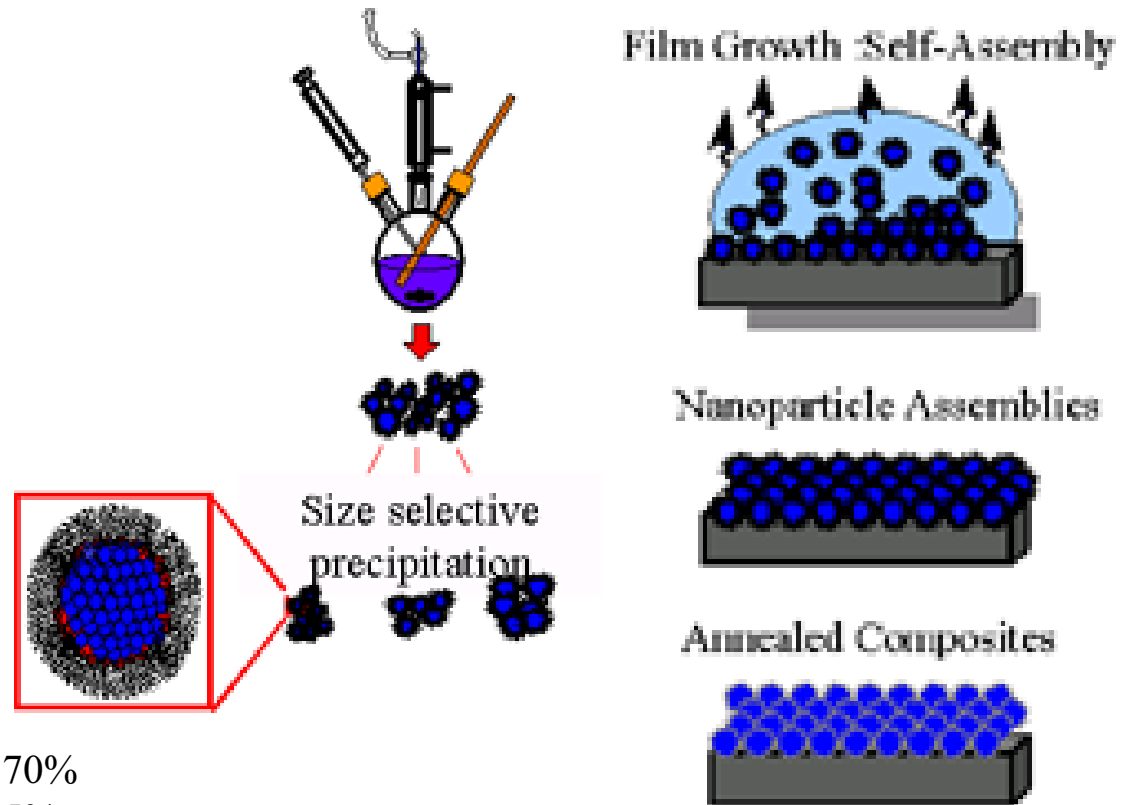
Future targets Niobdates

DARPA supported personnel:

Visiting Scientist Franz Redl 70%

Staff: C.B Murray 5%

Additional costs covered by IBM

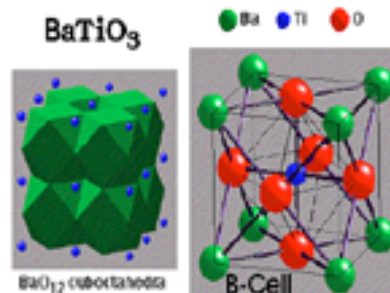
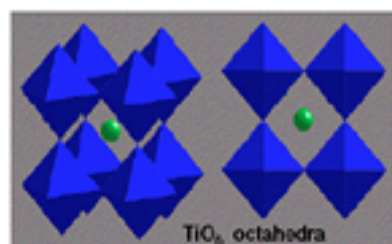


Key Opportunities to Control of Ferroic Nanomaterials

- **Size and compositional control of the individual nanoparticle:**
 - Particle size must be small enough to be single domain smaller than $\sim 200\text{nm}$ but not so small that tetragonal structure is lost I.e. larger than 50nm
 - Must have enough polarizability character to have tunability but no coercivity
 - Carbon and Hydroxyl functions must be minimized in the final structures
- **Engineering Nanoparticles shape control domain structure:**
 - Playing off of shape & crystal anisotropy may lower energy to reversal and loss.
 - Certain novel shapes may not sustain domain walls and thus allow single domain behavior at larger sizes.
- **Multicomponent assembly may allow the mixing of properties or new properties in composites:**
 - Intimate mechanical and dipolar coupling of grains of dissimilar composition provides opportunity.
 - Controlled assembly of independently tunable ferroic particle building blocks is a long term goal.
- **These techniques can not all be developed simultaneously. So we take the problem in 3 pieces, (1) Composition & Size, (2) Novel Shapes and (3) Assemblies to allow some learning in parallel.**

Size and Compositional Control in Titanates

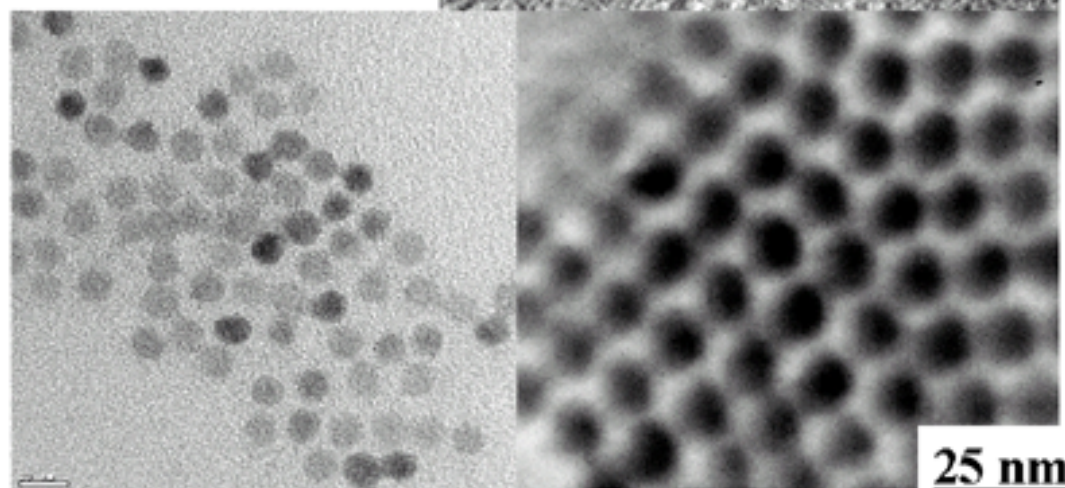
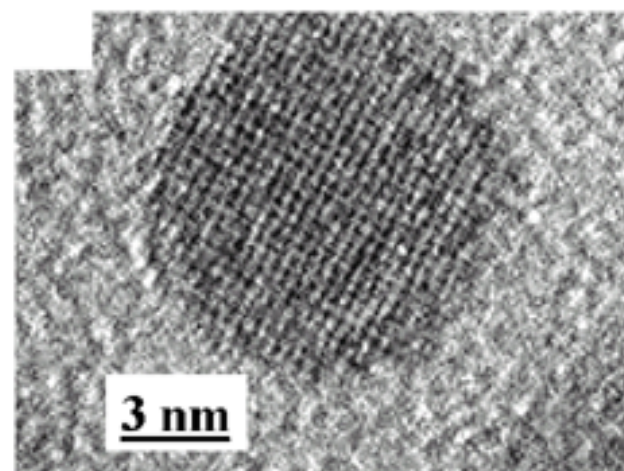
Challenges of scale-up from 100mg-10g scale



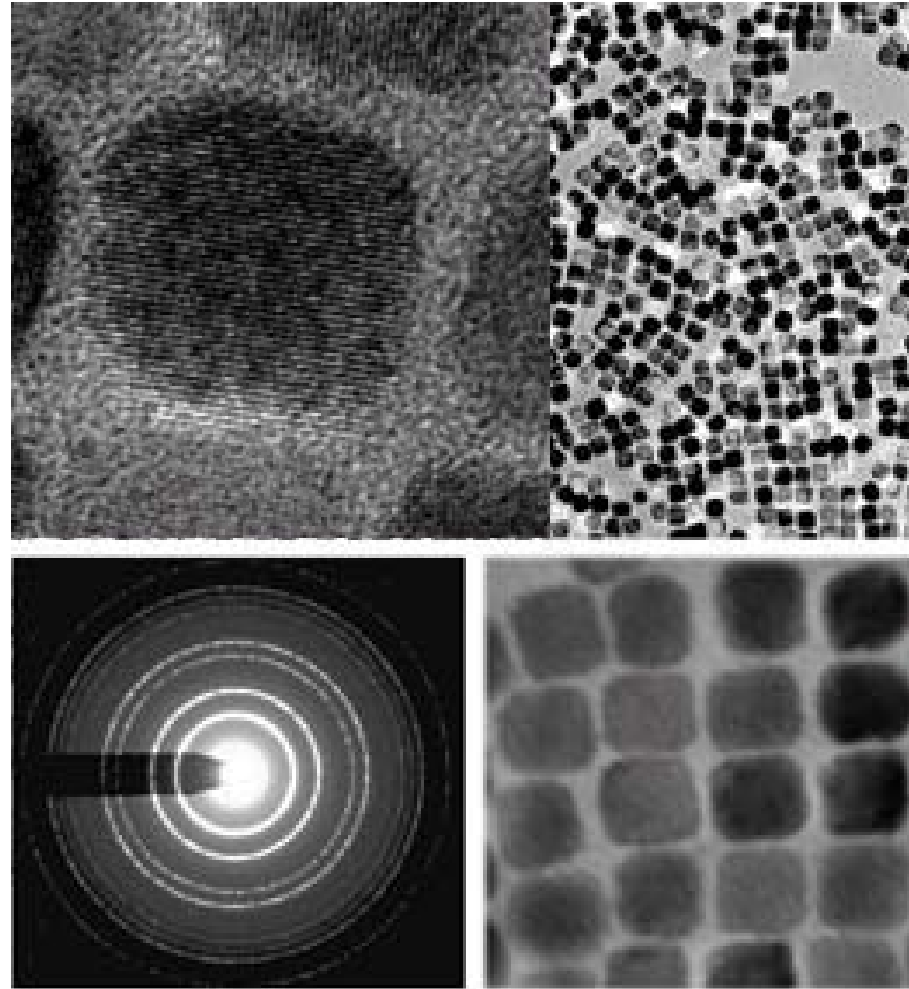
Ferroelectric Nanocrystals BaTiO₃

Synthesis of Mg Quantities complete in Q2

Challenge for Q3
to extend
synthesis extend
to SrTiO₃.



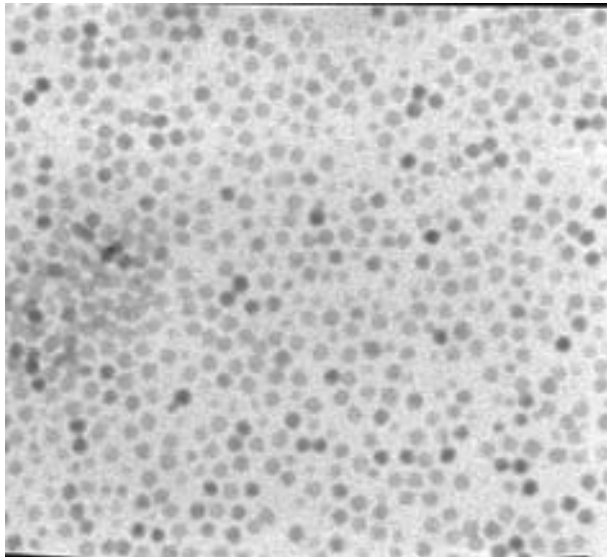
12 nm SrTiO_3 for Strontium titanium isopropoxide
Milligram quantities preparation complete Q3 but mixed
 BaSrTiO_3 takes a couple more months.



Mixed BaSrTiO₃ Nanoparticles

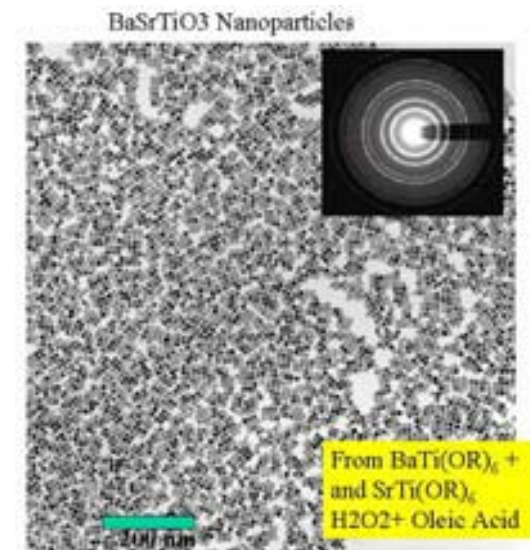
Milligram Quantities complete Q5.

BaSrTiO₃ synthesis from injection of
Individual Ba and Sr alcoxide precursors.



average size 8 nm
Bimodal population
(Most runs look worse)

React Ba and Sr precursors
to make mixed alcoxide
prior to initiating growth



Scale Up of Reactions from Milligram to multi-gram scale:

(1) Ocylether to expensive for scale-up solvent
re-optimize reactions for phenyl ether at 1/10th the price.

Begin processing Ba and Sr alcoxide monomers producing.

(2) Polymeric precursors at a fraction of the original polymers cost from vendor.

(3) Build and commission pilot reactor with 2 liter capacity up from Original 20ml scale.

(4) Average yield rise from 50-100mg to closer to 5-10 grams.
Reaction times between 1-3 days depending on temp & desired size

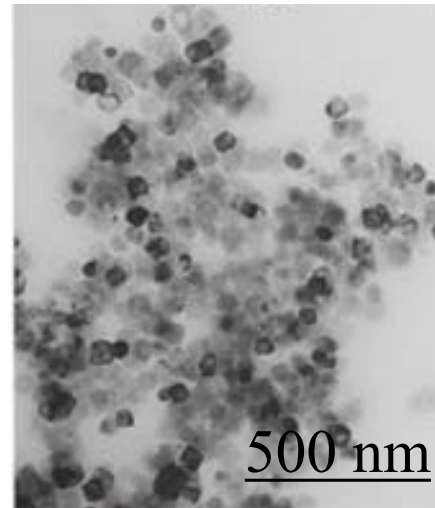
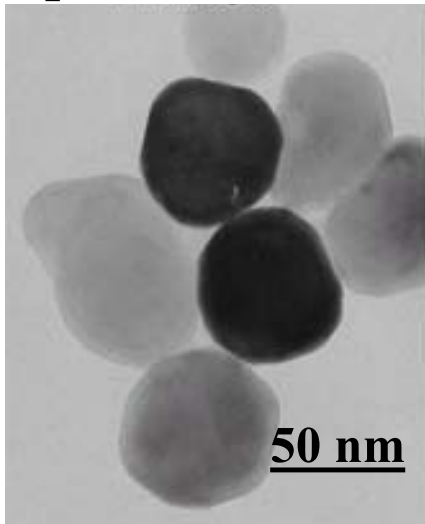
Results of 5 to 10 reactions combined to provide samples delivered to Rockwell for further tests.

Some 400gms of nanoparticle delivered to date.

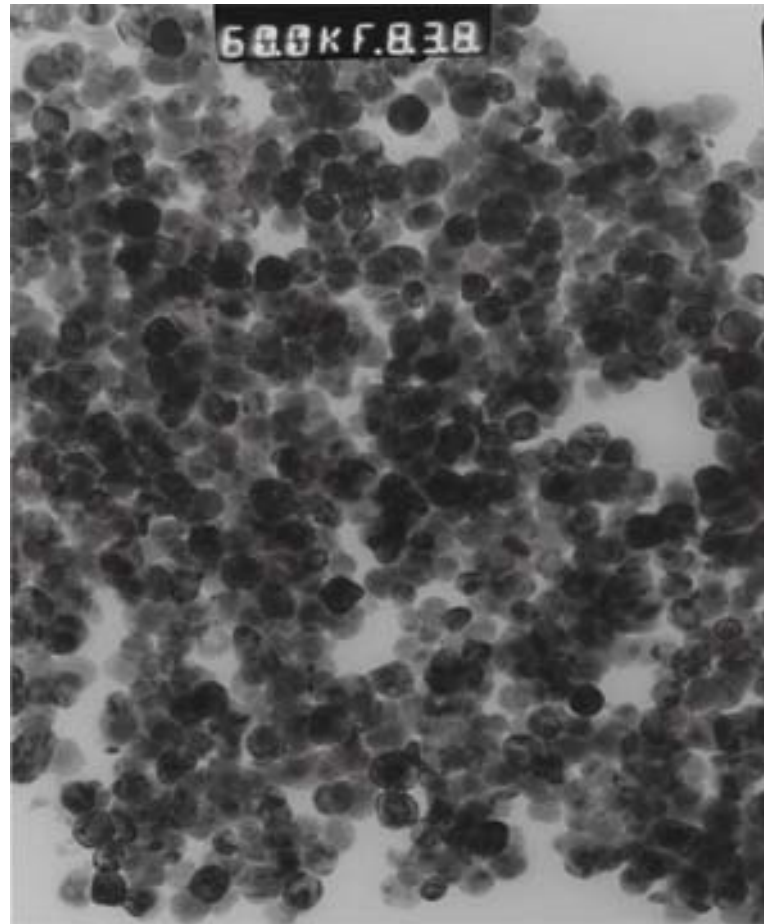
Quality of scale-up materials:


The average composition of the material is comparable to small batches but there is a greater variation in particle size $\sim 20\%$. Larger batches more readily secured to run over the weekend extending growth and allowing large sizes to be accessed. Average sizes move toward targets of 40-70nm range.

Examples from SrTiO_3 with post synthesis anneal to remove organic.



Synthesized and annealed BaTiO₃ powder~60nm Particle size





Design & Assembly of Two Component Nanomaterials

Shouheng Sun

Chuck Black

Franz Redl

Kyung-Sang Cho

Hao Zeng

Robert Sandstrom

Chris Murray

The precise control of composition size and shape on the nanoscale allows materials properties to be engineered.

Examples finite size effects include:

- Tunable optical properties of semiconductor Q. Dots. (quantum confinement)

- Coulomb blockade effect in metal nanostructures.

- Superparamagnetic effects in magnetic nanoparticles.

- Granular giant magneto-resistance.

- Superparaelectric phenomena in nanostructured ferroelectrics.

- Surface plasmons in noble metal nanostructures (Photonics & Plasmonics).

The next frontier is to control the interaction of nanostructures:

Engineering the cross-coupling of properties to reveal new emergent behavior.

We are looking for new materials in a world where $1 + 1 \geq 2$

i.e. the whole is greater than the sum of the parts

Materials Science needs to move toward controlled complexity:

Collective Phenomena:

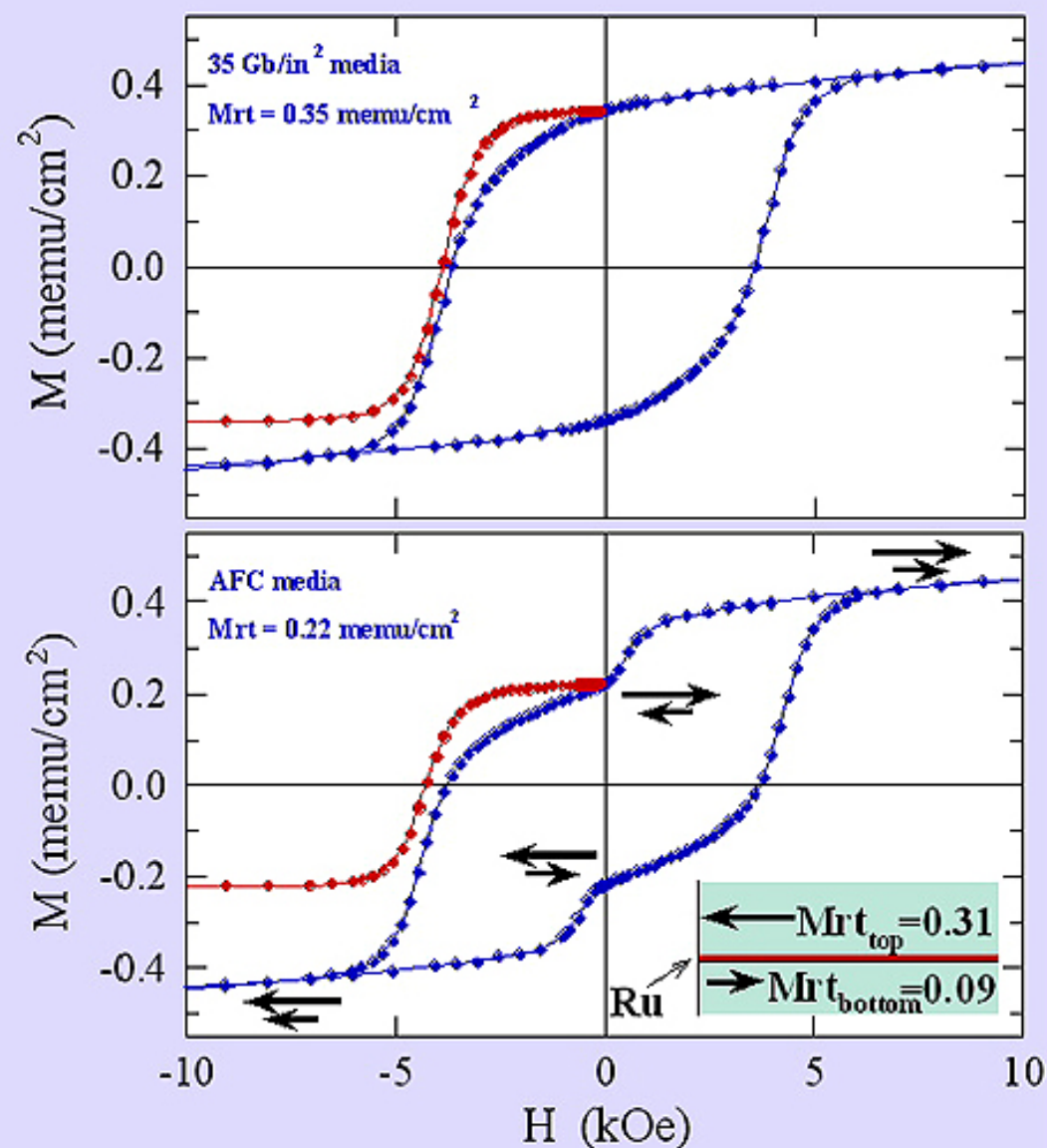
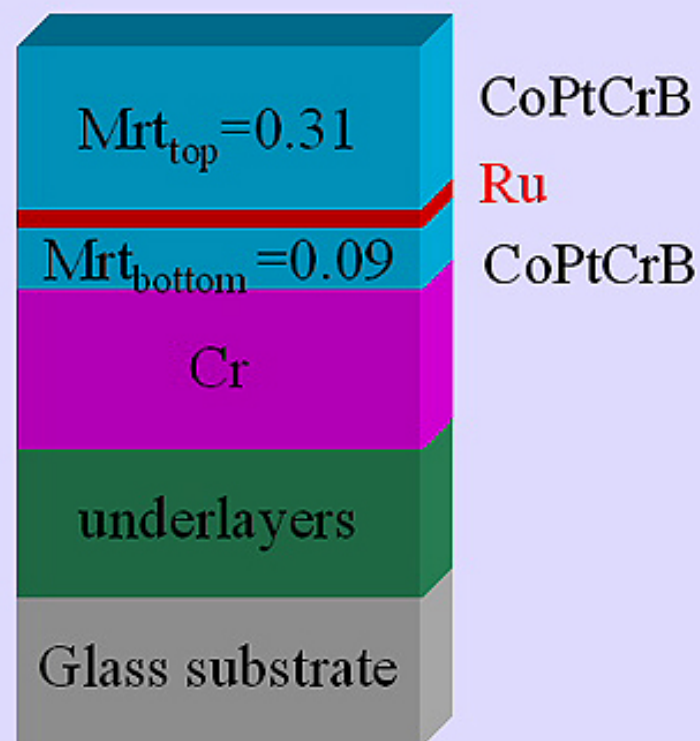
All the interesting things in chemistry & physics arise from the interplay and interference of the properties of more basic building blocks.

Nature teaches us that complex, highly functional & efficient systems can assemble from simple building blocks. These systems in turn can show complex and intelligent behavior.

Our challenge is to build more complex but controlled materials in the hope of observing, understanding and ultimately harnessing emergent behavior in these new systems.

Nanoparticles make ideal building blocks with tunable electronic, optical, magnetic and electrostatic properties and a tendency to self-organize make them ideal building blocks.

AFC media magnetization response to magnetic field



Spring-Exchange Magnetic
Nanocomposites:
Designing High energy product
Magnetic systems.
i.e. Simultaneously High M_s & High HC

Exchange-spring nanocomposites

H. Zeng & S. Sun

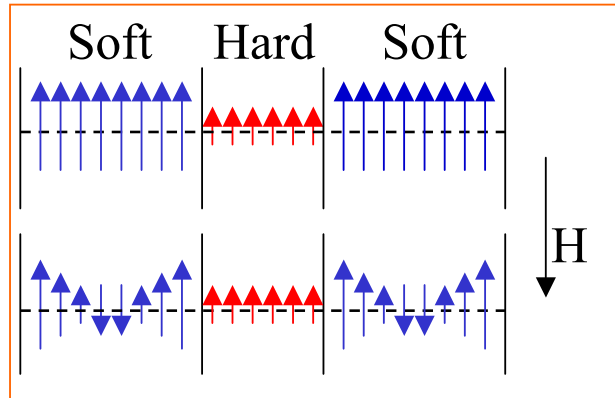
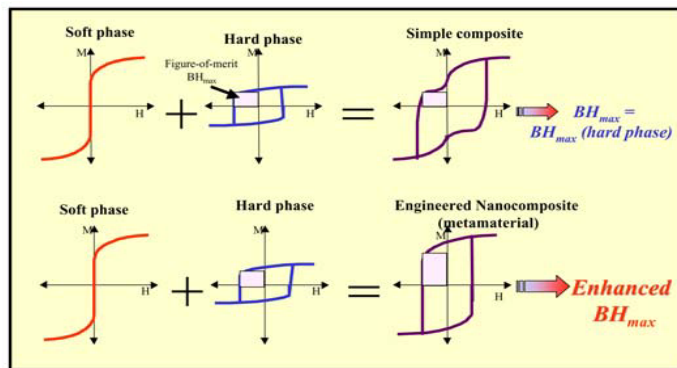


Illustration of a modulated hard-soft exchange-coupled system



Magnetic hysteresis loops for a non-exchange coupled system (top) and an exchange-coupled system (bottom).

➤ An exchange-spring composite contains two modulated phases that are in intimate contact with one being magnetically hard and another magnetically soft.

➤ The system can store high density magnetic energy because it has both large coercivity and high magnetic moment, and is ideal for future permanent magnetic nanodevice applications.

➤ The key to effective exchange-coupling is to control the size of the soft phase at $\sim < 10\text{nm}$.

➤ Self-assembly has been proven to be a unique way of forming exchange-spring nanocomposites.

Magnetic Nanomaterials for Functional Nanodevices

Researchers: Shouheng Sun, Hao Zeng, Min Chen

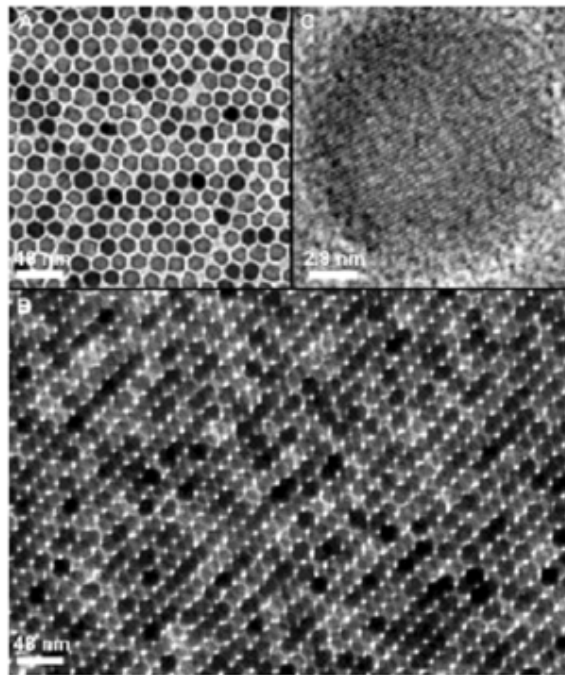
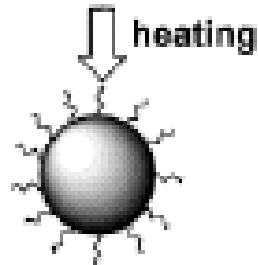
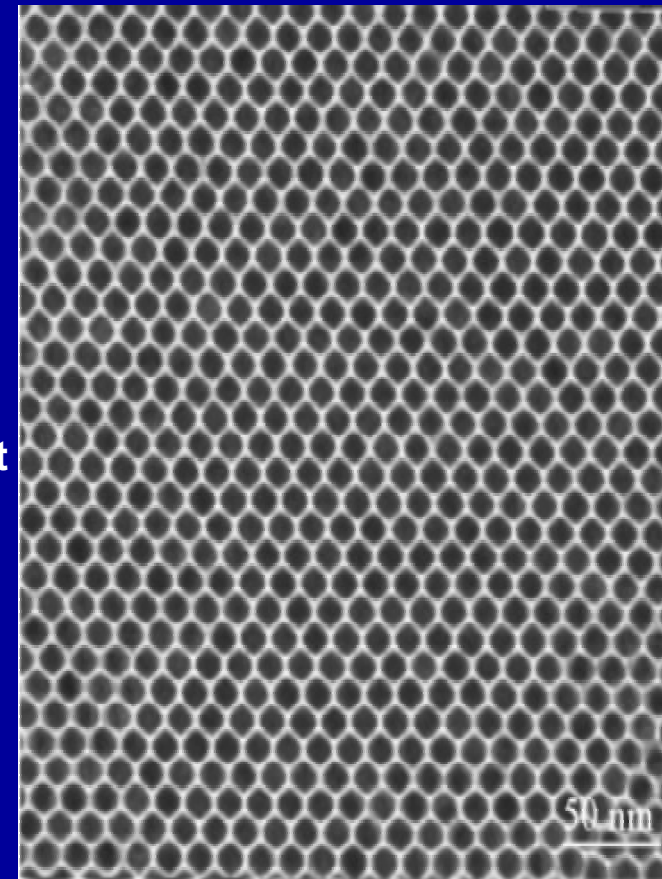


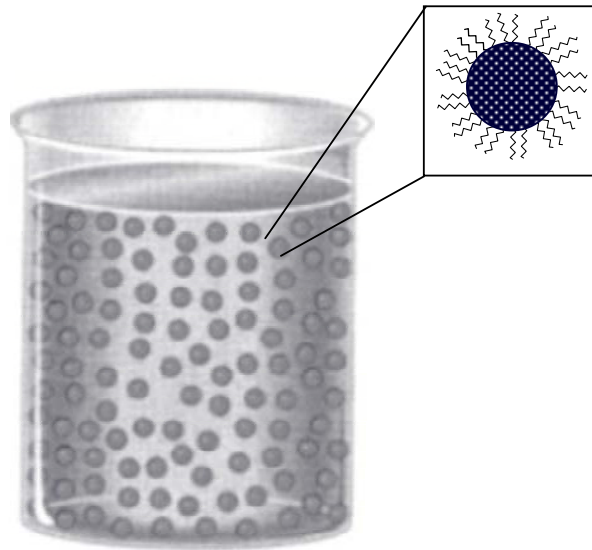
Figure 1. TEM bright field image of 16-nm Fe_3O_4 nanoparticles deposited from their dodecane dispersion on amorphous carbon surface and dried at 60 °C for 30 min: (A) a monolayer assembly, (B) a multilayer assembly, (C) HRTEM image of a single Fe_3O_4 nanoparticle. The images were acquired from a Philips EM 430 at 300 KV.

Single component
Self-assembly

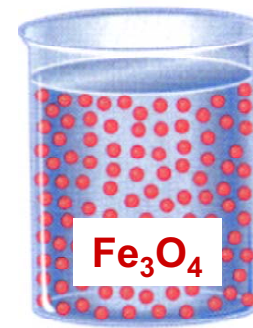
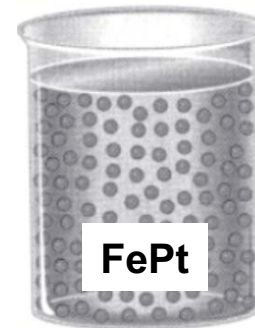


Self-assembled Fe_3O_4 NPs

Hard-soft exchange-coupled nanocomposites via self-assembly of two kinds of NPs



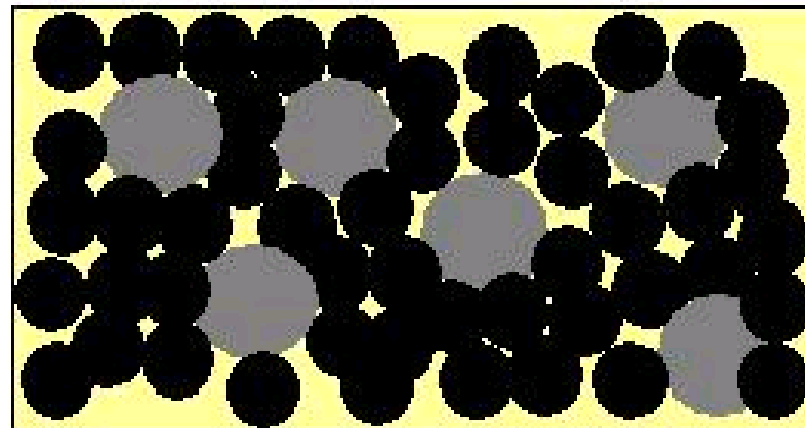
A nanoparticle dispersion in an organic solvent. The particles are stabilized by a layer of organic surfactant to prevent them from aggregation.



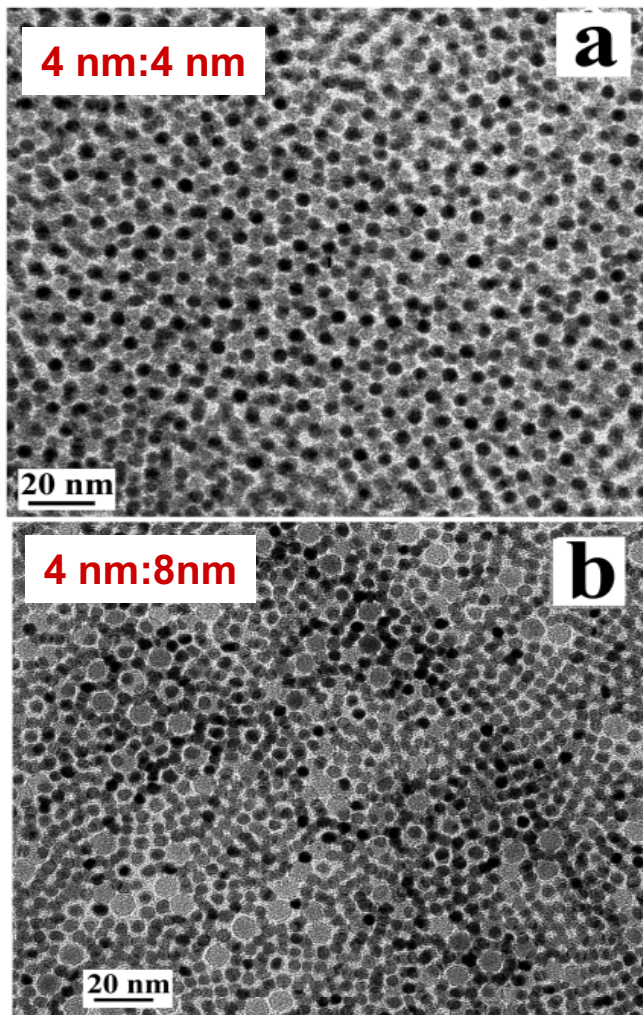
(1) Self-Assembly to mix two kinds of nanoparticles



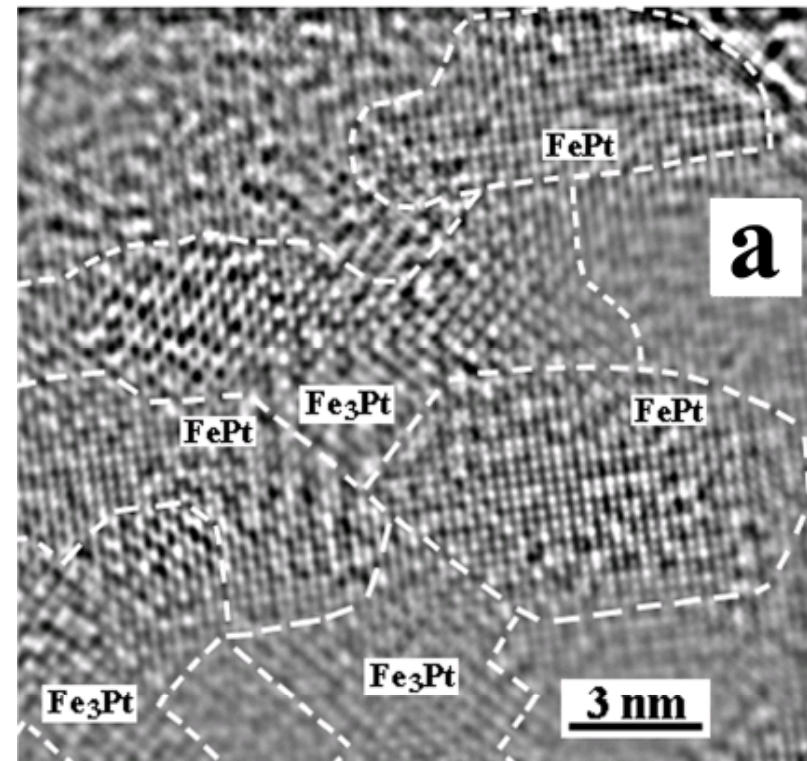
(2) Reductive annealing to reduce metal oxide to metal and to remove organic surfactants.



Hard-soft exchange coupled nanocomposite

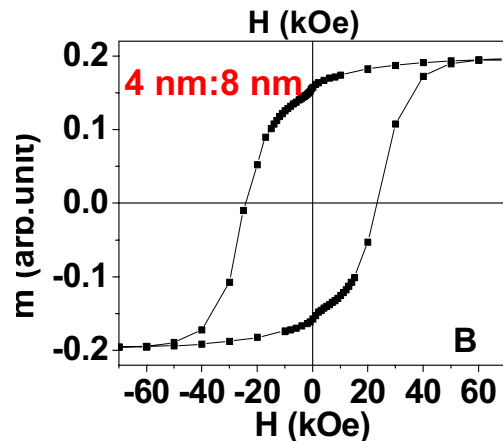
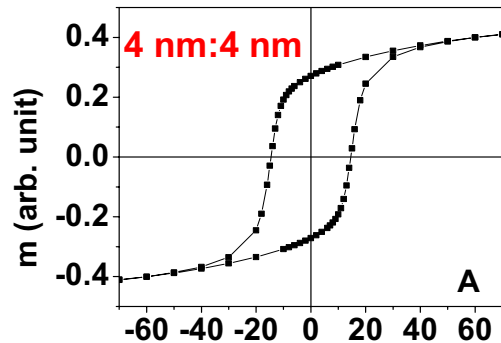


TEM images of two different binary assemblies prepared directly from particle dispersions of 4 nm FePt nanoparticles as well as 4 nm Fe₃O₄ and 8 nm Fe₃O₄.

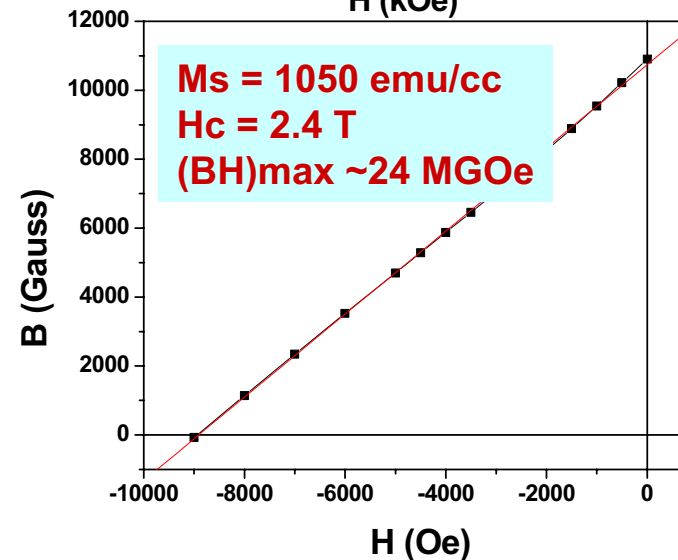
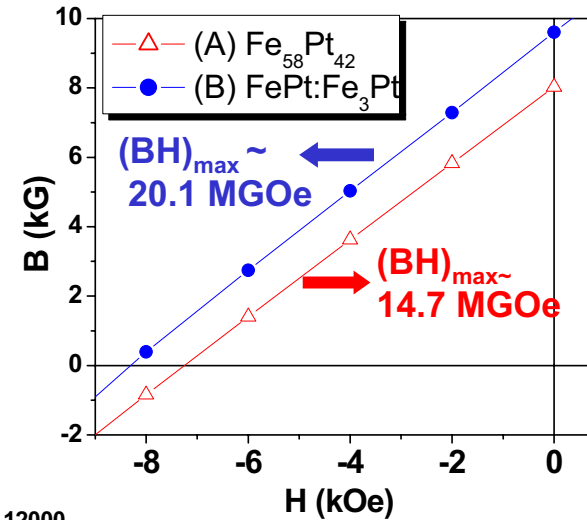


HRTEM image of an exchange-coupled nanocomposite (FePt-Fe₃Pt) made from 4 nm FePt and 4 nm Fe₃O₄ nanoparticles under reductive annealing. Shown here is a modulated structure with FePt and Fe₃Pt in intimate contact, resulting in exchange-coupling.

Nanocomposite magnetics



Hysteresis loops at room temperature with the composites from 4nm:4nm and 4nm:8nm nanoparticles respectively.

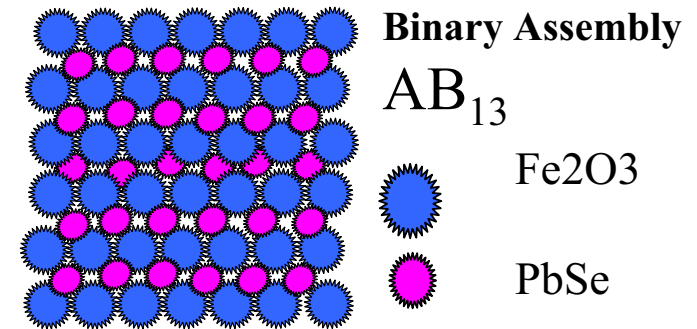


$(BH)_{max}$, energy product, reflects the ability for a composite to store the magnetic energy, the larger the better.

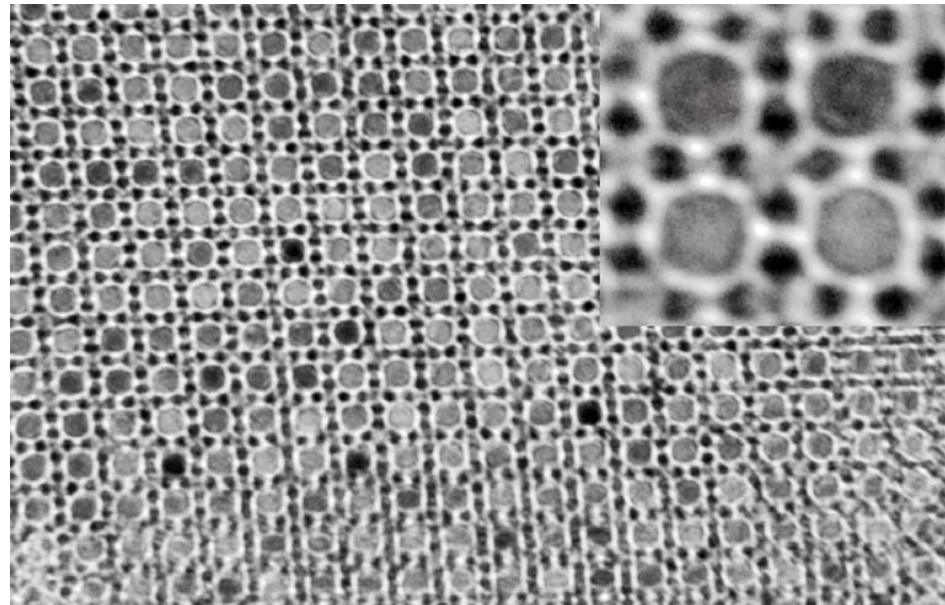
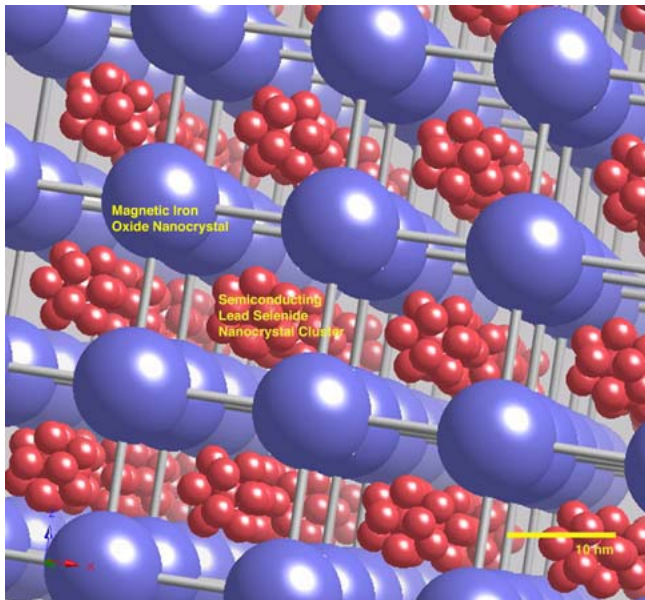
Binary Nanocrystal Array's a New Class of Nanostructured Materials

Franz Redl, Kyung-Sang Cho and C. B. Murray

Nanocomposites of:
Ferromagnets, Noble Metals, Semiconductor QDs,
Semimetals, Ferroelectrics, Superconductors, may
all be possible to explore for
New emergent properties.

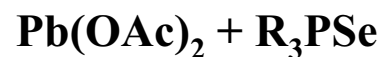
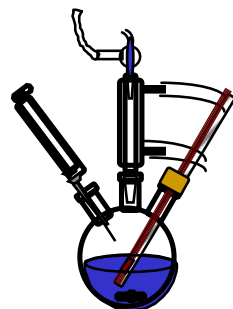


New Near IR Magneto-Optic Composite ~13nm Fe₂O₃ and 5nm PbSe Q.Dots
Packed in an AB₁₃ (NaZn₁₃) structure with 4.5 Million atoms in the unit cell.



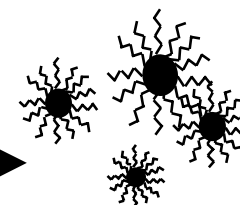
Wet Chemical Synthesis of PbSe Nanocrystals and Superlattices

Synthesis



oleic acid,

R_3P , $T=150\text{ }^\circ\text{C}$

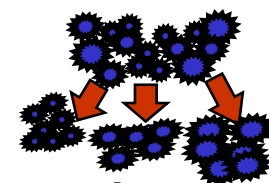


PbSe

R= octyl

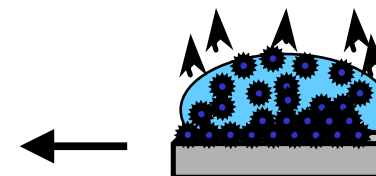
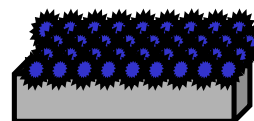
Size Selective Processing

Size selective precipitation in solvent/ non solvent pairs like hexane-methanol

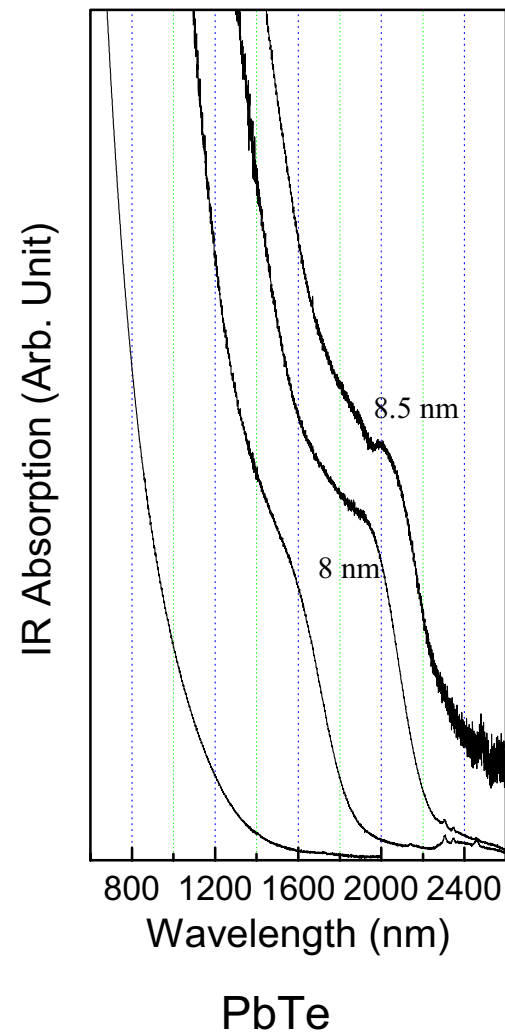
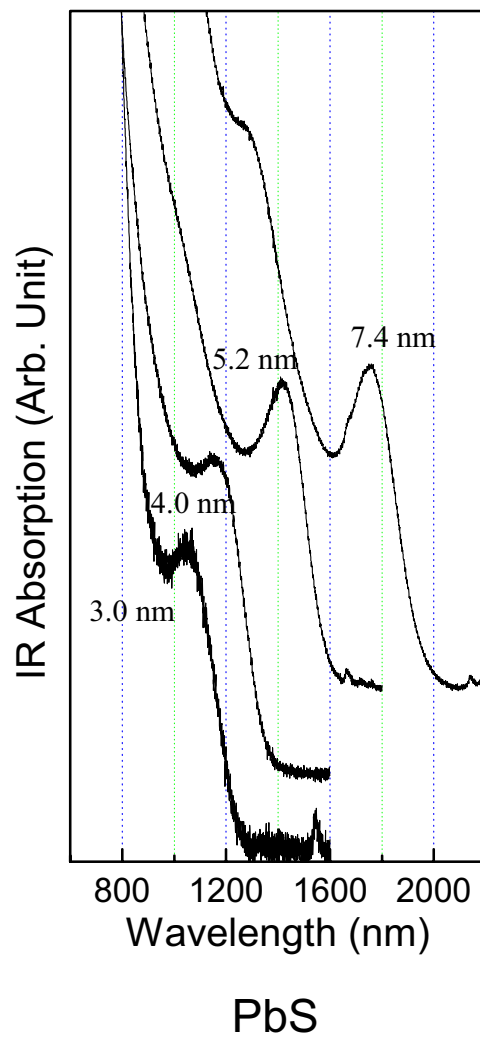
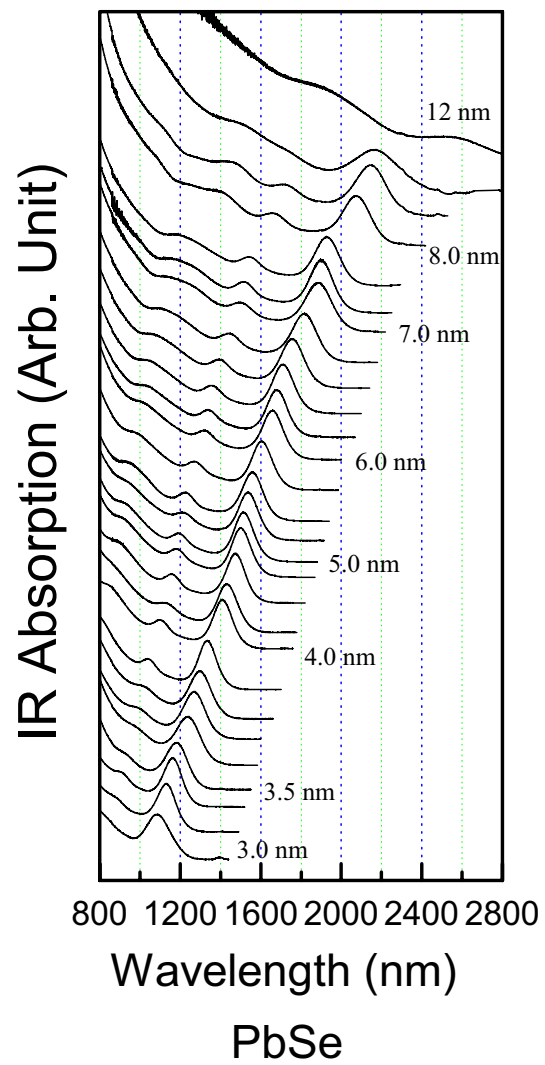


Self Assembly

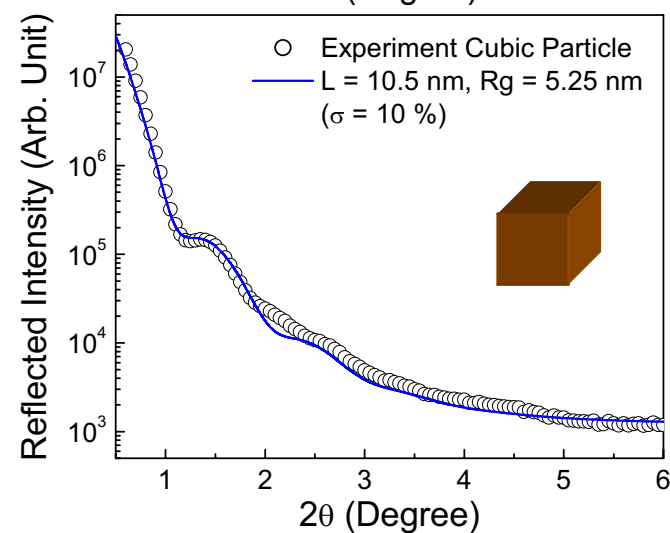
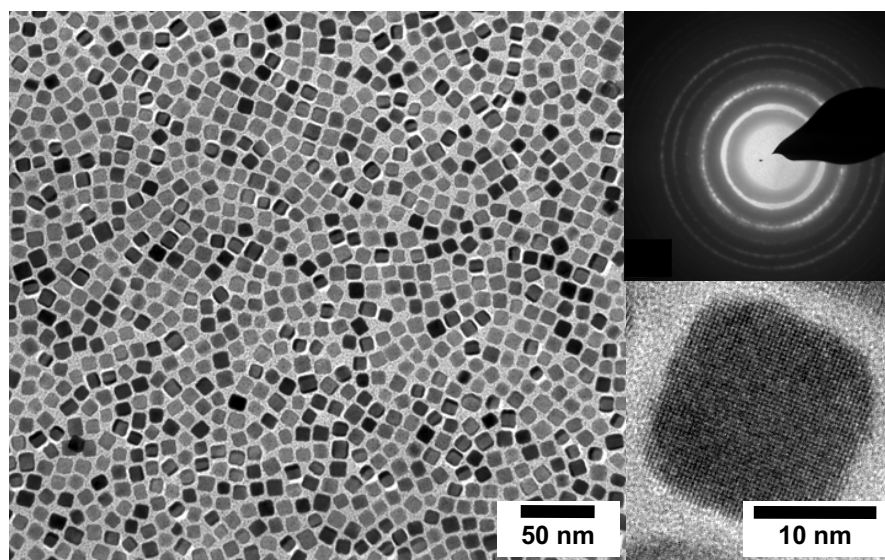
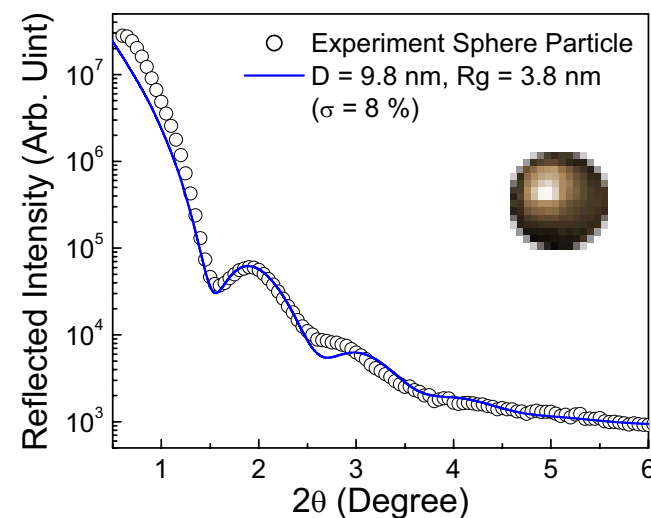
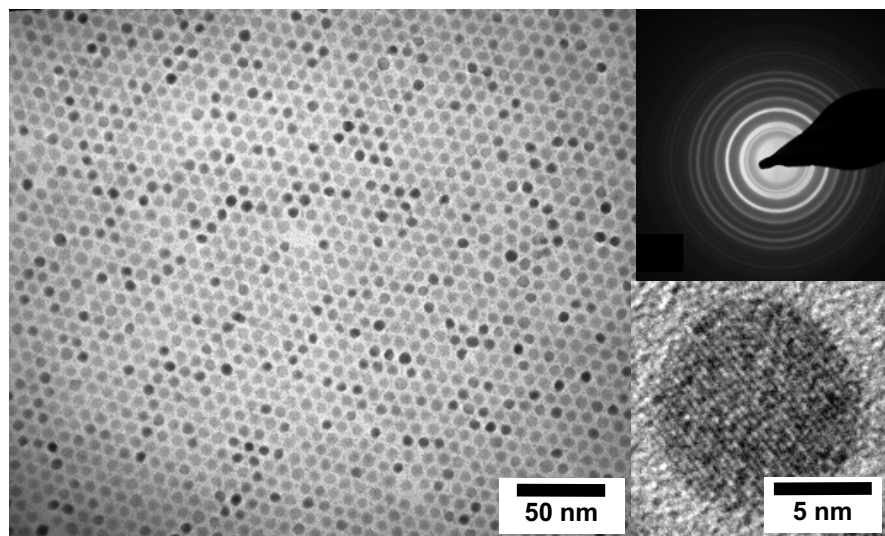
Evaporation of the solvent

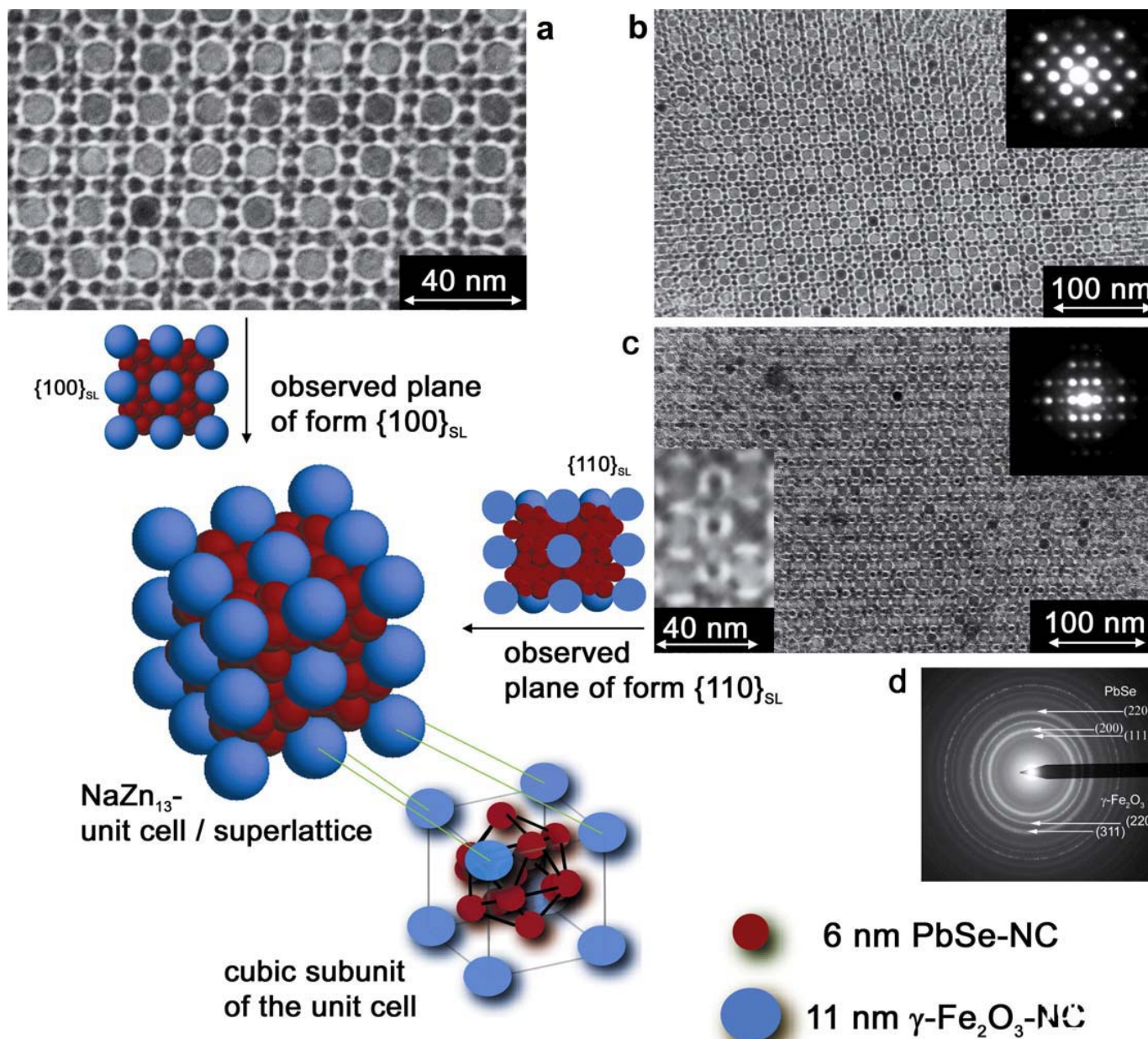


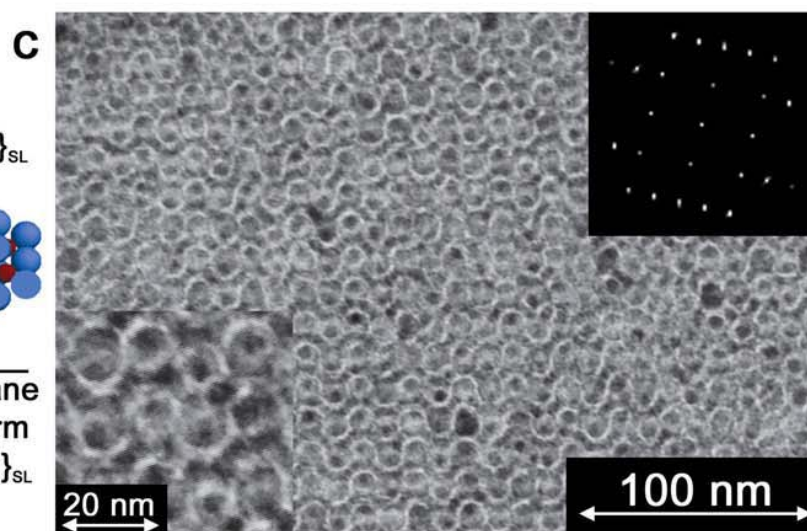
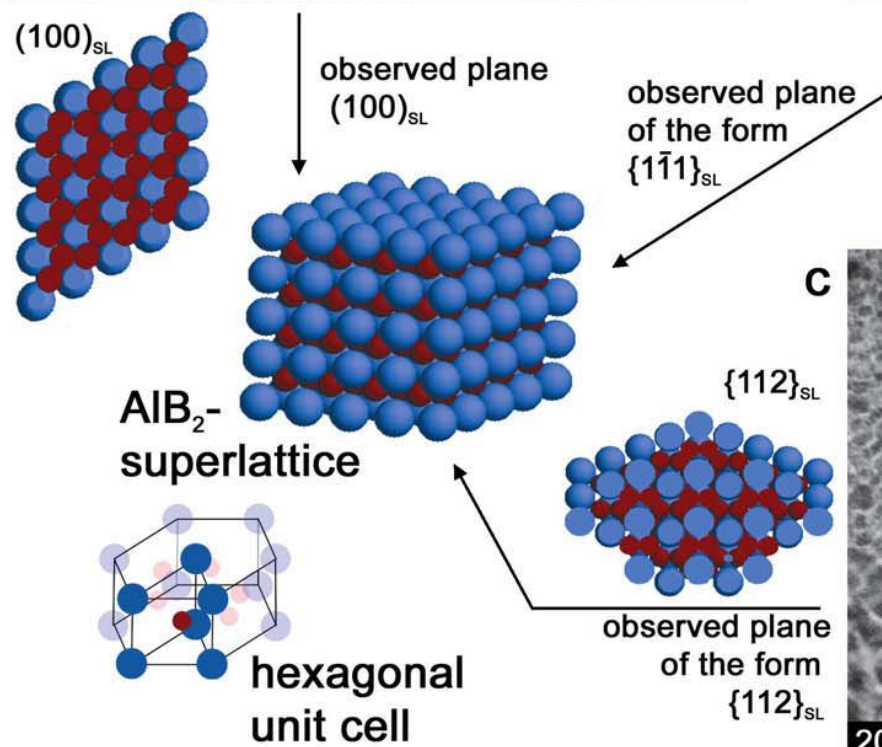
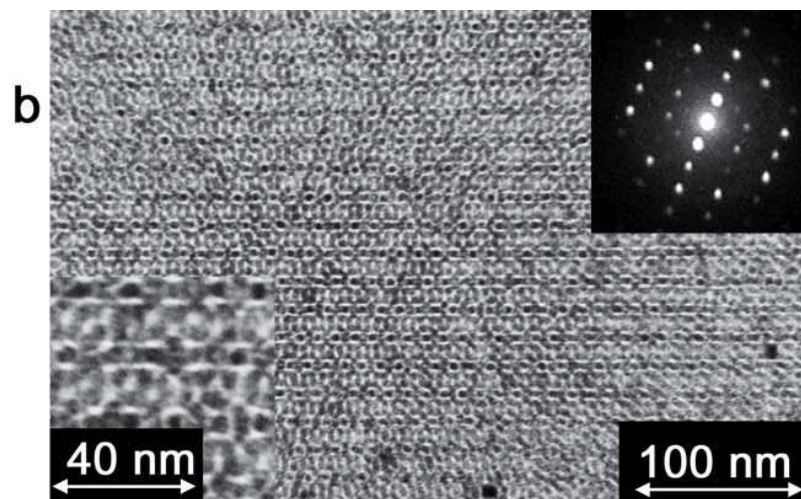
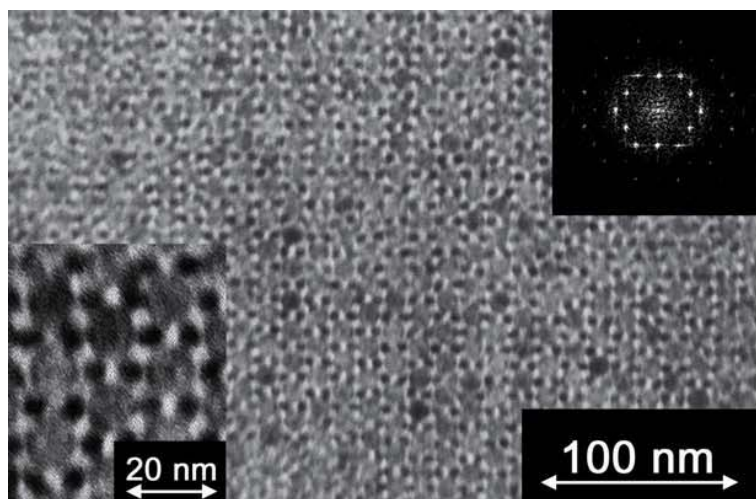
IR Absorption of Lead Chalcogenides NCs



Shape Change from Sphere to Cubic and SAXS in Polymer Matrix







Preliminary results on AB_5 ($CuCa_5$) binary superlattice

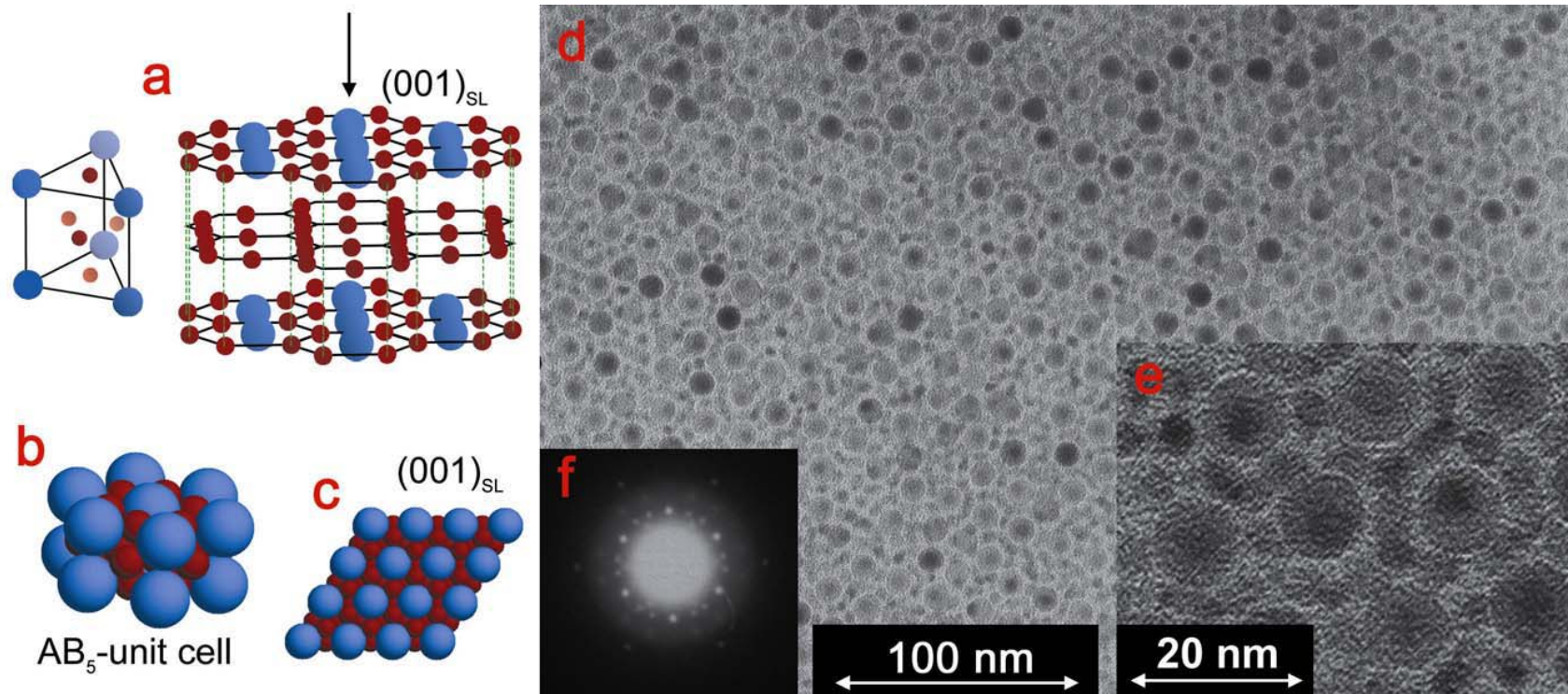
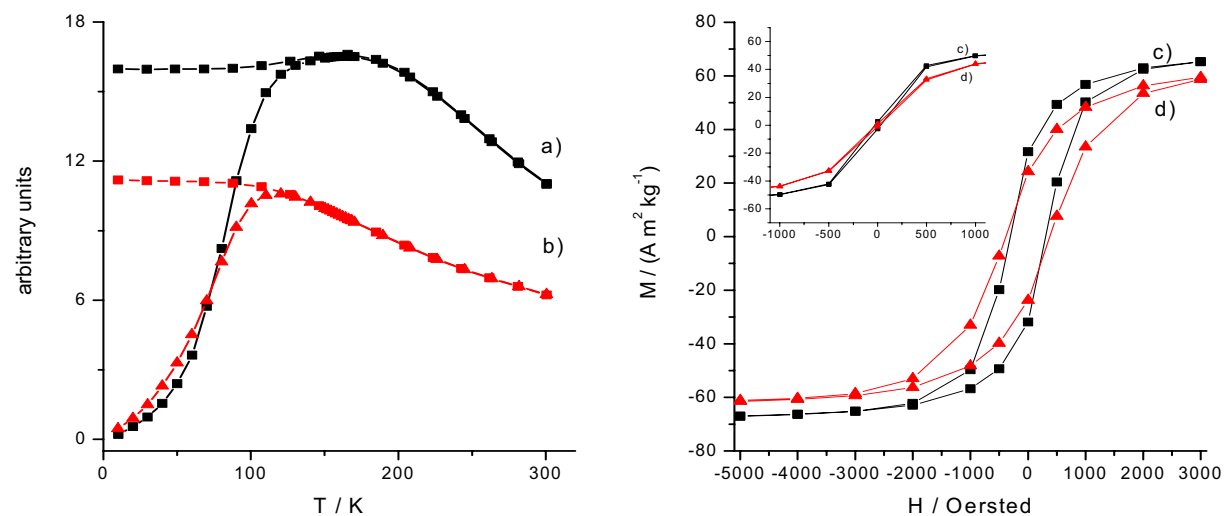
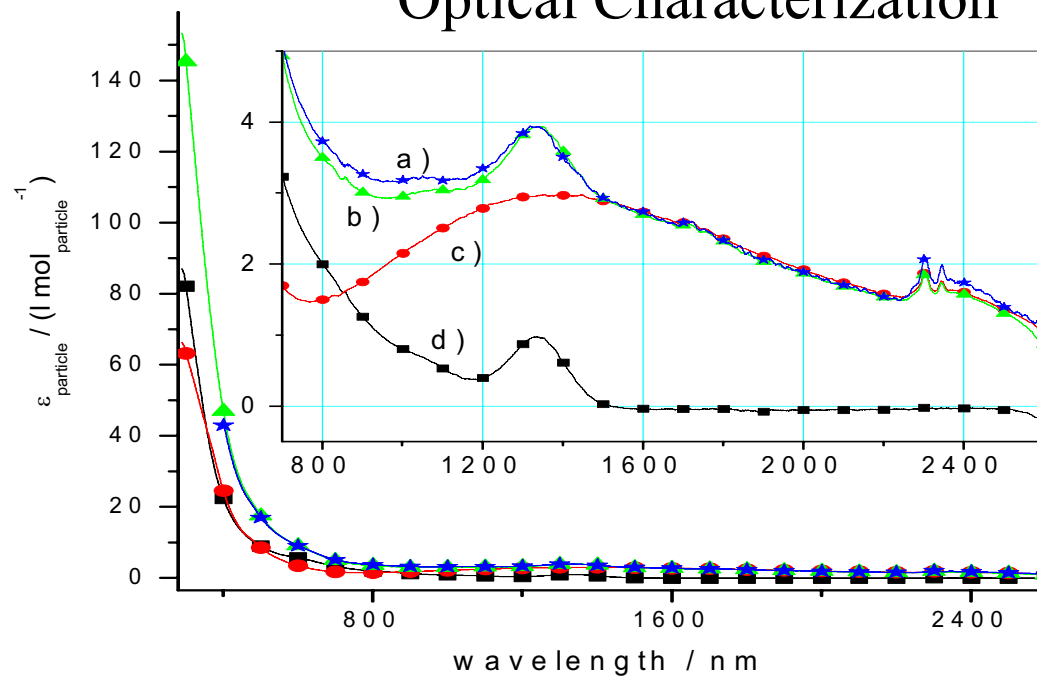


Figure 4: TEM micrographs and sketches of AB_5 superlattices (isostructural with intermetallic phase $CaCu_5$, SG 191) of 11 nm $\gamma\text{-Fe}_2\text{O}_3$ and 6.3 nm PbSe NCs. **a**) Depiction of the $CaCu_5$ structure as trigonal face-centred prism or layers. **b**) Hexagonal AB_5 unit cell. **c**) Depiction of the $(001)_{SL}$ plane. **d**) Projection of the $(001)_{SL}$ plane. **e**) Projection of the $(001)_{SL}$ plane at high magnification. **f**) Small angle electron diffraction pattern from a $6 \mu m^2$ $(001)_{SL}$ area.

Magnetic characterization of the Binary Arrays

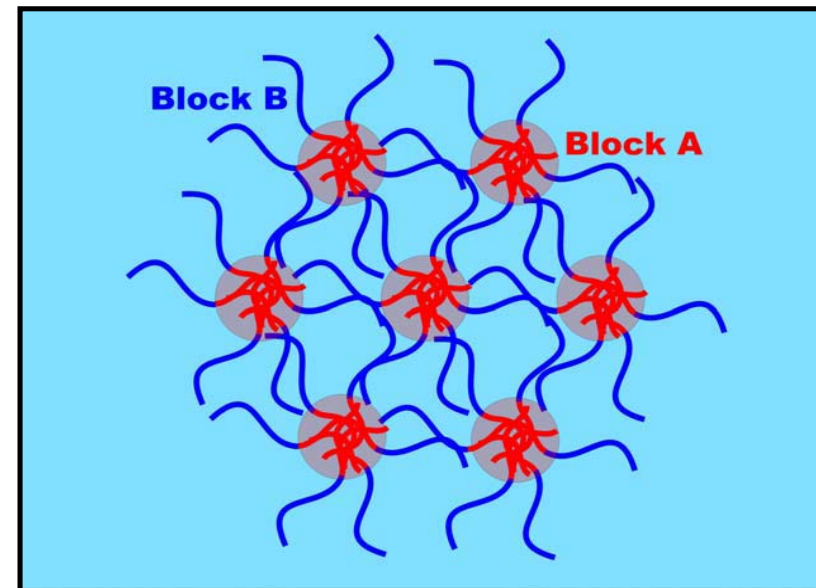
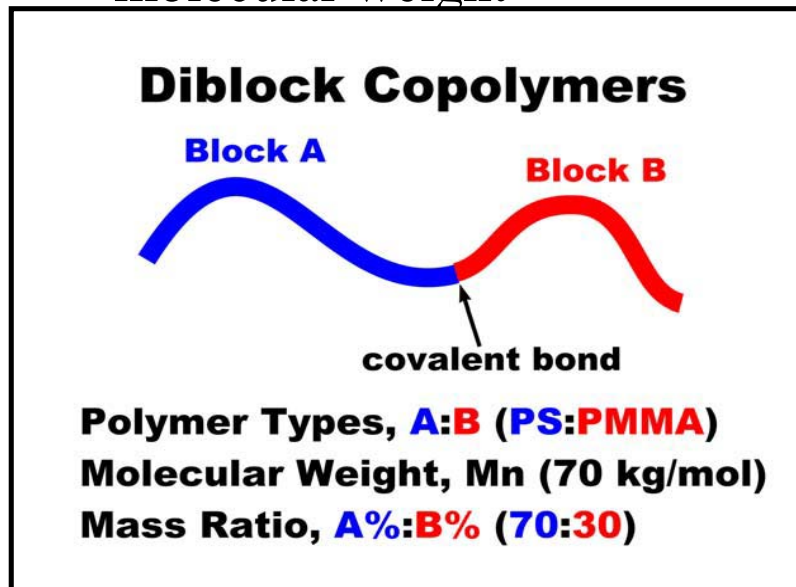


Optical Characterization



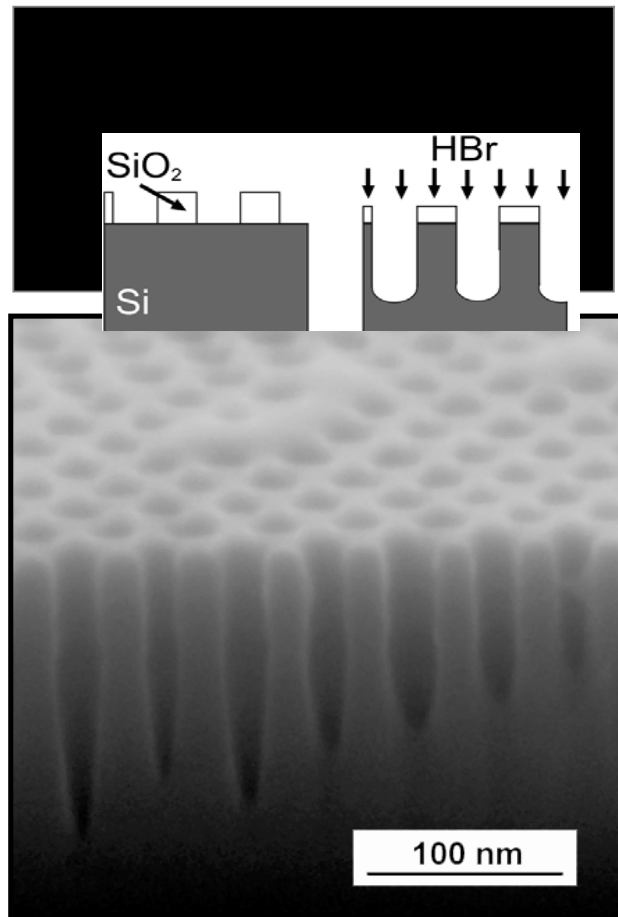
polymer self assembly

- Diblock copolymer molecules self organize into ordered phase morphologies
- Nanostructure dimensions (~ 10 -100 nm) depend on polymer molecular weight

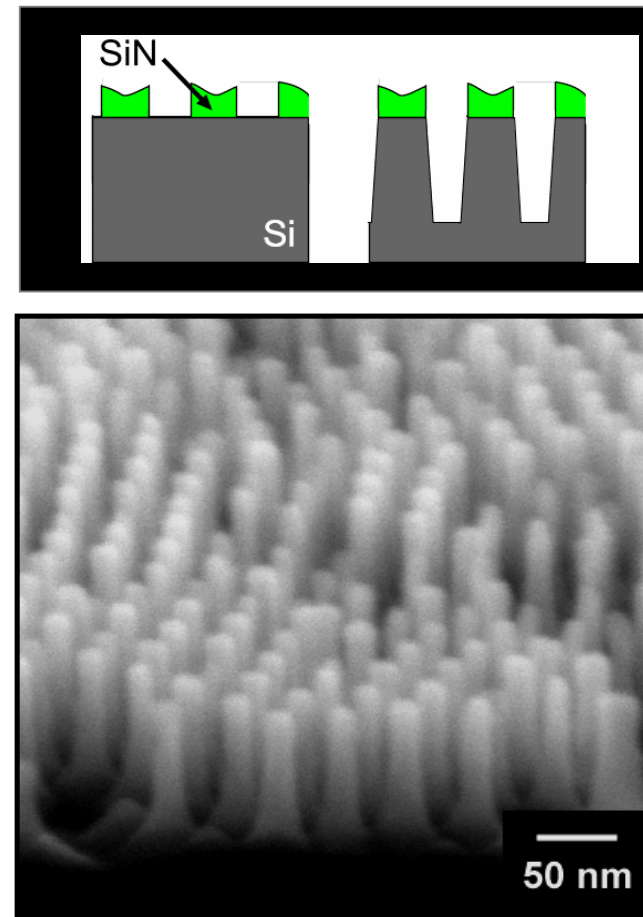


- - process integration - -

high-aspect-ratio silicon structures



nanotextured Si surface



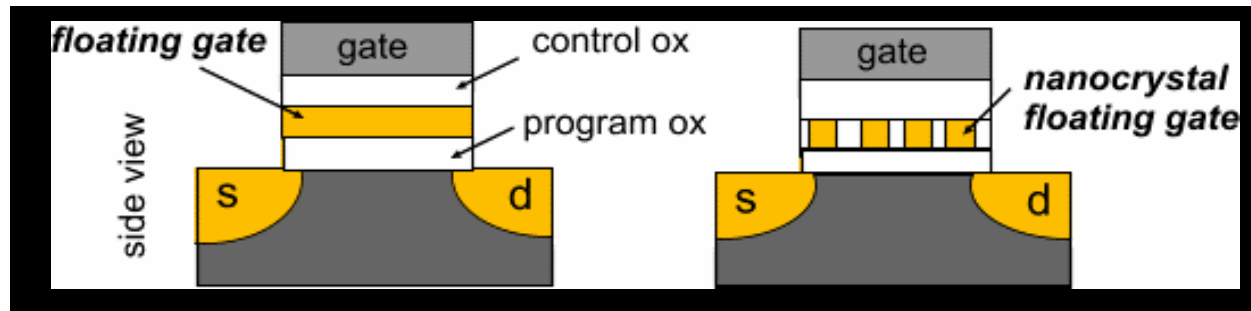
dense silicon pillar array

C. T. Black and K. Guarini

- - applications - -

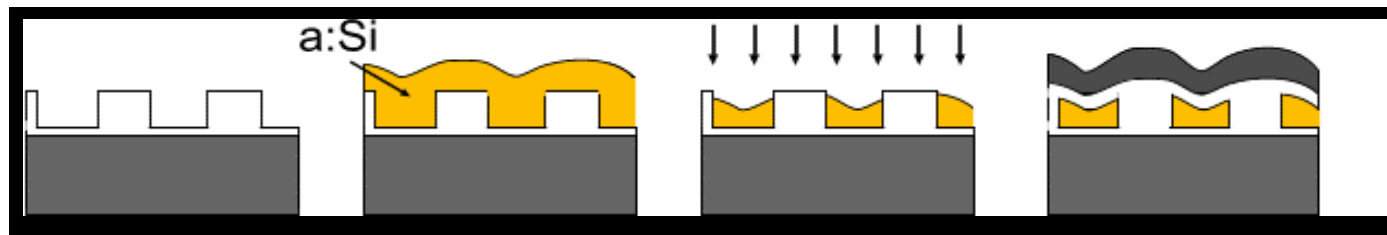
nanocrystal memories may improve FLASH scaling

nonvolatile memory



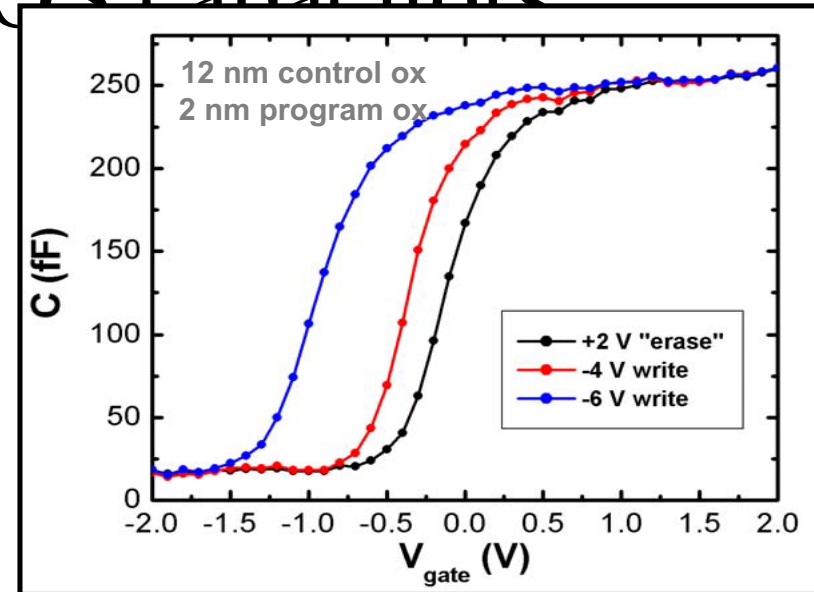
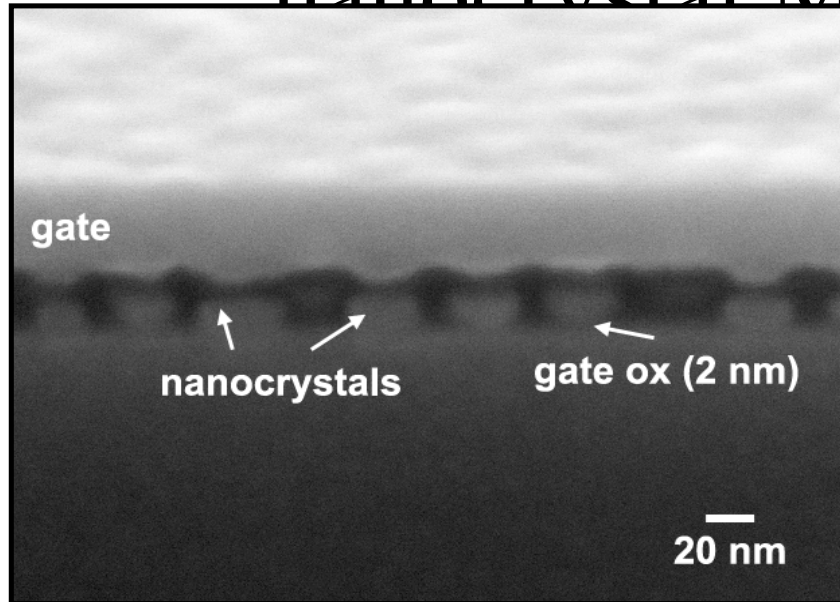
potential advantages:

- improved charge retention for same program ox thickness
(lower power, faster, improved cyclability)
- reduced stress-induced leakage current
- (possibly) multi-bit storage via single-electron charging effects
(with suitable nanocrystal size/uniformity)



- - applications - -

nanocrystal MOS capacitors



- nanocrystal MOS capacitors show ΔV_{FB} at low write voltages:
 - $\Delta V_{\text{FB}} \sim 0.25 \text{ V}$ for -4 V write
 - $\Delta V_{\text{FB}} \sim 0.75 \text{ V}$ for -6 V write
- **in progress:** evaluation of effect of control ox thickness, program ox thickness, and substrate doping
- **next:** evaluation of device retention time, write speed, & cyclability

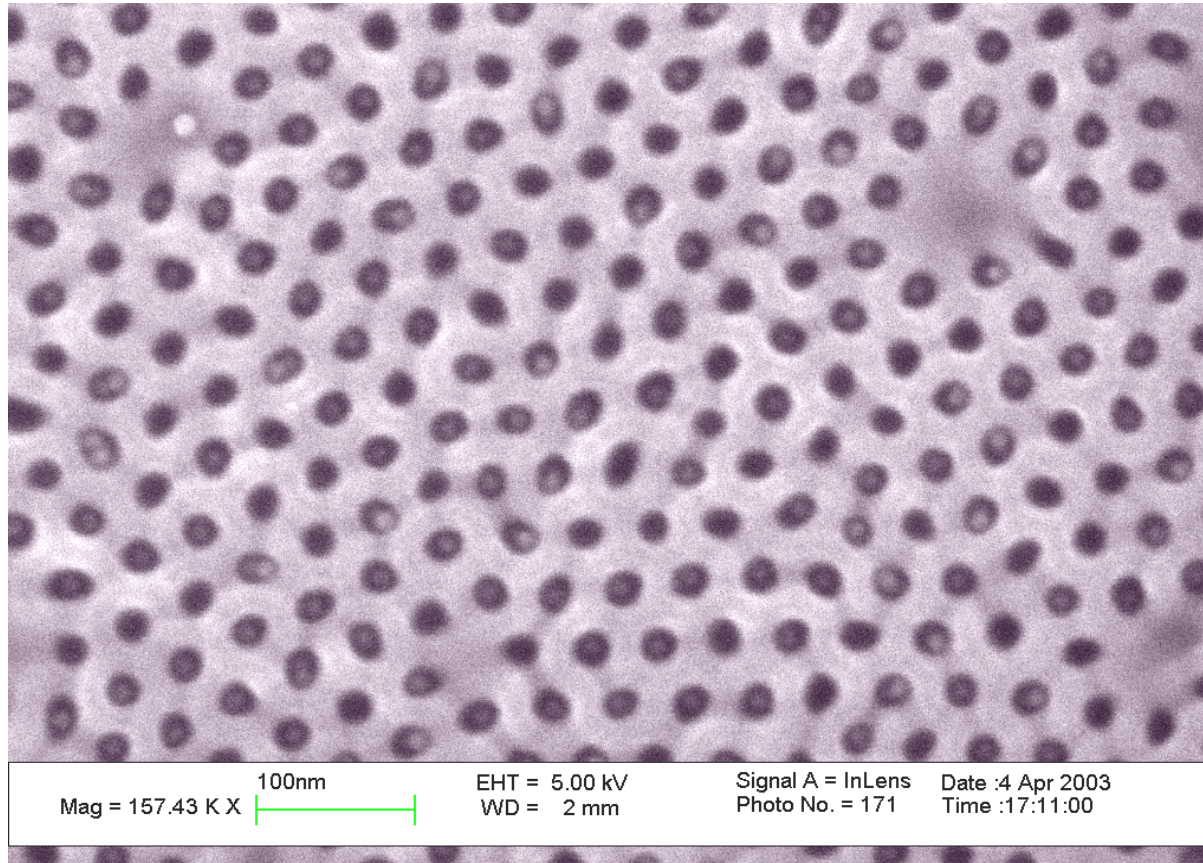
patent disclosure YOR8-2003-0152

Self-assembled Templates to Organize Nanoparticles

NanoDimpling and NanoRoughening

total # of template holes = 227
total # of 1 nanoxials/hole = 167
total # of 2 or more nanoxials/hole = 3
total # of no nanoxials = 57
75% coverage for 45sec wait

"particles on surface" test for
90s etched in SF₆+CF₃Br
on 14nm ϕ Fe_xO nanoxials - 45s



Pmma/PS Diblock copolymer template etched into silicon has 20nm ϕ with 40nm spacing and Fe_xO 14nm ϕ nanoxials
R.L.Sandstrom (NanoScale Materials & Devices Group) April 22, 2003

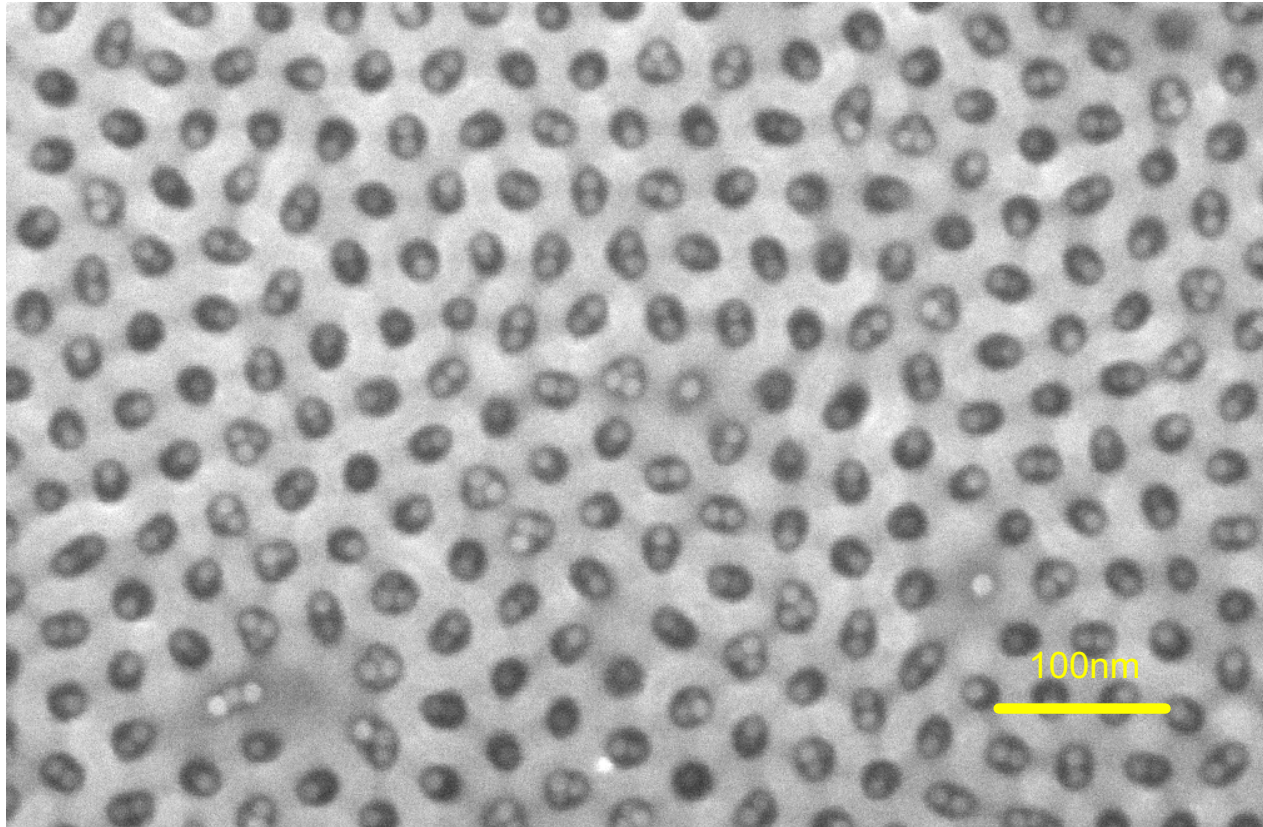


R. Sandstrom, C. T. Black & C. B. Murray

NanoDimpling and NanoRoughing

(total # of template holes = 230) (total # of 1 nanoxtals/hole = 56) (total # of 2 nanoxtals/hole = 151) (total # of 3 nanoxtals/hole = 23)

100% nanoxtals/hole coverage for 45sec nanoxtal residence wait time



Pmma/PS Diblock Copolymer Template has 20nm ϕ with 40nm spacing and Fe_xO 12-14nm ϕ nanoxtals
R.L.Sandstrom (NanoScale Materials & Devices Group) April 24, 2003

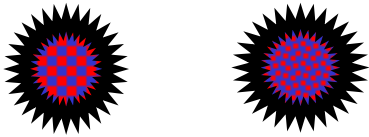


R. Sandstrom, C. T. Black & C. B. Murray

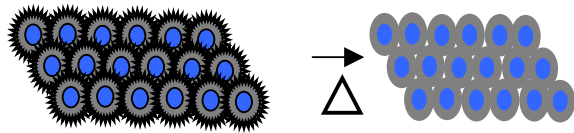
Complex Compositions and Multi-Component Structures

Simultaneous Reaction

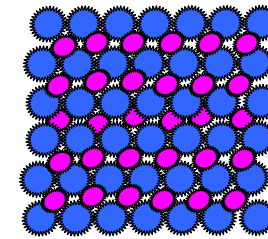
A & B Compounds & Alloys



Anneal to remove Organic



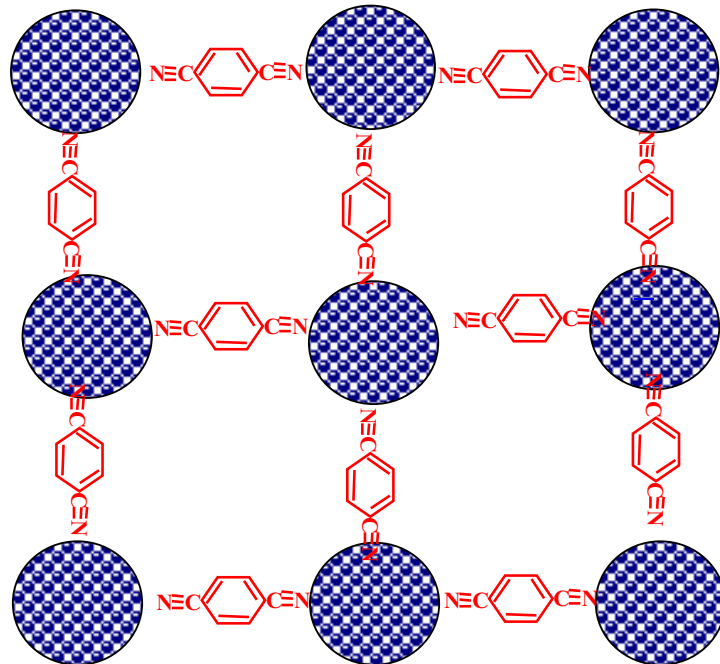
Ferromagnets,
Noble Metals,
Semiconductor QDots,
Ferroelectrics,
Superconductors



Binary Assembly
 AB_2 & AB_{13}



Customize organic linkers (molecular wires)



Dicyanobenzene linked Cobalt Nanocrystals

